

Polymer/Silica Nanocomposite System

Miroslav Janíček

Bachelor Thesis
2007



Tomas Bata University in Zlín
Faculty of Technology

Univerzita Tomáše Bati ve Zlíně

Fakulta technologická

Ústav inženýrství polymerů

akademický rok: 2006/2007

ZADÁNÍ BAKALÁŘSKÉ PRÁCE

(PROJEKTU, UMĚLECKÉHO DÍLA, UMĚLECKÉHO VÝKONU)

Jméno a příjmení: **Miroslav JANÍČEK**
Studijní program: **B 2808 Chemie a technologie materiálů**
Studijní obor: **Chemie a technologie materiálů**

Téma práce: **Polymer/Silica Nanocomposite System**

Zásady pro vypracování:

Elaborate a literar study focused on the following two points:

- | Treatment and modification of silica and nanosilica**
- | Using nanosilica in polymer system**

Elaborate a short summary of the advantages and disadvantages of polymer/silica nanocomposite system

Rozsah práce:

Rozsah příloh:

Forma zpracování bakalářské práce: **tištěná/elektronická**

Seznam odborné literatury:

Rothon, R. N. Particulate fillers for polymers, Shrewsbury, Rapra Tech., 2001, ISBN 185957310X.

Wypych G. Handbook of Fillers, Toronto-New York, ChemTec Publishing, 1999, ISBN 1884207693.

Greenwood, N. N. Chemie prvků, Praha, Informatorium, 1993, ISBN 8085427389.

Vedoucí bakalářské práce: **Ing. Lucie Kovářová, Ph.D.**
Ústav inženýrství polymerů

Datum zadání bakalářské práce: **11. listopadu 2006**

Termín odevzdání bakalářské práce: **21. května 2007**

Ve Zlíně dne 5. února 2007


prof. Ing. Ignác Hoza, CSc.
děkan




prof. Ing. Milan Mládek, CSc.
ředitel ústavu

ABSTRACT

Presented bachelor thesis deals with nanocomposite systems based on polymer matrix filled with inorganic particles of silicon dioxide (silica) in range of nanometres. This document is understood as short summary of contemporary investigated problems. First part describes the filler – methods how to prepare nano-particles and also possible surface modifications are mentioned. Properties of newly acquired materials are delineated in the second part. Only several “main” polymer matrices are mentioned due to a broad spectra of available resins. Mechanical and rheological properties are emphasised as the thermal behaviour is outlined as well.

Keywords: Silica, Polymer nanocomposite, Mechanical properties, Thermal behaviour

ABSTRAKT

Tato bakalářská práce se zabývá problematikou plnění polymerní matrice částicemi oxidu křemičitého (siliky) s rozměry v řádu nanometrů. Je uchopena jako literární rešerše současných řešených problémů v této oblasti. První část textu je zaměřena na popis plniva – zmíněny jsou jak metody jeho přípravy, tak i modifikace povrchu částic. Druhá část práce se poté zabývá jednotlivými případy plnění polymerů nano-silikou, přičemž jsou sledovány především „základní“ skupiny plastů se zaměřením na změny v mechanických a reologických vlastnostech a tepelném chování nově vzniklých materiálů.

Klíčová slova: Silika, Polymerní nanokompozit, Mechanické vlastnosti, Tepelné chování

ACKNOWLEDGEMENTS

I want to say a word of thanks to my supervisor – Dr. Lucie Kovářová, namely for her patience, advices, rebukes and commendation as well.

I thank to my parents – Libuše and Miroslav Janíček, for their unflagging interests in my study. I am also appreciative of their encouragement as the material support too.

My thanks are meant to all my friends and schoolfellows and all another people, who helped me or advised me – namely the crew of central library.

PODĚKOVÁNÍ

Chtěl bych poděkovat vedoucí mé práce – Ing. Lucii Kovářové, Ph.D., za její trpělivost, rady, výtky i slova chvály.

Mé díky směřují také k mým rodičům – Libuši a Miroslavu Janíčkovým, za jejich zájem o mé studium, jakož i duševní a materiální podporu.

Musím poděkovat také všem, kteří jakkoliv přispěli připomínkami nebo radou – mým přátelům a spolužákům a také pracovníkům univerzitní knihovny za jejich ochotu pomoci při vyhledávání v archivu a v internetových databázích.

TABLE OF CONTENTS

INTRODUCTION.....	7
1 SILICON DIOXIDE AS NANO-SIZED PARTICLES.....	8
1.1 PREPARATION OF NANO-SCALED SILICA PARTICLES.....	11
1.1.1 “Wet” processes.....	11
1.1.2 Thermal processes.....	12
1.1.3 Hollow particles.....	14
1.2 MODIFICATIONS OF SILICA.....	15
1.2.1 Hydrophobization of nano-silica surface.....	16
1.2.2 Functionalization of nano-silica surface.....	18
2 POLYMERS FILLED WITH NANO-SCALED SILICA.....	22
2.1 POLYETHYLENE/SILICA.....	22
2.2 POLYPROPYLENE/SILICA.....	29
2.3 POLYSTYRENE/SILICA.....	37
2.4 POLY(METHYL METHACRYLATE)/SILICA.....	42
2.5 POLYESTERS/SILICA.....	46
2.5.1 PET/Silica.....	46
2.5.2 PBT/Silica.....	49
2.6 POLYAMIDE/SILICA.....	51
2.7 EPOXY RESIN/SILICA.....	54
2.8 POLYURETHANE/SILICA.....	58
CONCLUSION.....	64
BIBLIOGRAPHY.....	65
LIST OF SYMBOLS AND ABBREVIATIONS.....	70
LIST OF PICTURES.....	72
LIST OF TABLES.....	78
LIST OF APPENDICES.....	79

INTRODUCTION

Composite materials are made out of mixture of two or more materials with the purpose to improve one or more desired properties. Nanocomposite systems are composite materials where one component is matrix and another component – called filler, has one or more characteristic dimensions in nanometre order [1]. Matrix usually represents major volume proportion where the filler is dispersed. Three main categories of fillers are differentiated: spherical particles, layered particles and fibrillar or tubular formations.

Composite materials reinforced by spherical particles with dimensions in micrometer orders are probably ones of most widely used types of composites in common applications [1], [2]. Increase of elastic modulus and yield strength of the matrix is one of the most frequent causes of filling. New properties of matrix material could be achieved by reducing the particle diameter into sizes of nanometres.

One of these properties could be affect of light that got through the material. Microscopic particles cause diffraction and dispersion of visible light. This makes ordinarily transparent resins opaque. Decreasing the particle diameter can make the resin transparent, or partially transparent, as Naganuma and Kagawa show in their study of effect of the size of silica in epoxy/SiO₂ composite system [3]. Another significant advantage is the decrease of filler load needed to achieve desired property, what is attributed to the increase of the specific surface.

In recent years, nano-structured organic-inorganic composites have received great attention because of both their academic interest and potential industrial importance.

It was concluded from the search in several databases (John Wiley & Sons, Ltd., Elsevier Ltd., and American Chemical Society provenience) that nano-scaled fillers, especially nano-sized silica, are new and just developing research area, in some measure, while micro-sized fillers have been known and studied for longer period. That is why the aim of this bachelor thesis is to be understood as an effort to give short summary of contemporary research on silica as the nanocomposite filler. Due to the broad spectrum of possible polymers, which could be filled, this work is restricted to several main polymer matrices.

1 SILICON DIOXIDE AS NANO-SIZED PARTICLES

Silicon is the second most widespread chemical element in the Earth's crust, but only the seventh in universe. Irregular spread out of silicon atoms probably happened during the formation of Earth [4]. On the Earth silicon mainly occurs in the upper mantle of the central core and in the crust. Predominantly the heavy metal oxides and silicates¹ are comprised in the core mantle while upper layers of the Earth are consisted of more lightweight silicate materials which surfaced as the Earth became cooler and solid. Different materials are formed during magma cooling². Exposition of these materials to erosion and transportation resulted in formation of sedimentary rocks – clay, sandstone etc. Another modifications could be passed under high pressures and temperatures.

In nature silicon can be never found free. It is always oxygen compound and primarily its coordinate number is 4. Basic group of these materials is SiO₂ and in the structure it could be found isolated, connected into chains, cycles, layers or three-dimensional structures.

Silicon dioxide (silica) is maybe the most investigated chemical compound – anyway after water [4]. Over twenty of silica phases exist and over ten of polymorphous forms of pure silica. However, the most frequent form is α -quartz, which is the main mineral component of rocks like granite or sandstone. In pure forms α -quartz is contained in crystal, alternatively impure α -quartz is amethyst, false topaz, etc.

Groupings of tetrahedrons {SiO₄}, which share joint vertex, create main crystal modifications of silica. The most thermodynamically stable form of silica in range of normal temperatures and common pressures is α -quartz. In this material the tetrahedrons are formed into helical chains. α -quartz could be transformed into β -quartz by an action of temperatures about 573°C. β -quartz has similar helical structure as α -quartz, but the structure is not so deformed as in α -quartz (angle O-Si-O is changed from 140° to 155° as showed in Fig. 1). Reaching temperature around 867°C the β -quartz is transformed into β -tridymite. During this process original Si-O bonds disappear and tetrahedrons {SiO₄} are rearranged into new hexagonal structure of β -tridymite. This structure is meta-stable, i.e. cooling less than 120°C transforms β -tridymite into stable α -tridymite – showed in Fig. 2.

¹ e.g. olivine (Mg,Fe)₂SiO₄

² Aproximate sequence of formation of crystalline minerals during the cooling of magma was compiled by N.L.Bowen: olivine, pyroxene, amphibole, biotite, orthoclase, muscovite, quartz, zeolites and hydrothermal minerals.

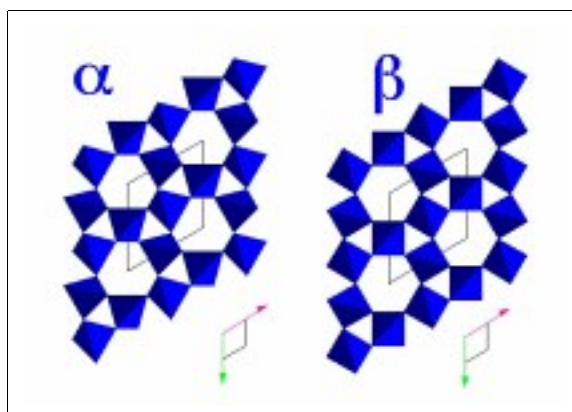


Fig. 1: Models of structure of α -quartz and β -quartz. (Borrowed from [5])

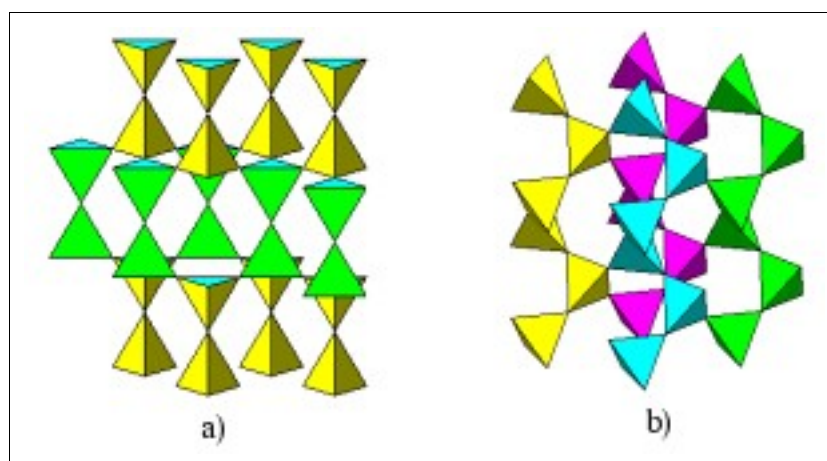


Fig. 2: Models of a) α -tridymite and b) α -quartz. (Borrowed from [6])

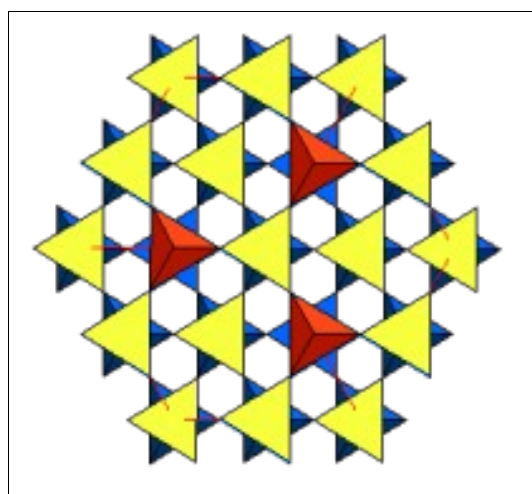


Fig. 3: Structure of α -cristobalite. (Borrowed from [7])

Vice versa heating the material over 1470°C could slowly transform β -tridymite into β -cristobalite, which can hold its structure as a metastable phase. β -cristobalite could be transformed into α -cristobalite (Fig. 3) by cooling down less than 200°C . Heating above a temperature of 1713°C under normal pressure fuses the material into liquid silicon dioxide. Processes are lucidly shown in Fig. 4.

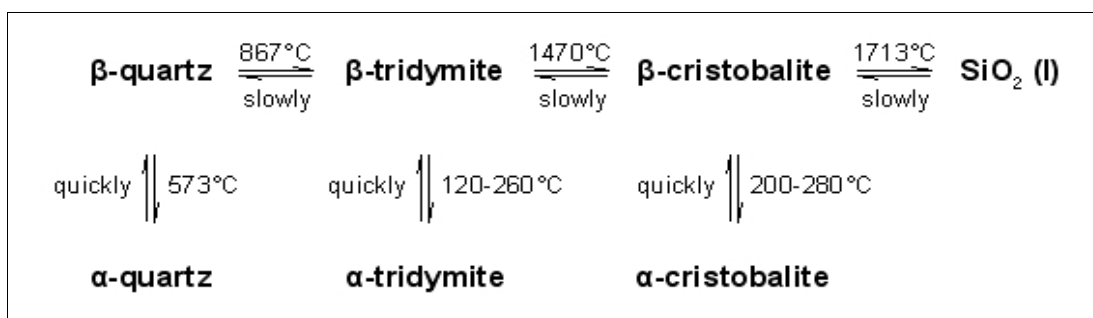


Fig. 4: Relations between crystal modifications of silica. (Reprinted from [4])

In contrast to above-mentioned crystal modifications forms of silica described in this work are amorphous.

Among earthy forms the diatomaceous earth (kieselguhr) and diatomite predominate. These rocks had been formed from shells of dead micro-organisms for millions of years. These organisms such as diatoms (shown in Fig. 5) or sponges are capable of synthesising biogenic silica *in vivo* [8, 9].

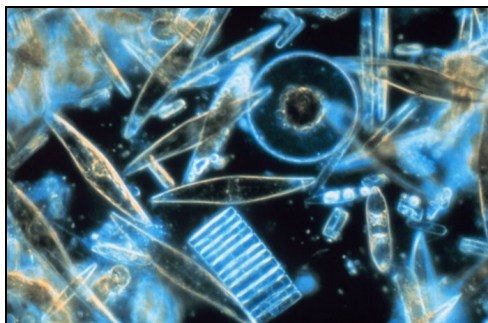


Fig. 5: Picture of diatoms through the microscope. (Borrowed from [8])

Silica is chemically resistant to all acids with the exception of fluorine acid (HF). It slowly dissolves in hot concentrated solutions of hydroxides of alkali metals and more rapidly in molten hydroxides or carbonates of alkali metals. In this process the silicates of relevant metal are obtained. From halogens, only fluorine easily attacks a molecule of silica under formation of silicon fluoride and oxygen.

The reactions of silica with metals are mainly used in glass and pottery technologies. Reactions under which the soluble sodium silicate and potassium silicate are formed are

also significant¹. Acquired soluble glass is dissolved in hot water under pressure. Solid particles of insoluble glass are filtered.

Watered-down solutions are used for preparation of silicate gels by acidulation. Acquired silica gel is amorphous form of silicon dioxide with very porous structure and large specific surface. After exsolution the silica gel is ridded of remaining electrolyte and finally the dust is dehydrated by calcination or by nebulization in hot air.

Silica gel is chemically inert and non-toxic. That is the reason of its wide usage in cosmetics or food industry as an anti-sinter agent. Moreover, silica gel is used as a part of flatting varnishes. Its applications as desiccant are also well-known.

Ultrafine silica² is produced by hydrolysis of silicon chloride under high temperatures in oxygenic flame of special burners. Production is described in chapter 1.1.2.

1.1 Preparation of nano-scaled silica particles

From a technological point of view, it is highly difficult to prepare nano-scaled particles by simple milling. The main problem is a broad distribution of particle sizes. Therefore the techniques of preparing small particles from their chemical precursors are used in practise. They allow a controlled growth of the particles and their aggregates. The methods how to prepare nano-scaled silica particles can be divided into two processes, “wet” and thermal.

1.1.1 “Wet” processes

In industry the mostly applied process, which take place in liquid state, is the preparation of silica gel by acidulation of aqueous solution of sodium silicate, which is made from sand. The advantage of this technique is the relatively low cost. However, the disadvantages are a various level of contamination by alumina and also the relatively wide distribution of particle sizes.

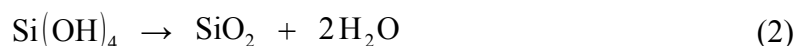
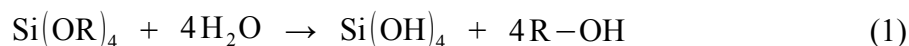
For preparing suspensions of particles with narrow distribution Stöber et al. [10] developed method often used for laboratory preparation of silica powder. This is the only method used for preparing nano-particles in studied literature, which deals with preparation and characterisation of fine silica. It consist in finding that the final particle size can be clearly determined by the concentration of water and ammonia in ethanol. Stöber method of preparation is based on a hydrolysis of tetraethers of silicic acid (tetraalkyl silicates) in

1 These reactions run in glass furnace where sand is fused with relevant carbonate at 1400°C

2 Often called pyrogenic or fumed silica

alcohol (methanol, ethanol) as medium under catalysis of ammonium and water. Firstly, the saturated ammonia solution in alcohol is prepared and mixed with water, consequently the alkyl silicate is added. The mixture is stirred or inserted in a water bath under ultrasonic vibrations. First part of the reaction (the hydrolysis under formation of silicic acid) is invisible. The observable part of the process is the condensation of silicic acid indicated by an increasing opalescence and led to turbid white suspension of silica. This process takes about two hours. Table in appendix A2 shows experimental arrangements, final median diameter and geometric standard deviation of silica spheres obtained by Stöber.

Bogush et al. [11] followed in Stöber research by elaborate a method of silica powder preparation from tetraethyl orthosilicate (TEOS). They prepared monodisperse particles in sizes around 40nm. Two equations which describe the hydrolysis and condensation are:



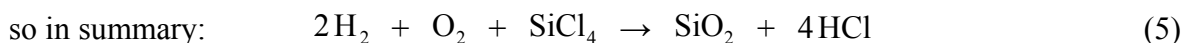
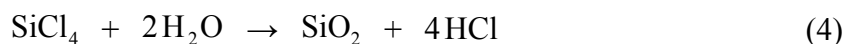
It was found that five factors influencing the size of final particles, namely concentration of TEOS, ammonia and water, type of alcohol used as the solvent and reaction temperature. Suspension of silica prepared by “wet” processes can be finally centrifuged and then desiccated or additionally treated before drying.

1.1.2 Thermal processes

The largest part of silica nano-particles production is taken by thermal processes, in spite of fact that detailed research of controlled growth of silica in suspensions was done.

Industrially the most used method of fine silica particles producing was developed for German chemical company Degussa AG by its researchers led by H. Kloefer [12]. This process uses silicon tetrachloride as silica precursor. It is produced by action of gaseous chlorine in fused metallic silicon. SiCl_4 is liquid with boiling point 57.6°C . Chloride vapour is mixed with oxygen and this gaseous mixture is combusted with hydrogen by special burners. This process carries several advantages. By varying the concentration of reactants, temperature of combustion and also dwell time of generated dust in burner chamber, it is possible to control the size of forming silica particles such as the surface properties [13]. Thermal hydrolysis of silicon tetrachloride allows the formation of mono-disperse particles with easily removable by-product (hydrochloric acid) and practically no contamination by reagents.

Reaction under which the fumed silica is created could be characterised by these equations:



Arrangement of production line¹ of fumed silica could be as showed in Fig. 6.

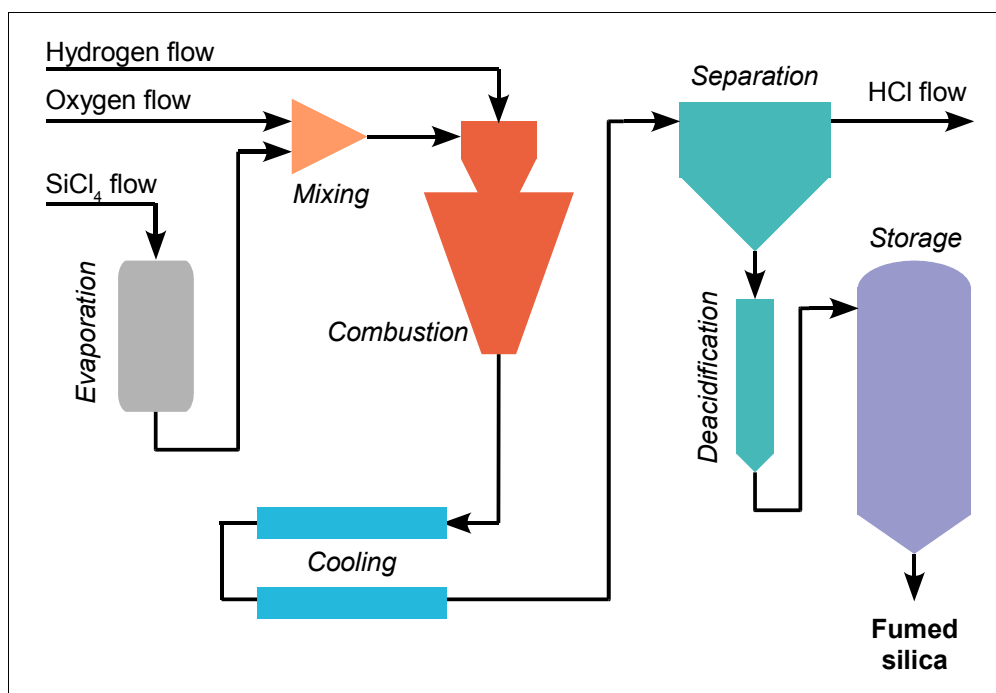


Fig. 6: Production of fumed silica – flow chart.

In literature which deals with polymer composites containing nano-scaled silica particles this filler is not prepared in laboratory but it is practically always purchased. Primarily it is one of a product line AEROSIL[®] developed and distributed by Degussa AG. The others are Sigma-Aldrich, Cabot corp. and other companies. These commercial products are used as purchased or firstly treated as described in chapter 1.2. Some technical data sheets of frequently used nano-dusts are included in Appendix A3.

In addition to preparation by combustion of silicon tetrachloride, there are other methods how to achieve fine silica powder, namely preparation in plasma flow or by an act of an electric arc. Some of them were studied for example by Balabanova [14, 15]. Wypych [16] mentions existence of “fused silica”, what is also a type of nano-dust. However, in articles studied in this thesis these types are not used. Therefore, only the fumed or precipitated silicas are presented.

¹ Presented chart is based on production line used by Degussa AG for producing AEROSIL[®] [12]

1.1.3 Hollow particles

Special case of silica nano-particles is hollow spheres or core-shell type particles. Techniques of their preparation have been intensively investigated. However these particles are not generally used as polymer fillers and only one method dealing with polymers is outlined.

Nano-sized hollow spheres are very important as extremely small containers, carriers, and reactors for encapsulation and micro-reactions in nanotechnology. Zhang et al. described in his work [17] the method of synthesis of these nano-sized hollow silica nano-spheres with a hole (commonly denoted as silica nano-bottles) by thermal destruction of polymer nano-particle used as template. This functional polymer particles was prepared by emulsion copolymerization of styrene (as major monomer) with (ar-vinylbenzyl)trimethylammonium chloride (as secondary monomer) which afford the quaternary ammonium species and with cross-linker – 4,4'-isopropylidene diphenol bimethacrylate.

The basis of the polymer particle preparation was studied by Chen et al. [18]. They use emulsifier-free emulsion of monomers and deionized water in nitrogen atmosphere. The reaction takes about twelve hours (for more see [17] and [18]).

The result of Zhang synthesis was cross-linked polymer nano-spheres with a uniform size of about 45 nm. Subsequently the silica nano-bottles were synthesised by adding dropwise TEOS into mixture of previously prepared polymer latex with ammonia in water under intense stirring. Prepared mixture was finally heated in autoclave at 100°C for 3 days. Afterwards the powder was washed and dried at normal temperature. Finally, polymer templates were removed by calcination at 550°C for 5h. The scheme of the entire process is in Fig. 7.

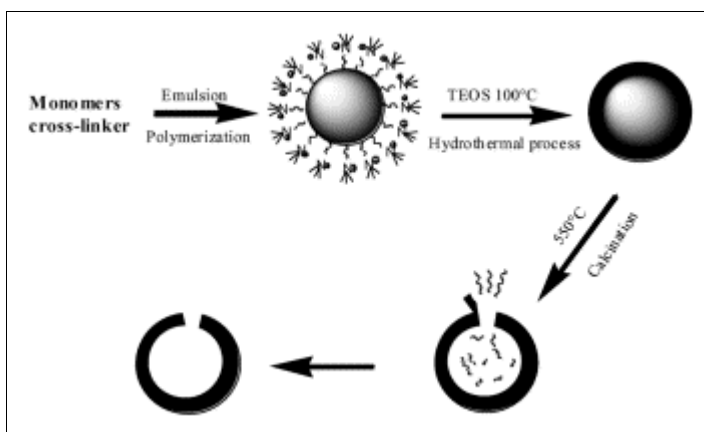


Fig. 7: Scheme of silica nano-bottle preparation. (Borrowed from [17])

1.2 Modifications of silica

Freshly-produced nano-particles prepared by thermal or “wet” process always carries hydroxyl groups bonded on silicon atom – called silanol group, which causes of characteristic properties. One of these properties is the ability of the spheres to connect by hydrogen bonds, but the more important is high air moisture absorption [12]. This hydrophilic character is attributed to the silanol groups whose “water attractiveness” can be affected by their mutual interactions as mentioned in [12]. Mutual interaction is related to particle diameter what was studied by Iijima et al. [19]. Following types of silanol groups and their interactions are distinguished:

1. Free silanol groups
2. Geminal silanol groups
3. H-bridged silanol groups
4. Siloxane groups

These types are clearly showed in Fig. 8. Fig. 9 shows ideas of Iijama et al. – the influence of particle size on silanol interactions.

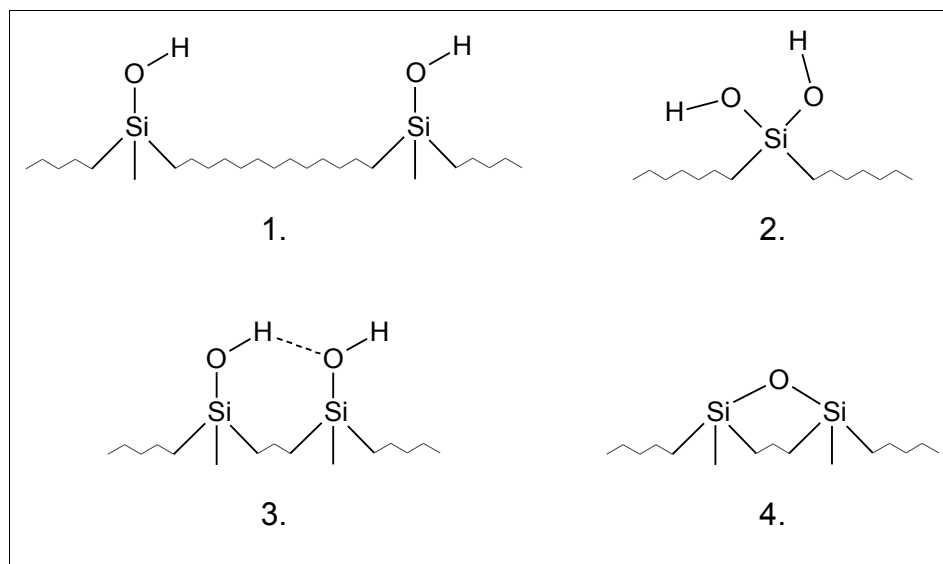


Fig. 8: Interactions between silanol groups: 1. free groups, 2. geminal group, 3. bridged groups, 4. siloxane group. (Reprinted from [12])

In the literature, the silica dust is often dried before use. Also numerous chemical reactions with fumed or precipitated silica have been described to make it hydrophobic. Some modifications from the simplest introduction of water repellent groups to the functionalization of the spheroids are described in this chapter.

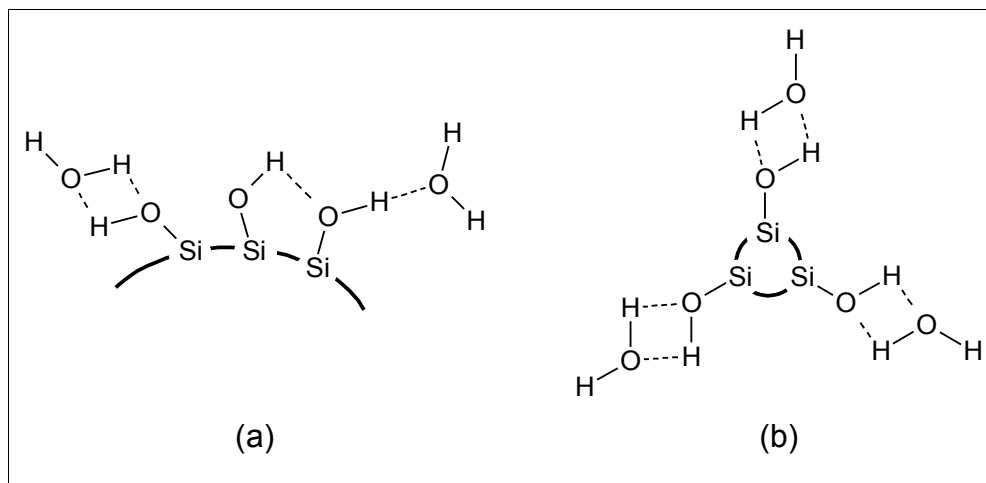


Fig. 9: The effect of particle curvature on surface silanol structure and the accessibility of water molecules. (a) bridged groups, (b) isolated groups. (Reprinted from [19])

1.2.1 Hydrophobization of nano-silica surface

Studied methods are based on the “elimination” of hydroxylic groups or on covering them by another water-repellent groups. In most cases it is organic molecule bearing silicon atom with bonded atom (usually chlorine) or functional group capable to substitute the silanol hydrogen with the “organic silicon”. Generally showed in Fig. 10.

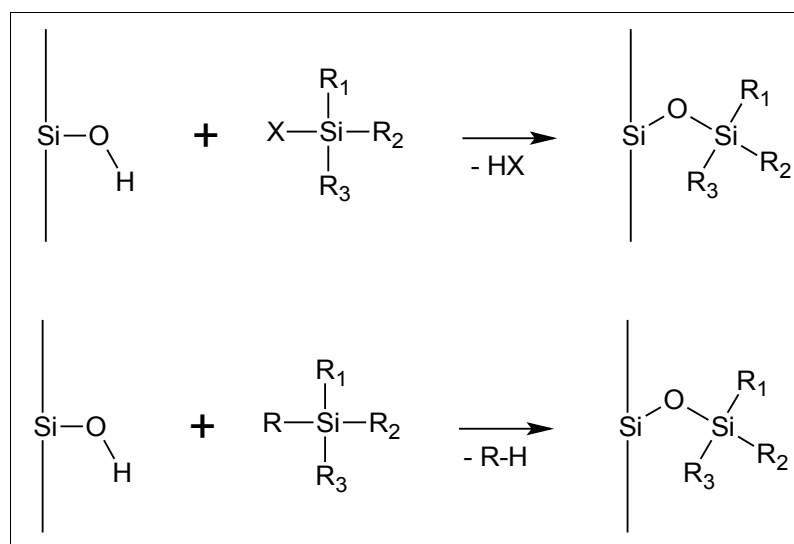


Fig. 10: Substitution of silanol hydrogen by organic silicon.

This molecules are denoted as silane coupling agents or grafting molecules. They are widely used for both the hydrophobization and the functionalization of the surface.

The simplest modification of fumed silica is the act of chlorotrimethylsilane, usually done in the same time as the silica is processed. The reaction is analogical to reaction showed in Fig. 10, where R_1 , R_2 and R_3 are methyl groups and X is chlorine. This powder is

produced by Degussa AG under name AEROSIL® R202, and no similar product can be found in Sigma-Aldrich catalogue. Fig. 11 shows the dramatical difference between natural fumed and treated silica.



Fig. 11: The difference between hydrophilic silica and hydrophobic silica silylate (the amount of water and dust is always the same). (Borrowed from [20])

If dichlorodimethylsilane or trichloromethylsilane is used, the more complicated structures and bondings parallel to particle surface arise (for details see [12] or [20]).

Besides reactions eliminating hydrogen chloride another reactions was studied. They are mainly based on esterification of the silanol group. For example Bagwe et al. [21] or Takahashi and Paul [22] used triethoxysilane as coupling agent of the amine. The substance of the process is hydrolysis and consequent reaction of *in situ* prepared alcohol with the particle surface as showed in Fig. 12. Ossenkamp et al. [23] points out that the esterification is equilibrous reaction and it is realised firstly by adsorption of the alcohol on the surface with H-bridge interaction and then by elimination of water molecule.

Shimada et al. [24] used 2-propenyl(3-chloropropyl)dimethylsilane (Fig. 13) as coupling agent with small tendency to hydrolysis than alkoxyhanes or else mentioned organosilicons.

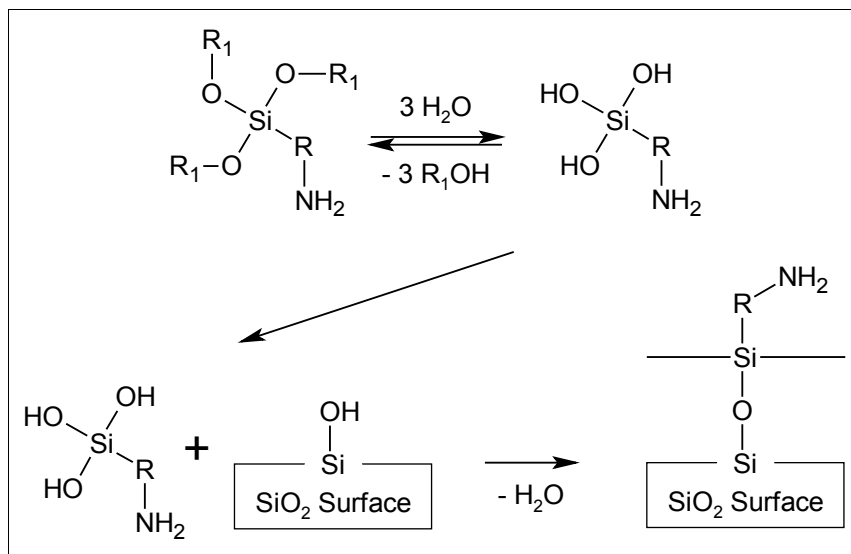


Fig. 12: Esterification of the particle surface. (Based on schemes in [21], [22])

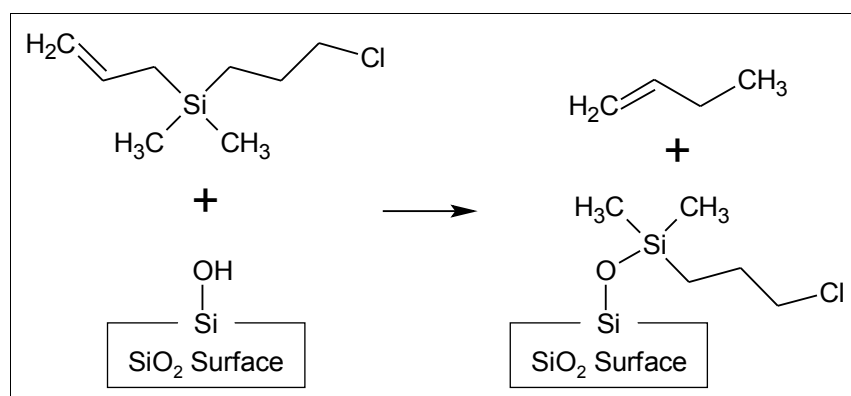


Fig. 13: Reaction studied by Shimada et al. (Based on schemes in [24])

Last two presented modifications are rather functionalizations than simple hydrophobizations because of the more specific substituents such as amino group or halogen. Linking up concrete molecules on silica particle surface made it more “related” to polymer matrix (as in cases of polymer grafted silica). In many examples this treatment improves mechanical properties of the composite, stability of the particle in matrix, or inner structure of the material what can be demonstrated for example by diverse gas permeation [22].

1.2.2 Functionalization of nano-silica surface

In relation to previous subhead, the desiderative molecules or functional groups are bonded on nano-spheres mainly by silane coupling agents. The functionalization of surface is also called grafting and bonded molecule is grafted molecule. This curing is done mainly to improve adhesion and stability in the matrix or to make the nano-particle polymerisation nucleus as demonstrated on following cases.

El Harrak et al. [25] modified surface by consequent reactions in stable colloidal medium to bond an initiator of polymerisation with particles. By this it was achieved the embedment of the filler to the matrix. The entire procedure takes place in dimethylacetamide. Also washing the suspension between single steps is done in colloid state to prevent irreversible particle aggregation. The first step is silanization with markaptopropyl triethoxysilane. Following second step is over-grafting reaction of the 2-bromoisobutyrate. The process is schematized in Fig. 14.

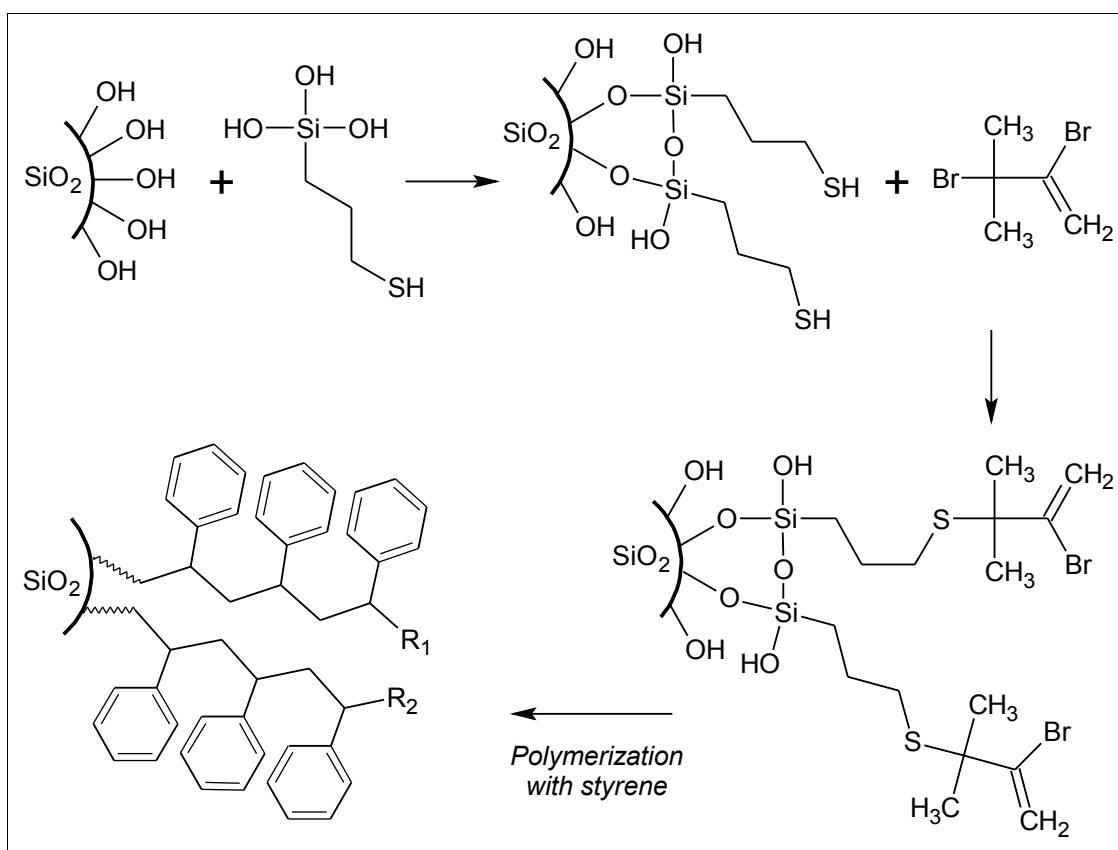


Fig. 14: Silica surface treatment studied by El Harrak et al. (Scheme based on [25])

The advantage of this technique is the ability to adjust the degree of grafting, which can be between 0.5 and 5 graft molecules on square nanometre. Finally, prepared particles were mixed with monomer (styrene) in which they initiated polymerisation.

Avella et al. [26] described surface cured silica acquired by reactions similar to El Harrak's. Silica in [26] was prepared by precipitating method mentioned in chapter 1.1.1. Avella used γ -aminopropyl triethoxysilane hydrolysed in water. The suspension of silica in ethanol was added to hydrolysed γ -aminopropyl triethoxysilane with mechanical stirring and the mixture was kept at 70°C for 24 hours. Consequently, the particles were dried at 80°C. The grafting reaction was done by mixing of solutions of the modified silica in chloroform and hexamethylenediisocyanate in chloroform. Final blend was stirred at room temperature

for another 24 hours. Finally this colloid was immersed dropwise to a solution of hydroxyl terminated poly(ϵ -caprolactone) – abbreviated as OH-PCL-OH, with low M_w (about 10,000 $\text{g}\cdot\text{mol}^{-1}$) in chloroform and additional 24 hours was given to the reaction.

The composite material was prepared by melting of new particles with poly(ϵ -caprolactone) with M_w about 60,000 $\text{g}\cdot\text{mol}^{-1}$ inside a mini-extruder operating at 150°C with a single mixing screw.

In Fig. 15 there is schematized processing of the poly(ϵ -caprolactone) grafted silica.

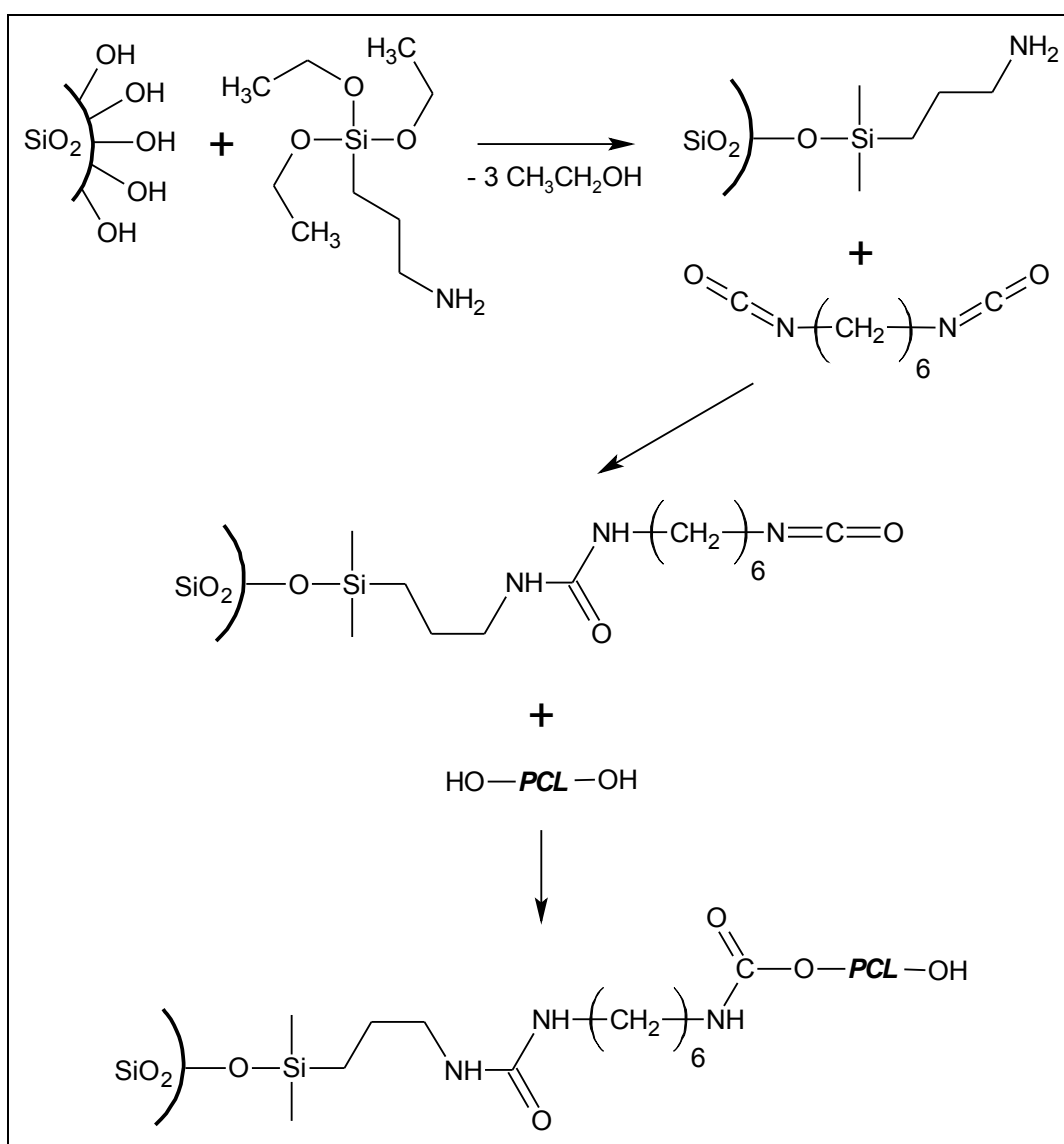


Fig. 15: Grafting poly(ϵ -caprolactone) on silica surface. (Scheme based on [26])

As it was mentioned previously there is possibility to bond the particle on the polymer chain. Takahashi and Paul [22] showed introduction of amino groups on silica surface. This modified material was mixed with polymer denoted as ULTEM® 1000 from GE Plastics (what is poly(ether imide)). The result is disruption of the cycle in main chain and grafting the particle (see Fig. 16).

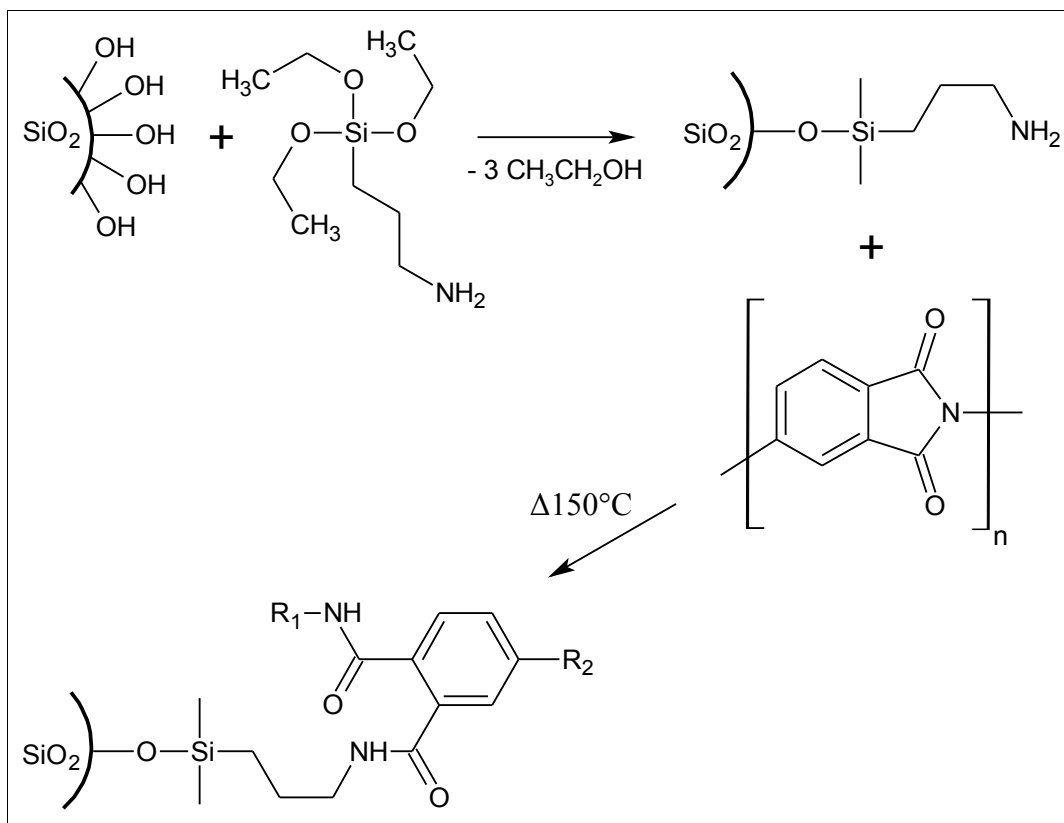


Fig. 16: Grafting of silica onto poly(ether imide) chain. (Scheme based on [22])

There are many other types of grafted silica, but almost always the basis is the reaction of substituted silane, which introduce another reactive group.

To the contrary, there are studies of grafting silica by more complicated chains and organic molecules not only to improve the fixation in polymer, but to introduce some decomposable groups for example in foaming procedures [27] or to compatibilize the surface of synthetic polymer matrix with inner environment of organism [28].

Another method how to couple the silica nano-particles to polymer could be irradiation of suspension of silica dust in liquid monomer by γ -ray as Rong et al. presented in [29]. Obtained system also contains some amount of unbounded chains of homopolymer beside grafted particles. This method is rare in studied literature and is not evolved here.

2 POLYMERS FILLED WITH NANO-SCALED SILICA

In this chapter the concrete nanocomposite systems are described. As it was touched on in introduction of this thesis, only several polymer matrices are included because of the huge amount of commercially available types. The selection was based on both the number of published articles of the specific resin and the commercial importance too.

2.1 Polyethylene/silica

Kontou and Niaounakis [30] focused their study on polymer matrix which takes about third of worldwide plastic production. They studied the influence of filling on properties of linear low density polyethylene (LLDPE). They investigated two matrices prepared by different methods – one by metallocene (abbreviated as mLLDPE) and second by traditional Ziegler-Natta (zLLDPE) catalysts. The filler was commercial product Aerosil® R972 – silica with surface modified by dimethyldichlorosilane. The impact of concentration of particles of diameter 16 nm was investigated.

Five blends were made of silica content from 2 wt% up to 10 wt%. Mixing was done in Brabender mixer at 170°C and rotation speed of the screw was 40 rpm. The silica powder was added to melted polymer in several small doses to achieve better dispersion. Finally the samples were compression moulded at 130°C.

Micrographs of the surface was obtained by scanning electron microscope. In Fig. 17 – 20 can be seen, that silica in mLLDPE creates larger agglomerates than in zLLDPE. Thermal properties was measured by DSC and obtained values are in Table 1. Dynamical mechanical result were obtained in terms of storage and loss modulus – plotted in Fig. 21 – 24 and summarised in Table 2. Moreover tensile stress-strain tests were done with results presented in Fig. 25 – 28 and Table 3.

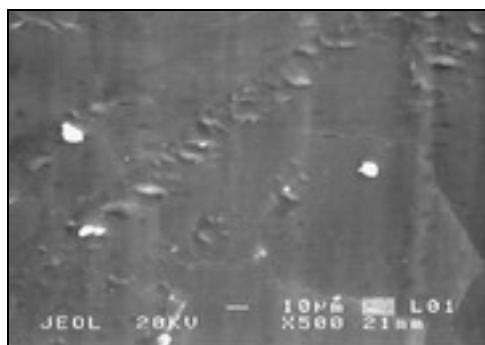


Fig. 17: SEM micrograph of the mLLDPE/SiO₂ nanocomposites with the silica content of 4 wt%. (Borrowed from [30])

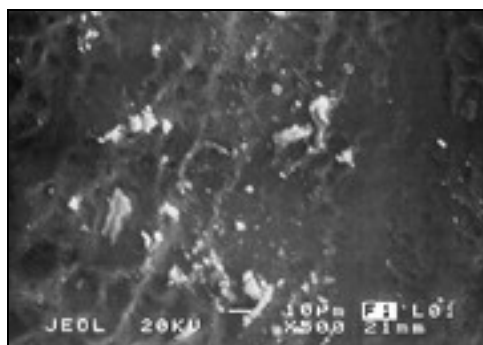


Fig. 18: SEM micrograph of the mLLDPE/SiO₂ nanocomposites with the silica content of 8 wt%. (Borrowed from [30])

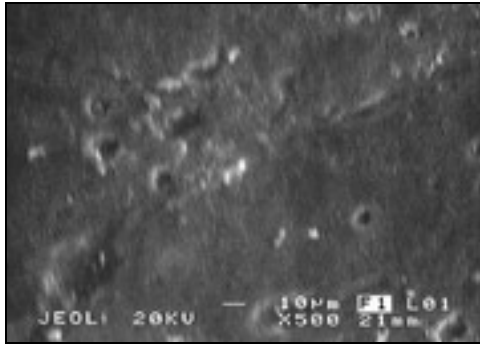


Fig. 19: SEM micrograph of the zLLDPE/SiO₂ nanocomposites with the silica content of 4 wt%. (Borrowed from [30])

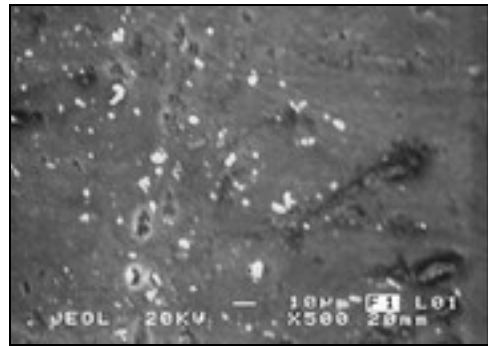


Fig. 20: SEM micrograph of the zLLDPE/SiO₂ nanocomposites with the silica content of 8 wt%. (Borrowed from [30])

Table 1. Obtained DSC data (Reprinted from [30])

Sample type (nano-SiO ₂) (wt%)	mLLDPE/SiO ₂				zLLDPE/SiO ₂			
	T_m (°C)	ΔH_m (J/g)	x_c (%)	T_g (°C)	T_m (°C)	ΔH_m (J/g)	x_c (%)	T_g (°C)
0	103.0	100.8	34.8	-40	127.1	113.7	39.2	-50
3	101.7	114.5	39.5	-30	125.0	119.0	41.0	-40
4	105.0	116.3	40.1	-30	126.1	116.3	40.1	-30
6	104.0	103.5	36.7	-30	125.8	110.3	38.0	-25
8	103.3	97.2	33.5	-40	123.8	108.8	37.5	-25
10	103.3	84.6	29.2	-15	126.4	103.6	35.7	-20

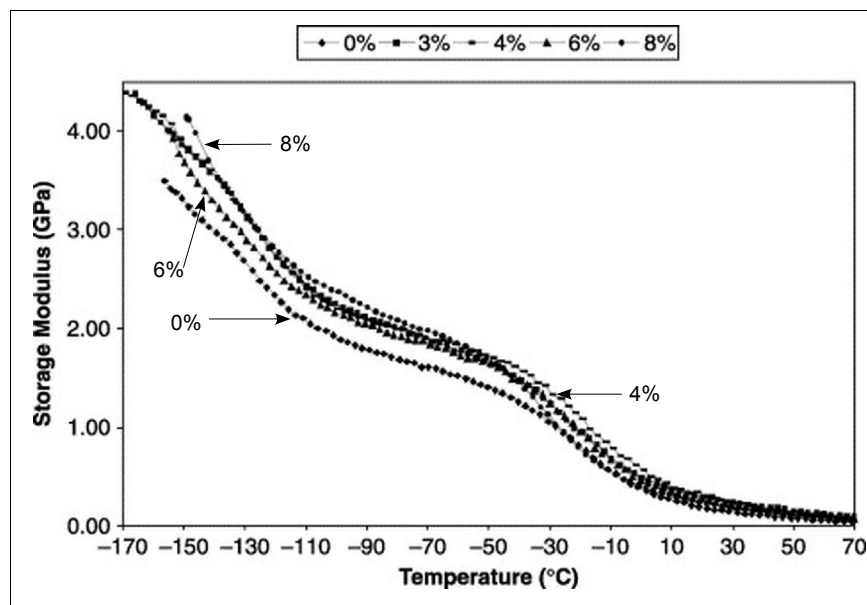


Fig. 21: Storage modulus (E') dependence on temperature of the mLLDPE/SiO₂ nanocomposites at frequency of 1 Hz. Percentages are percent by weight of particles load. (Borrowed from [30])

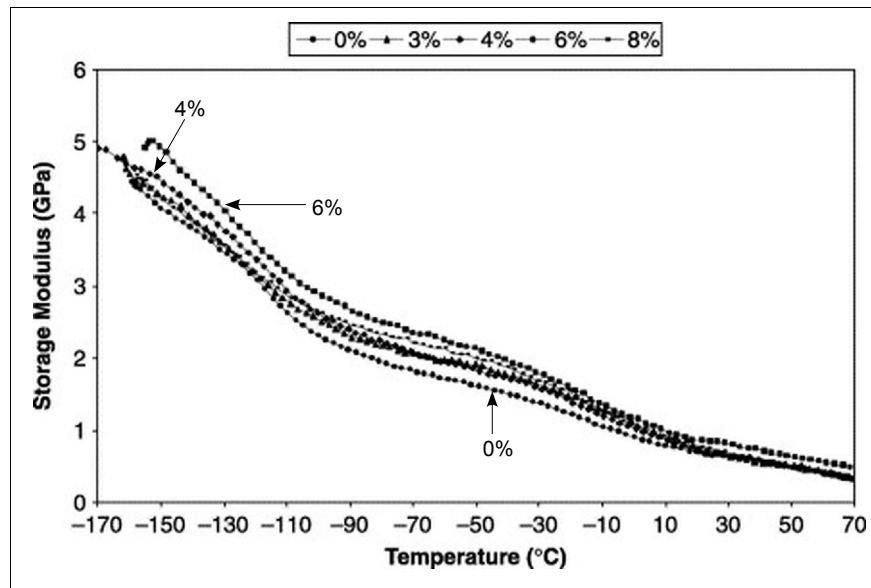


Fig. 22: Storage modulus (E') dependence on temperature of the zLLDPE/ SiO_2 nanocomposites at frequency of 1 Hz. Percentages are percent by weight of particles load. (Borrowed from [30])

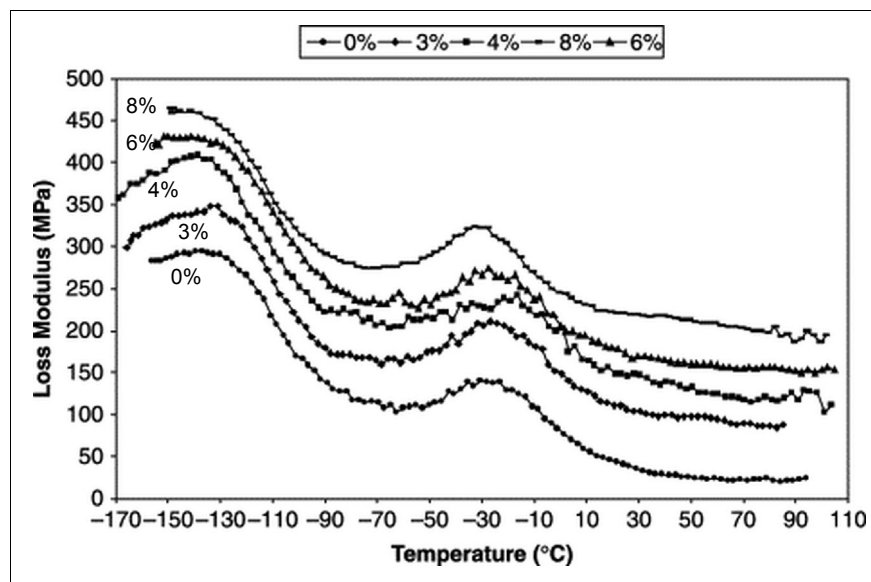


Fig. 23: Loss modulus (E'') dependence on temperature of the mLLDPE/ SiO_2 nanocomposites at frequency of 1 Hz. Percentages are percent by weight of particles load. The curves are shifted in the y-direction to make them distinguishable. (Borrowed from [30])

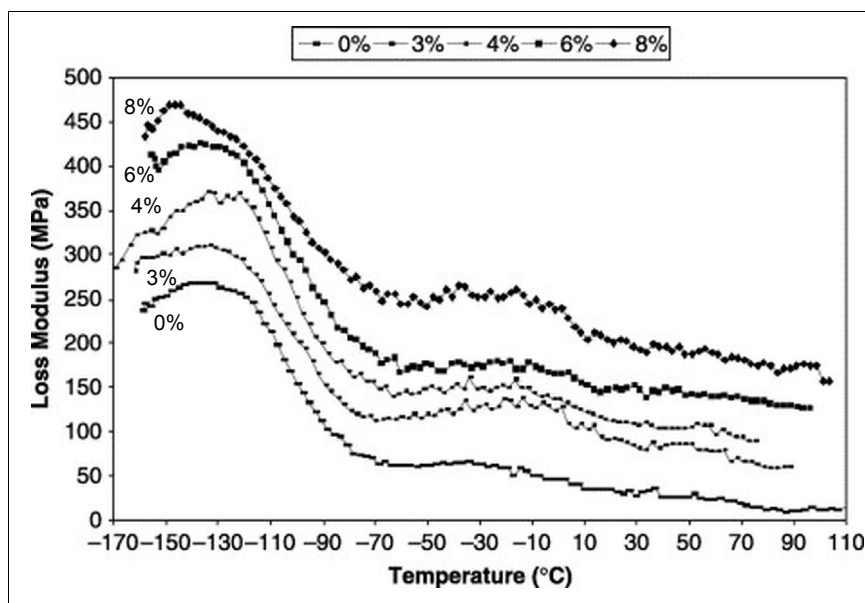


Fig. 24: Loss modulus (E'') dependence on temperature of the zLLDPE/SiO₂ nanocomposites at frequency of 1 Hz. Percentages are percent by weight of particles load. The curves are shifted in the y-direction to make them distinguishable. (Borrowed from [30])

Table 2. DMA results (Reprinted from [30])

Sample type (nano-SiO ₂) (wt%)	mLLDPE/SiO ₂ loss modulus				zLLDPE/SiO ₂ loss modulus			
	peak position (°C)		peak position (MPa)		peak position (°C)		peak position (MPa)	
	T_{γ}^1	T_{β}^2	T_{γ}	T_{β}	T_{γ}	T_{β}	T_{γ}	T_{β}
0	-136	-30	0.29	0.14	-139	-40	0.32	0.12
3	-135	-26	0.32	0.21	-136	-28	0.33	0.16
4	-135	-20	0.39	0.23	-135	-29	0.27	0.17
6	-137	-22	0.34	0.18	-137	-31	0.30	0.11
8	-145	-32	0.31	0.17	-145	-37	0.39	0.17
10	-147	-31	0.28	0.18	-142	-22	0.40	0.16

- 1 T_{γ} – γ -transition temperature. The γ -transition could be cooperative angular motion to give local configurational changes. It is relative to glass transition.
- 2 T_{β} – β -transition temperature. This transition is related to side chains motion and in case of PE it is similar to the glass transition.

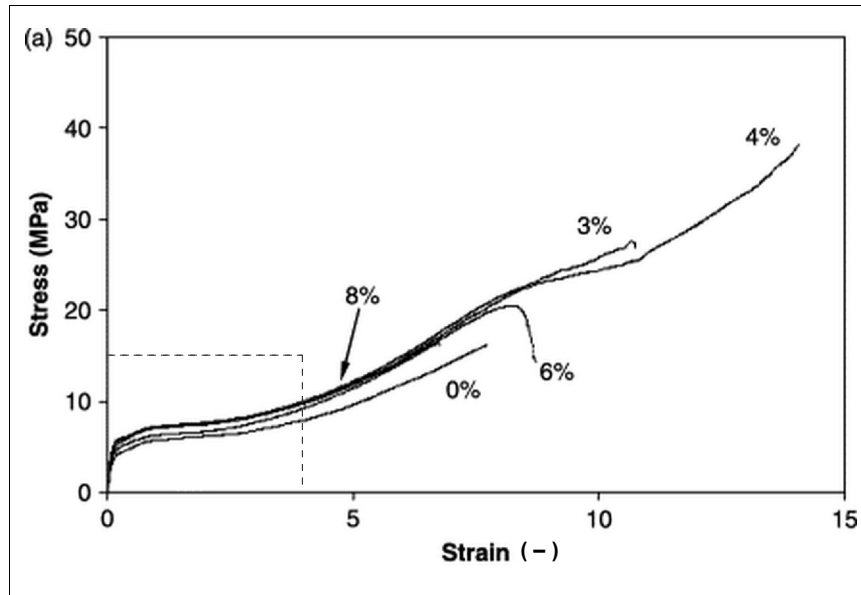


Fig. 25: Tensile stress–strain curves of the mLLDPE/SiO₂ nanocomposites. Percentages are percent by weight of particles load. (Borrowed from [30])

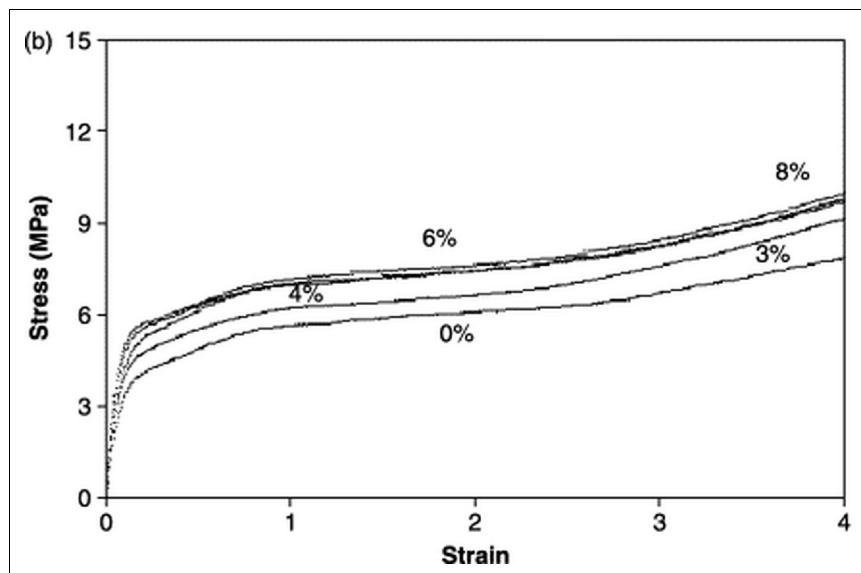


Fig. 26: Tensile stress–strain curves of the mLLDPE/SiO₂ nanocomposites in the low strain range – detail indicated by rectangle in Fig. 25. Percentages are percent by weight of particles load. (Borrowed from [30])

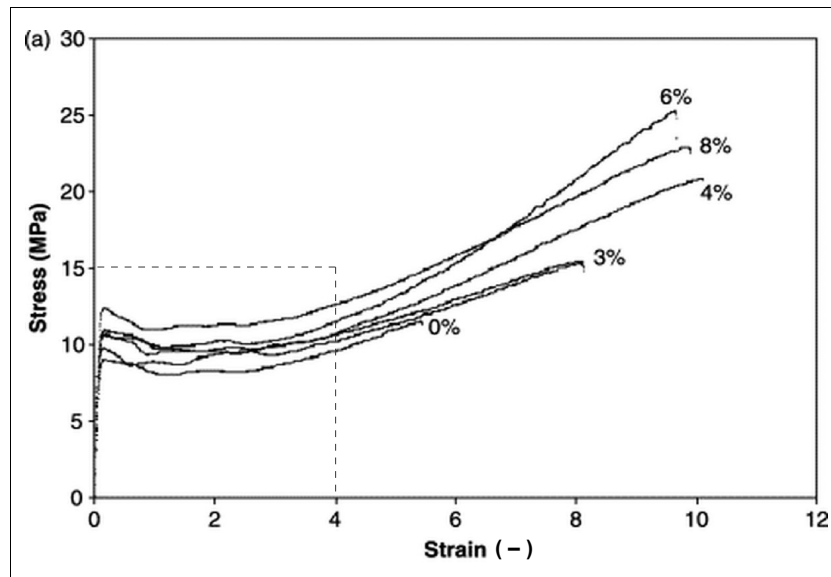


Fig. 27: Tensile stress–strain curves of the zLLDPE/SiO₂ nanocomposites. Percentages are percent by weight of particles load. (Borrowed from [30])

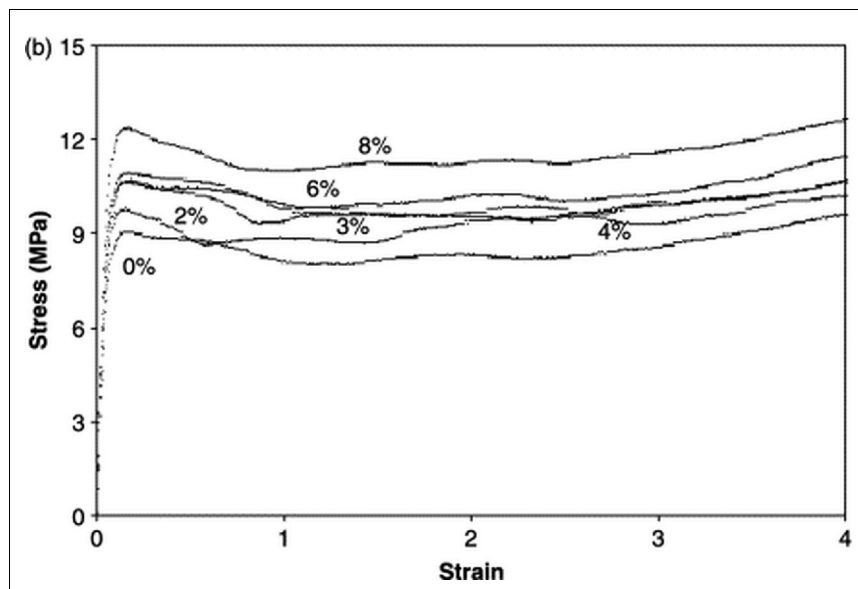


Fig. 28: Tensile stress–strain curves of the mLLDPE/SiO₂ nanocomposites in the low strain range – detail indicated by rectangle in Fig. 27. Percentages are percent by weight of particles load. (Borrowed from [30])

Table 3. Tensile properties (Reprinted from [30])

Sample type (nano-SiO ₂) (wt%)	Elastic modulus (MPa)	Yield stress (MPa)	Strain at break (-)	E_c/E_m^1 (-)	Elastic modulus (MPa)	Yield stress (MPa)	Strain at break (-)	E_c/E_m (-)
0	51	3.7	7.8	1.00	230	10.5	5.5	1.00
3	55	4.2	10.8	1.23	237	11.0	8.1	1.03
4	70	5.0	14.0	1.36	240	9.0	10.0	1.04
6	82	5.4	8.3	1.61	245	11.0	9.5	1.07
8	103	5.5	11.0	2.03	280	12.9	9.6	1.22
10	65	7.2	9.0	1.28	153	10.8	9.0	0.66

Acquired data confirm that low fraction of filler can rapidly change properties of original matrix. Optimum in case [30] was established as 4 wt% of SiO₂, what is considerable difference between the amount of particles in microscopic range. As Kontou and Niaounakis mentioned, 20 wt% filling with micro-sized silica is needed to achieve similar performance. Also was learnt that silica content more than 8% is detrimental to the properties of the LLDPE composites. Finally it was concluded that nano-fillers do not only increase the stiffness of the LLDPE matrix, but also modify morphology and introduce new energy-dissipation mechanisms.

Besides LLDPE there is another “special” type of PE – the high density polyethylene (HDPE). This material was filled with silica in Zhang's et al. work [31]. In this paper, dependence of silica content in matrix was not investigated – in all samples the weight concentration of modified nano-dust was 0.75 wt%. This amount was chosen on the basis of previous researches (namely [29] and [32]), where the very effective modifications were observed at fillings up to 2 wt%, as Zhang interjected.

The particles were at mean diameter 10 nm and they were grafted by several polymer chains, which were synthesised *in situ*. Whole process is similar to [29] or [32] – silica was suspended in monomer and this system was irradiated by γ -rays to initiate the polymerisation and also to activate the particle surface, what leads to bonding onto forming chains. Styrene, butyl acrylate, methyl methacrylate and butyl methacrylate were used as monomers. Modified nano-dust was consequently mixed with HDPE in high speed blender and obtained material was extruded by twin-screw extruder at approximately 190°C. Prepared masterbatch was injection moulded into testing shapes.

1 Fraction of modulus of composite (E_c) to modulus of pure matrix (E_m)

Accomplished tests confirmed that filling HDPE with silica can be an effective way how to improve some matrix properties. These improvements strongly depended on the nature of grafted chains as can be seen in Fig. 29 or in Fig. 30.

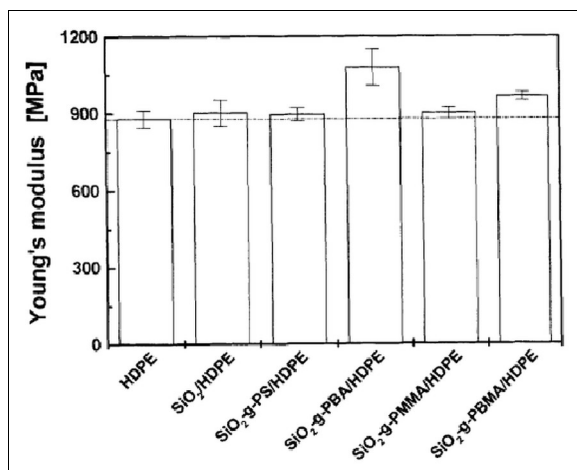


Fig. 29: Young's modulus of HDPE reinforced by different modifications of silica (Borrowed from [31])

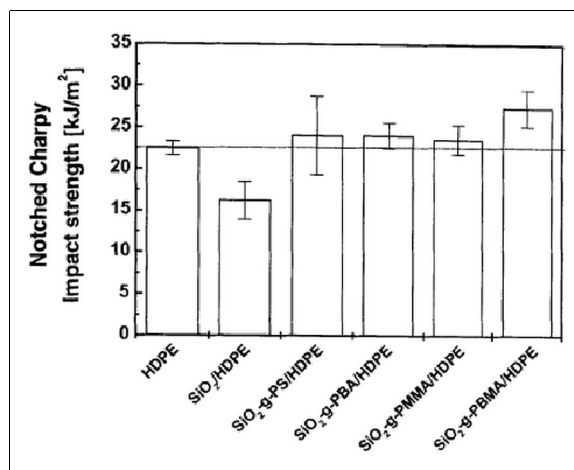


Fig. 30: Notched Charpy impact strength of HDPE reinforced by different modifications of silica (Borrowed from [31])

2.2 Polypropylene/silica

Ones of firsts who investigated the preparation and qualities of polypropylene filled with nano-sized silica was Rong et al. [29]¹ and Wu et al. [32].

An isotactic polypropylene homopolymer was filled with polystyrene grafted silica and also poly(ethyl acrylate) grafted silica particles [32]. The used nano-dust was at mean size of 15 nm. The silica was grafted onto forming chains during the process of *in situ* polymerisation initiated by γ -rays irradiation. Then the obtained particles were mixed with small amount of iPP and consequently the masterbatch was diluted with neat PP in twin-screw extruder. Pellets were injection moulded into shape of testing bars.

Tensile properties were investigated (Fig 31). A broad study of the morphology of the fracture surface was done. Several micrographs are here presented (Fig. 32, Fig. 33). As it can be seen, the unfilled PP has relatively smooth fracture surface in contrast to filled ones. Surface of PP/SiO₂ is more rough and only small plastic deformations could be found. Composites prepared from modified particles has dramatically different fracture morphology – huge amount of fibrils is observed as in Fig. 32 (d) and (e). When the filler load approaches value of about 2.7 vol% a number of cavities appear on the surface of PP/SiO₂ what is caused by debonding of the untreated particles. Grafted silica creates agglomerates surrounded by the concentric fibrillar matrix (pointed by upper arrow in Fig. 33 (c) and (f)).

¹ Mentioned in part dealing with filler modifications – chapter 1.2.2.

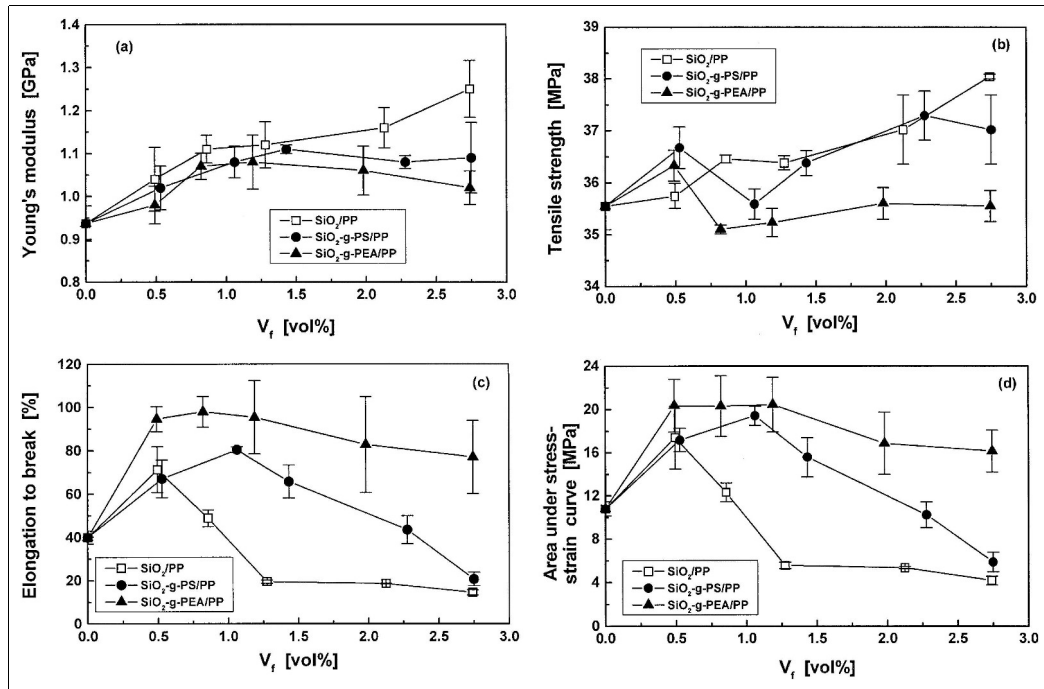


Fig. 31: Tensile properties of PP composites as a function of nano-SiO₂ volume fraction: (a) Young's modulus, (b) tensile strength, (c) elongation at break, and (d) area under stress-strain curve. Crosshead speed was 50 mm·min⁻¹. (Borrowed from [32])

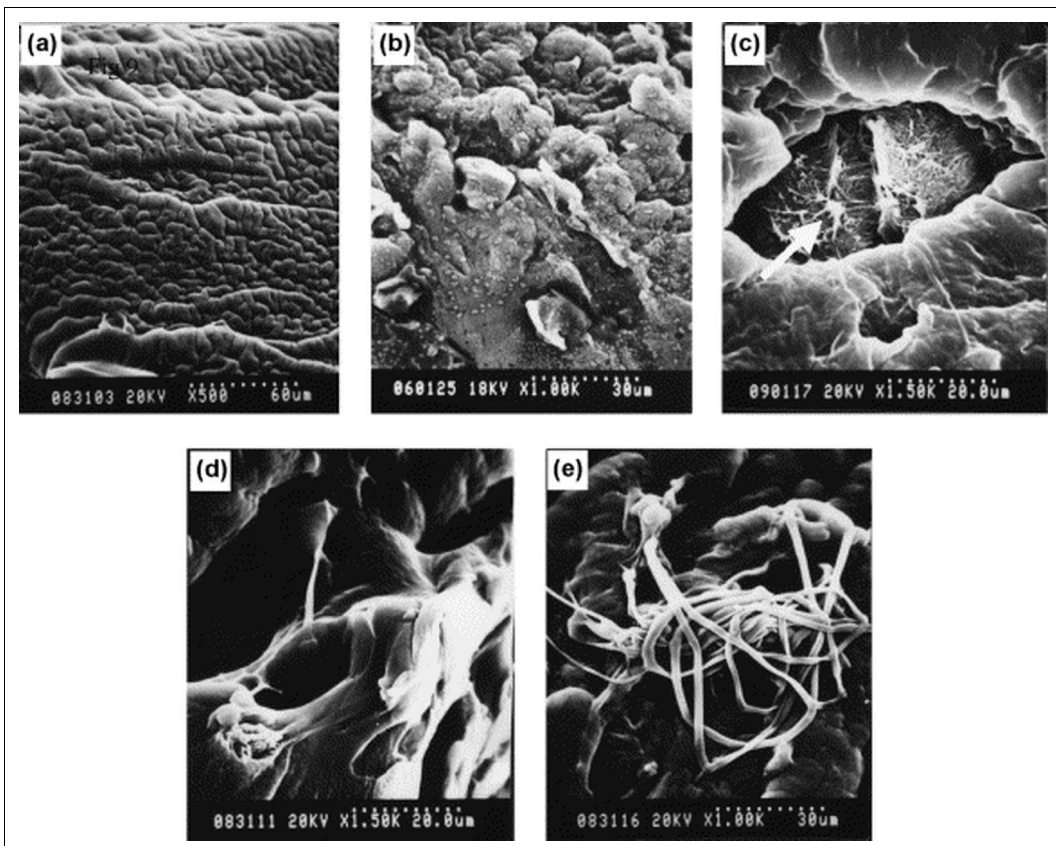


Fig. 32: SEM pictures of tensile fractured surface of: (a) neat PP; (b) and (c) PP/SiO₂ (silica content 0.86 vol%) at different magnification; (d) PP/SiO₂-g-PS (silica content 1.06 vol%); (e) PP/SiO₂-g-PEA (silica content 0.86 vol%) (Borrowed from [32])

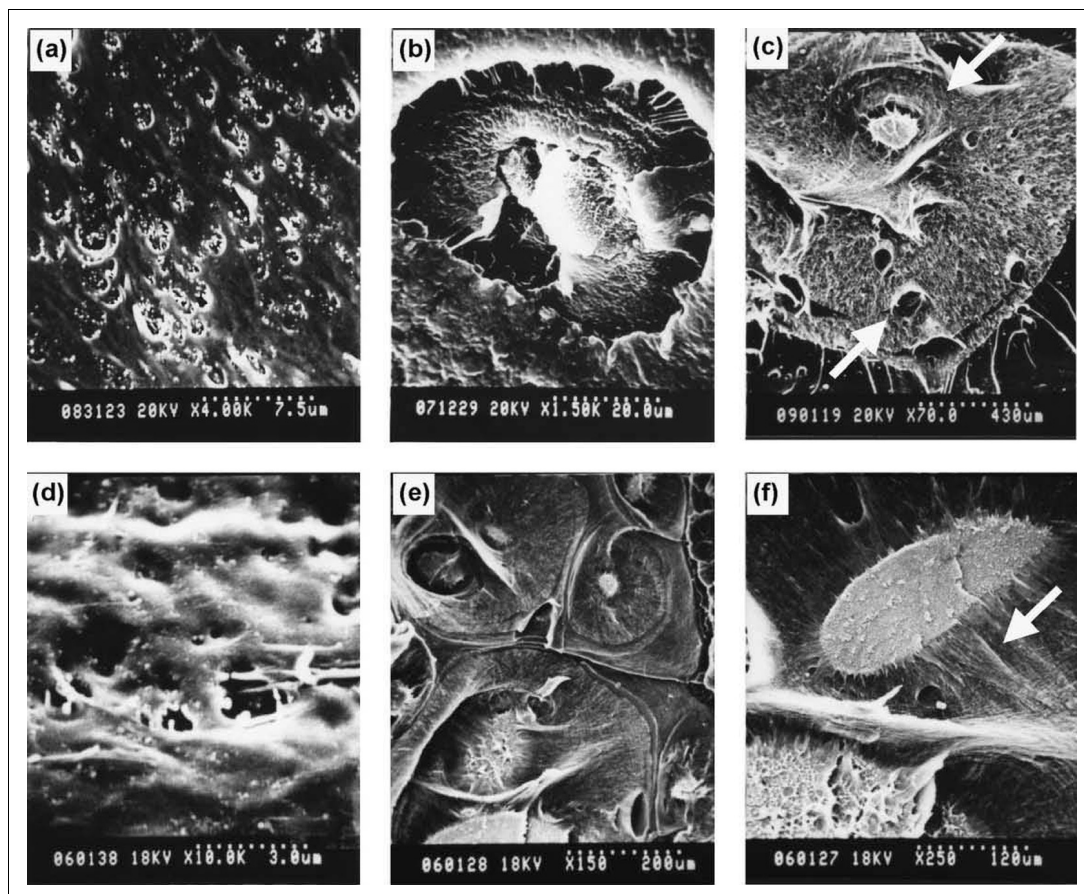


Fig. 33: SEM micrographs of tensile fractured surface of: (a) and (b) PP/SiO₂ (silica content 2.74 vol%); (c) and (d) PP/SiO₂-g-PS (silica content 2.75 vol%); (e) and (f) PP/SiO₂-g-PEA (silica content 2.75 vol%). Micrographs are at different magnitudes. (Borrowed from [32])

In the conclusion of [32] there was ascertained that the technique of the final composite preparation also plays noticeable role in the material properties, namely the silica loading speed and number of screws of the extruder (single or twin).

Wu et al. have continued in his research by elaborating [33], where the precipitated silica is used and where the composite properties as dependence of chains grafted on particle surface are investigated. For comparison the fumed silica was used as well. Also in this case the matrix was commercial isotactic polypropylene. Grafting and polymerisation of macromolecular chains from monomers was done by irradiation of γ -ray as in [29] or [32]. Grafted chains were polystyrene (PS), poly(methyl methacrylate) (PMMA), poly(ethyl acrylate) (PEA) and poly(butyl acrylate) (PBA). The final composite material was mixed in twin co-rotating miniextruder. Afterwards, the testing bars were prepared by injection-moulding. The mechanical test were done with results presented in graphs denoted as Fig. 34 – 37 (the influence of silica modification and concentration) and Fig. 38 – 41 are the comparisons of silica origins.

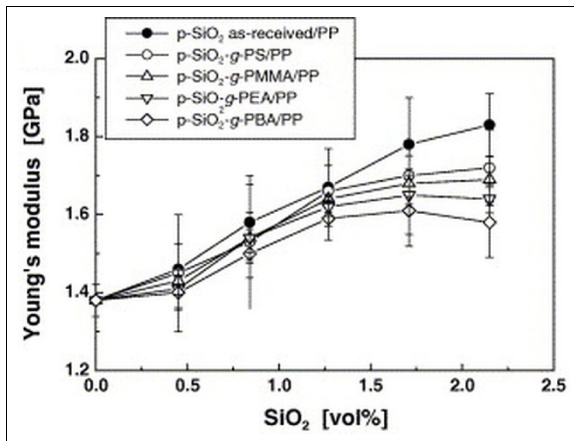


Fig. 34: Young's modulus as a function of silica content (Borrowed from [33])

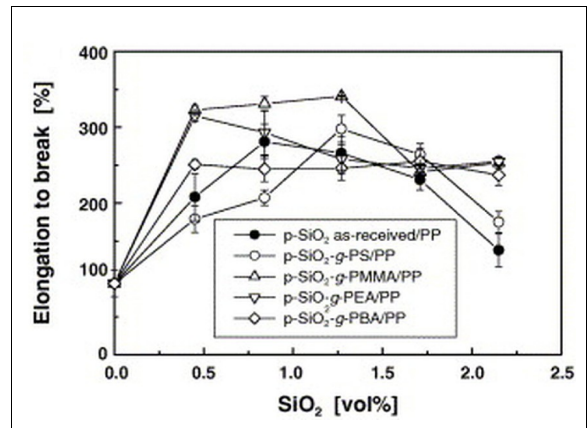


Fig. 35: Elongation at break as a function of silica content (Borrowed from [33])

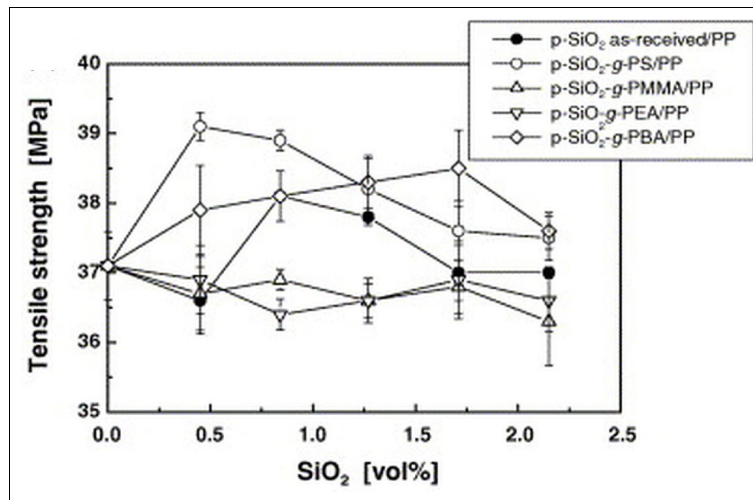


Fig. 36: Tensile strength as a function of silica content (Borrowed from [33])

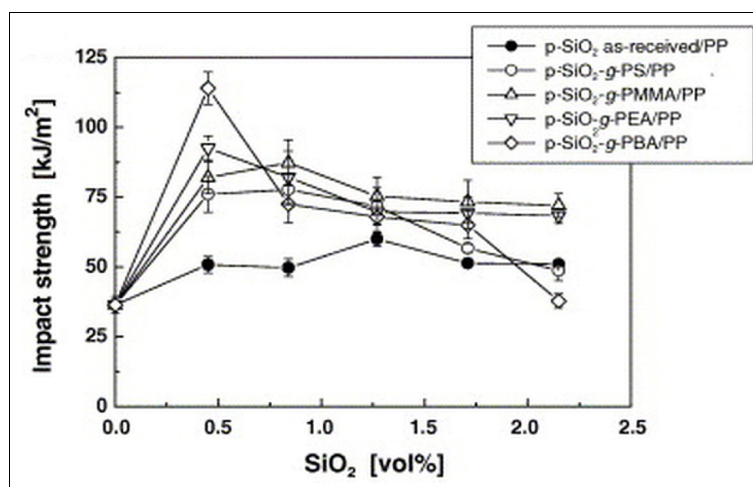


Fig. 37: Impact strength as a function of silica content (Borrowed from [33])

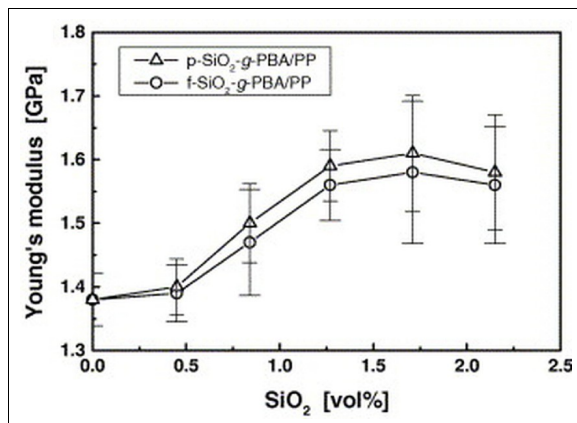


Fig. 38: Young's modulus versus silica content – the comparison of different silica types: *p*-SiO₂ – precipitated and *f*-SiO₂ – fumed silica (Borrowed from [33])

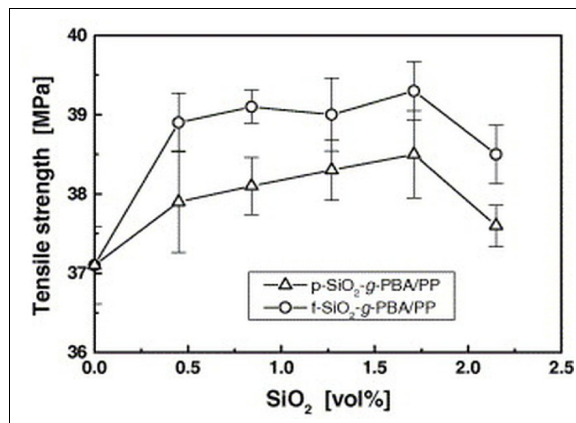


Fig. 39: Tensile strength versus silica content – the comparison of different silica types: *p*-SiO₂ – precipitated and *f*-SiO₂ – fumed silica (Borrowed from [33])

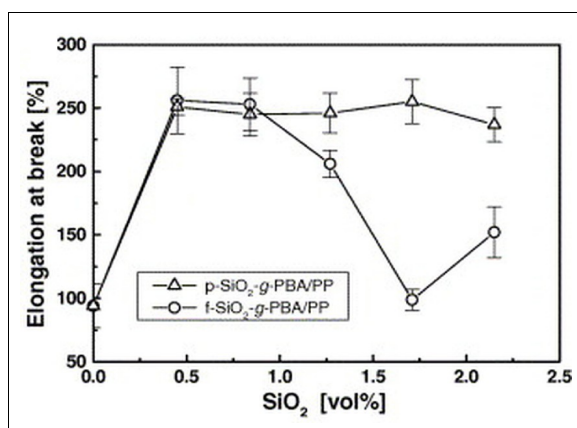


Fig. 40: Elongation at break versus silica content – the comparison of different silica types: *p*-SiO₂ – precipitated and *f*-SiO₂ – fumed silica (Borrowed from [33])

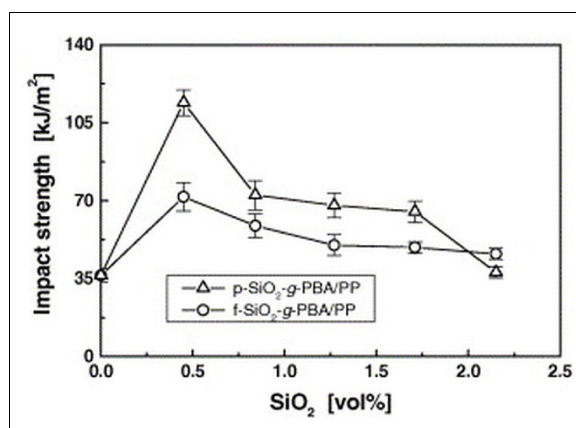


Fig. 41: Impact strength versus silica content – the comparison of different silica types: *p*-SiO₂ – precipitated and *f*-SiO₂ – fumed silica (Borrowed from [33])

It was found that the silica prepared by precipitation has relatively the same impact on mechanical attributes as fumed silica has. When the bearing of the particle concentration is investigated, the important ascertainment is the observation of strong changes even if the concentration of nano-dust is only about 0.5 vol.%. It was noted that the grafted polymer nature plays significant role in the alternation of the properties. Unfortunately, in [33] neither data were summarised in tables nor exact values were given.

Zhou et al. [34] describes in the introduction of his work the main difficulty of filling polymers by silica. It is the procuration of good distribution of particles, what is difficult because of the tendency of silica to create aggregates. In [34] the good dispersion is solved by modification of nano-particles by grafting poly(glycidyl methacrylate) generated from glycidyl methacrylate and consequent blending of obtained particles in polymer matrix with some amount of modified polymer chains. The modified polymer was aminated PP

(polypropylene grafted with NH_2), which can be obtained by melt mixing of maleic anhydride grafted PP and hexamethylenediamine in batch mixer. The blends of grafted silica, modified PP and “pure” PP were prepared in compositions as showed in Table 4 by mixing at 180°C for 15 min. with rotor speed 60 rpm. Finally the standard bars for mechanical tests were injection moulded.

The samples were investigated by transmission electron microscopy. It was confirmed that grafted silica has better distribution in comparison with untreated one as can be seen in Fig. 42 – 45.

Results of mechanical testing are plotted in graphs in Fig. 46. And finally DSC measurement was done with results showed in Table 5 and in Table 6. Compared were both the composition of final blend (all combinations – with or without silica, with or without modified PP and so on) and influence of grafted silica concentration.

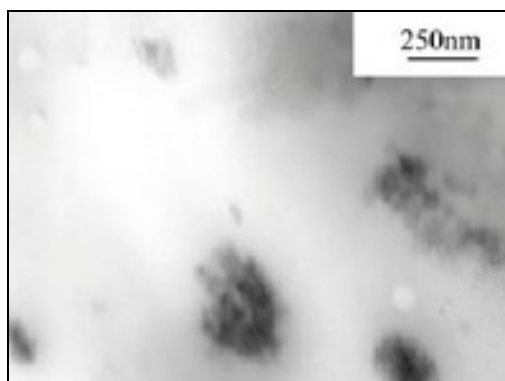


Fig. 42: TEM micrograph of untreated SiO_2/PP (silica particles load 3 wt%) (Borrowed from [34])

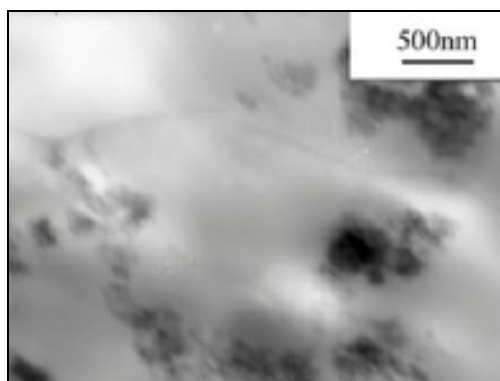


Fig. 43: TEM micrograph of untreated SiO_2/PP (silica particles load 5 wt%) (Borrowed from [34])

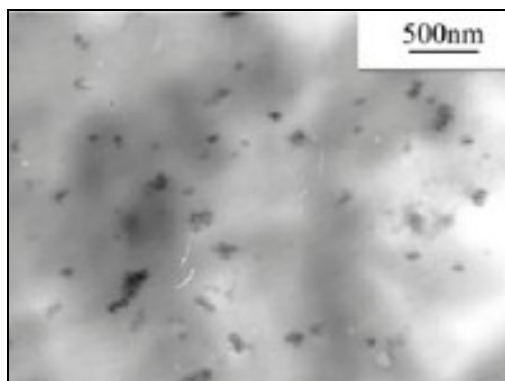


Fig. 44: TEM micrograph of $\text{SiO}_2\text{-g-PGMA}/\text{PP}$ (particles load 3 wt%) (Borrowed from [34])

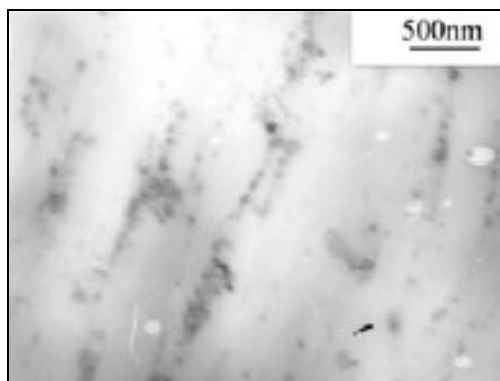


Fig. 45: TEM micrograph of $\text{SiO}_2\text{-g-PGMA}/\text{PP-g-NH}_2/\text{PP}$ (particles load 3 wt%) (Borrowed from [34])

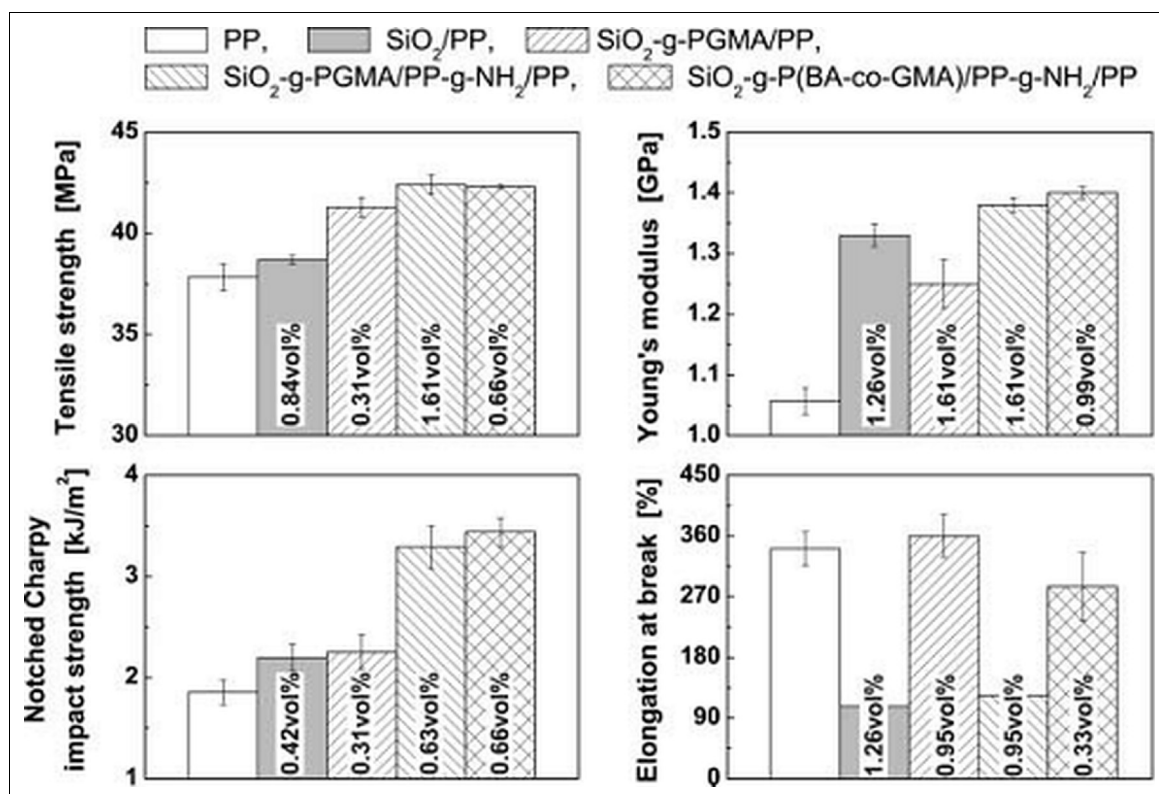


Fig. 46: Results of mechanical tests of different blends. The highest material property of blends was observed with presented particle volume ratio. (Borrowed from [34])

Table 4. Melt flow indexes (MFI) and equilibrium torques recorded at steady-state (10 min. after feeding) in the mixer of PP and its composites (Reprinted from [34])

Materials	Weight ratio	MFI (g/10 min.)	Equilib. torque
PP	100	11.0	4.1
SiO ₂ -g-PGMA/PP	3:97	10.2	4.4
SiO ₂ -g-PGMA/PP-g-NH ₂ /PP	3:10:87	8.4	5.9
SiO ₂ -g-PGMA/PP-g-MA/PP	3:10:87	13.3	4.6
SiO ₂ -g-PGMA/PP-g-MA/HMDA/PP	3:10:0.17:87	10.0	5.1
PGMA/PP-g-NH ₂ /PP	0.9:10:87	9.9	-

Table 5. DSC results of PP and its composites (Reprinted from [34])

Materials	Weight ratio	T _m (°C)	T _c (°C)	x _c (%)
PP	100	164.8	115.8	54.3
PP-g-NH ₂ /PP	10:90	163.5	116.4	55.1
SiO ₂ /PP	3:97	164.2	116.9	54.8
SiO ₂ -g-PGMA/PP	3:97	165.3	118.6	52.2
SiO ₂ -g-PGMA/PP-g-MA/PP	3:10:87	165.7	125.6	61.1
SiO ₂ -g-PGMA/PP-g-NH ₂ /PP	3:10:87	165.8	125.5	58.1
SiO ₂ -g-PGMA/PP-g-MA/HMDA/PP	3:10:0.17:87	166.0	123.8	56.6

Table 6. Influence of SiO₂-g-PGMA content on crystallization and melting behaviours of PP composites (Reprinted from [34])

Materials	Weight ratio	T _m (°C)	T _c (°C)	x _c (%)
PP	100	164.8	115.8	54.3
SiO ₂ -g-PGMA/PP-g-NH ₂ /PP	1:10:89	165.8	125.4	57.9
SiO ₂ -g-PGMA/PP-g-NH ₂ /PP	2:10:88	165.6	125.7	59.7
SiO ₂ -g-PGMA/PP-g-NH ₂ /PP	3:10:87	165.8	125.5	58.1
SiO ₂ -g-PGMA/PP-g-NH ₂ /PP	5:10:85	165.4	126.8	61.6

As a result of [34] the reactive compatibilisation technique for improving performance of PP/nano-silica composites was developed. Accordingly, the reactive compatibilized system shows a significant synergetic effect as viewed from tensile and impact properties of the composites. However, the strong interfacial interactions causes a reduction in failure strain. DSC data shows increase of crystallization temperatures when grafted particles and modified polymer is mixed into matrix. Still and all, the temperature shows low dependency on filler concentration as the melting temperature too.

The crystallisation of isotactic polypropylene containing silica particles was investigated by Nitta et al. [35]. They have studied the influence of concentration and particle diameter on the number of nuclei arose and the speed of spherulite growth.

In their experiments isotactic polypropylenes with high isotacticity (98-99%) and different molecular weight were used as matrix. Silica particles were treated with silane coupling agents carrying hydrophobic methyl and octyl chains to improve the miscibility. The composite was prepared by simple melt mixing in corotating twin-roller at 180°C – firstly the iPP was fused and then silica dust was added. Each blend had been mixed for 10 min.

Polarizing optical microscope was used to observe the crystallisation processes. It was noticed that growth rates of spherulites in iPP/SiO₂ are reduced as the content of silica particles increases. Every addition of silica dust brings reduction of distance between particles what leads to null growth rate of spherulites when the inter-partical distance reaches to the end-to-end distance of iPP chains. In Fig. 47 – 49 the dependence of spherulite growth rates on silica content and diameter is plotted. These graphs also clearly show that micro-scaled particles have negligible influence on the rate of spherulite growth.

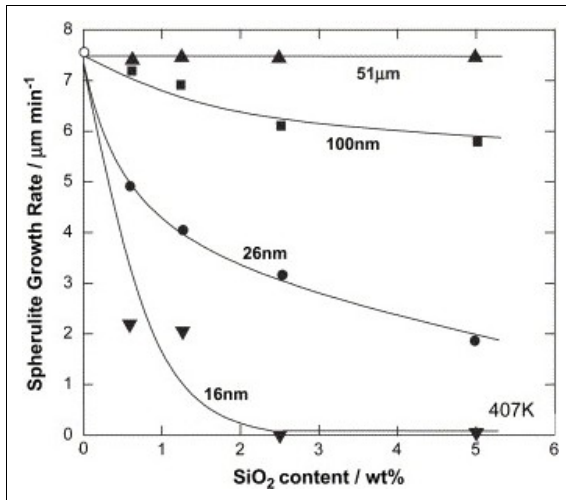


Fig. 47: The dependence of the spherulite growth rates on silica content isothermally measured at 407K. (Borrowed from [35])

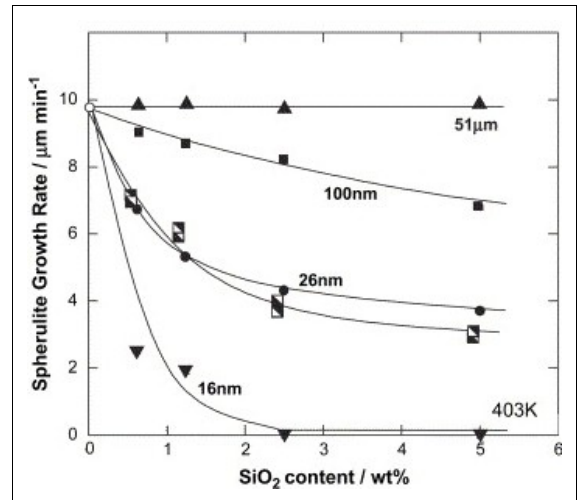


Fig. 48: The dependence of the spherulite growth rates on silica content isothermally measured at 403K. (Borrowed from [35])

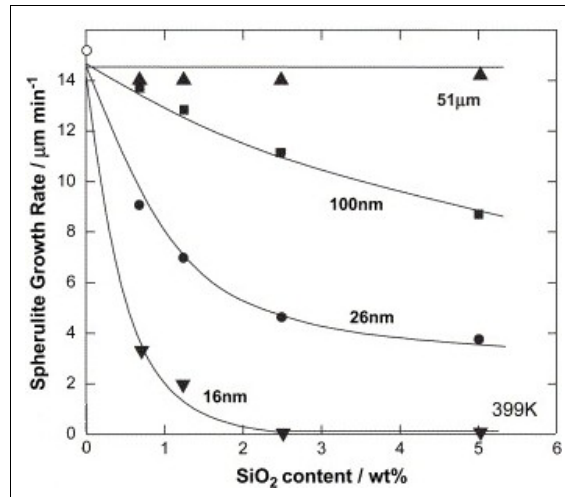


Fig. 49: The dependence of the spherulite growth rates on silica content isothermally measured at 399K. (Borrowed from [35])

2.3 Polystyrene/silica

Bartholome et al. [36] prepared polystyrene matrix filled with polystyrene grafted silica nano-particles. Grafting was started by bonding triethoxysilyl terminated alkoxyamine initiator (denoted as A in Fig. 50) on particle surface. Consequent controlled growth of polystyrene chains in presence of alkoxyamine initiator (denoted as B) was done. By varying the conditions of the grafting treatment Bartholome et al. was able to achieve different graft density and different chain length. Obtained samples are summarised in Table 7.

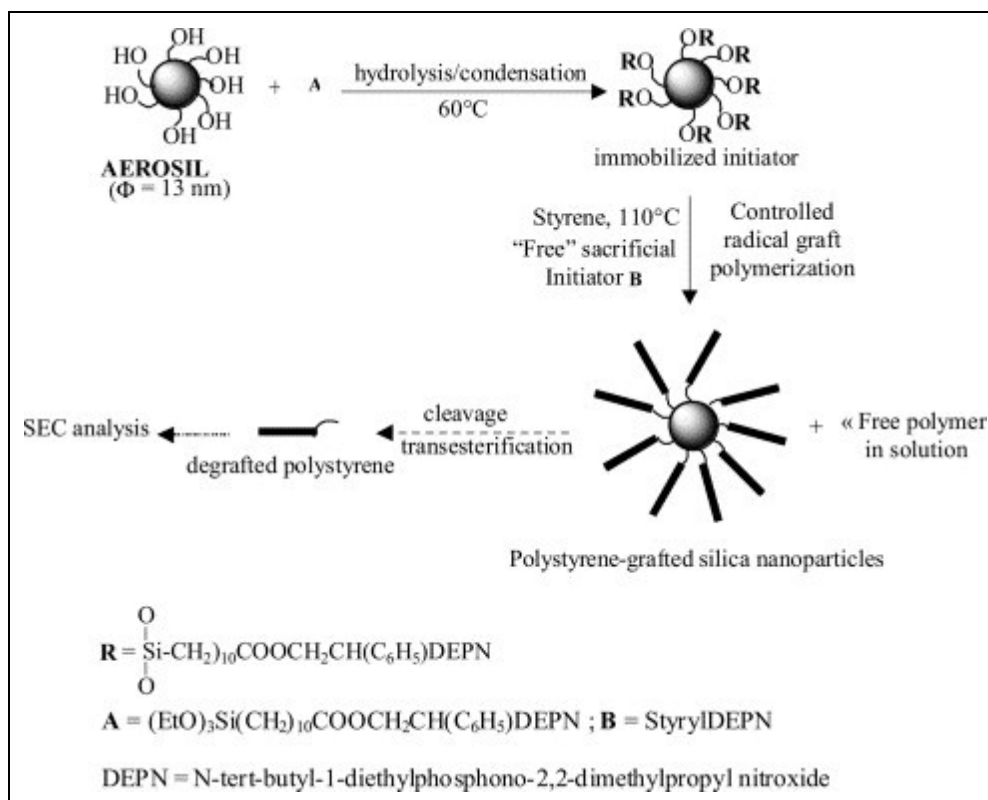


Fig. 50: The scheme of grafting silica by PS chains (Borrowed from [36])

Table 7. Polystyrene grafting densities, molecular weights of the grafted PS chains and hydrodynamic diameters of a series of PS-grafted silica samples (reprinted from [36])

Sample No.	Grafting density ($\mu\text{mol}/\text{m}^2$)	M_n of the grafted chains (g/mol)	Hydrodynamic diameter determined by DLS (nm)
1	0.05	14,800	316
2	0.05	60,000	144
3	0.27	60,000	181
4	0.33	30,900	150
5	0.37	38,700	165
6	0.32	56,000	175
7	0.28	60,000	189

The grafted silica and pure PS ($M_n = 100,000 \text{ g}\cdot\text{mol}^{-1}$) were introduced in benzene and the final blend was lyophilized and obtained powder was compression moulded at 160°C over 10 min. and then investigated. Fig. 51 and 52 are presented here to show the different filler dispersion in matrix.

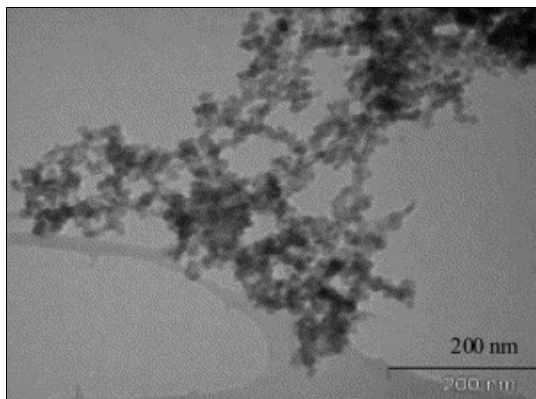


Fig. 51: TEM micrograph of unmodified silica gel (Borrowed from [36])

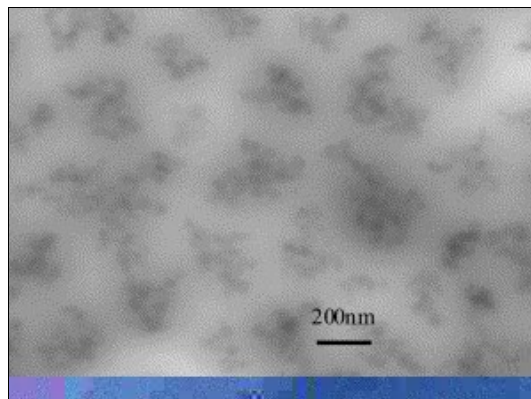


Fig. 52: TEM micrograph of PS/silica gel – sample 3 (Borrowed from [36])

The study of viscoelastic properties brought out that the elastic behaviour of the suspension considerably decreases the secondary elastic plateau even if the molecular weight of the grafted chains is above the critical molecular weight of entanglement of polystyrene ($M_e = 18,000 \text{ g}\cdot\text{mol}^{-1}$). Bartholome et al. explained this by decreasing of the size of silica aggregates of the grafted silica in comparison to untreated particles. The major role of the viscoelastic behaviour of nanocomposite was also ascribed to the graft density. Two samples with same graft chain length but different graft density were compared in Fig. 53 and Fig. 54. The “gel” behaviour disappears as G' no longer exhibits plateau and the macromolecular flow occurs, in the low frequency range. In this fact Barholome et al. emphasised the contradict to conclusions of Dageou et al. [37] and points out that converse results are caused by different nature between nano-silica (used in [36]) and colloidal silica (used by Dageou).

Fig. 55 shows that even a small amount of short chains is effective to avoid the gel effect. Fig. 56. shows the comparison of storage shear modulus of blends of different samples, pure PS and unmodified silica.

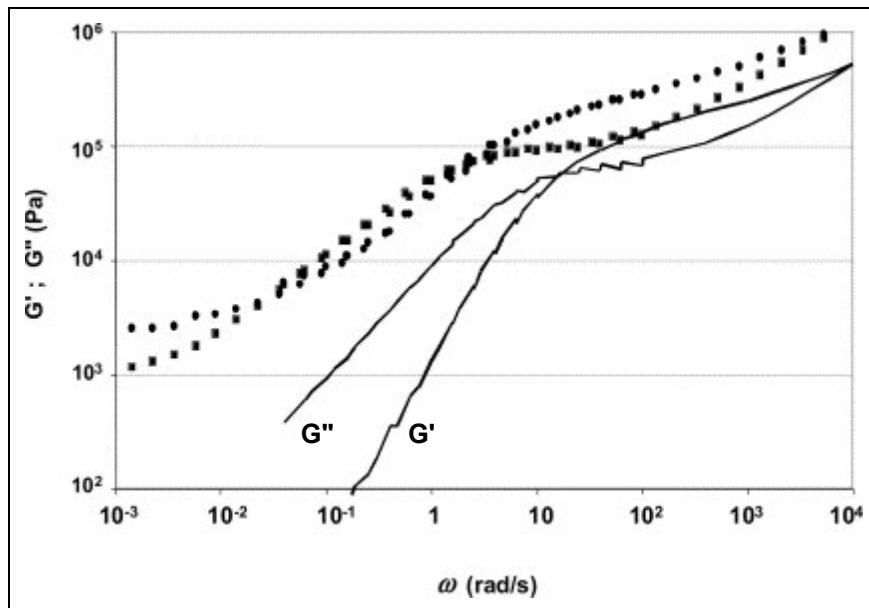


Fig. 53: Complex shear modulus versus frequency: Master curves ($T_{ref} = 160^\circ\text{C}$). PS-grafted silica ($\bullet G'$, $\blacksquare G''$) (sample 2) and poly-styrene matrix (—). (Borrowed from [36])

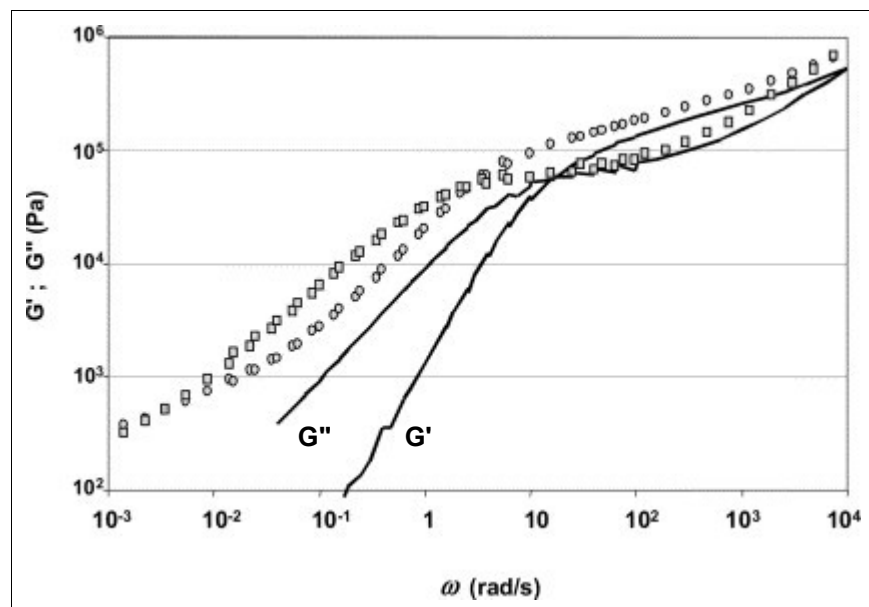


Fig. 54: Complex shear modulus versus frequency: Master curves ($T_{ref} = 160^\circ\text{C}$). PS-grafted silica ($\circ G'$, $\square G''$) (sample 3) and poly-styrene matrix (—). (Borrowed from [36])

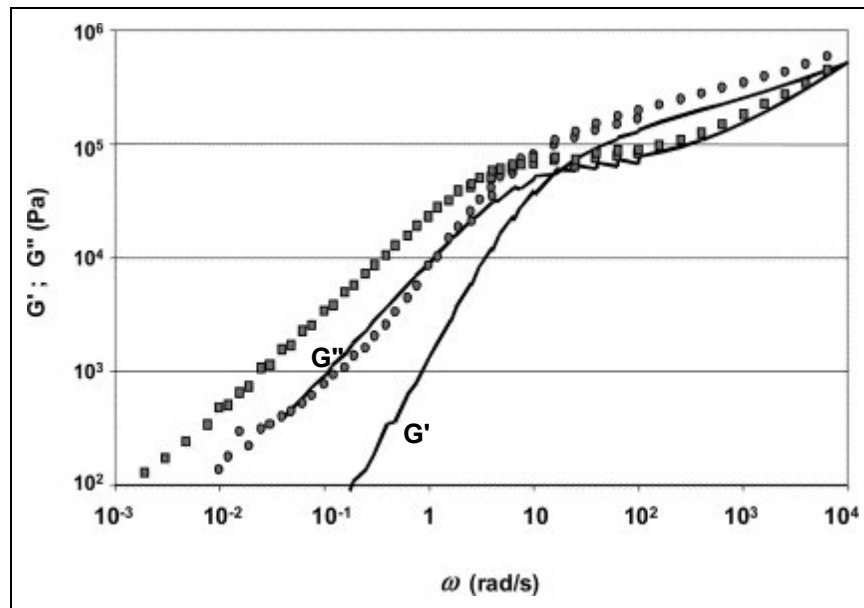


Fig. 55: Complex shear modulus versus frequency: Master curves ($T_{ref} = 160$ °C). PS-grafted silica ($\bullet G'$, $\blacksquare G''$) (sample 1) and polystyrene matrix (—). (Borrowed from [36])

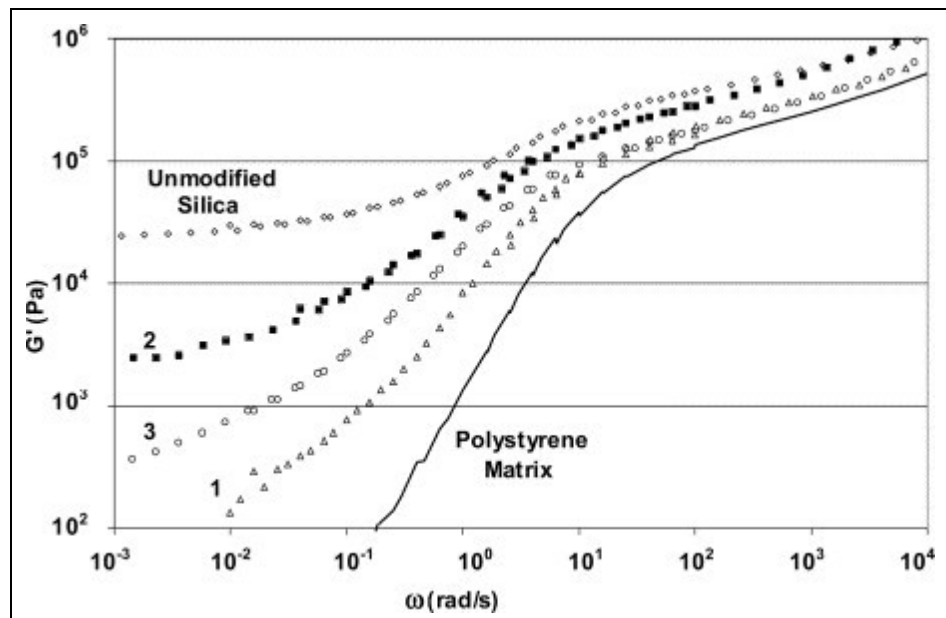


Fig. 56: Storage shear modulus of blends of polystyrene and PS-grafted silica (samples 1 – 3 in Table 7) (Borrowed from [36])

2.4 Poly(methyl methacrylate)/silica

Poly(methyl methacrylate) films filled with nano-silica were studied by Liu et al. [38] with interest in high filled composite. Silica used in their work was in size 10 – 20 nm and it was firstly treated. The surface was grafted by “non-silane“ coupling agent – the alylglycidylether. Nanocomposite material was consequently prepared by polymerisation of MMA initiated by benzylperoxide with grafted silica dispersed in monomer. Films of PMMA/silica with weight ratio of silica of 70% showed extreme high hardness and surface planarity and also good thermal stability, but without positive changes in thermal degradation of PMMA.

More complex study was done by García et al. [39]. They have prepared nanocomposite of PMMA and silica particles of main diameter 12 nm with no surface modification. All materials were purchased and used as received. The PMMA was diluted in toluene and mixed with suspension of silica in the same solvent. The nano-dust content varied in matrix from 1 to 35 wt% as summarised in Table 8 together with glass transition temperature. The dilution was magnetically stirred at 50°C and after inspissate the creamy blend was then spread on glass and heated at 140°C to eliminate residual toluene. Finally the material was compression moulded into 130 µm thick films at temperatures from 135°C up to 150°C. Then the SEM, DSC, TGA, FTIR and isothermal chemiluminescence (CL) was applied. The obtained SEM images are here presented in Fig. 57. Graphs of TGA and CL are showed in Fig. 58 – 61.

Table 8. Compositions and glass transition temperatures (Reprinted from [39])

<i>Sample</i>	<i>wt% of silica</i>	<i>T_g (°C)¹</i>
PMMA	0	104.6
PMMA-1	1.0	-
PMMA-3	2.9	107.6
PMMA-5	4.8	107.6
PMMA-7	6.6	-
PMMA-9	9.1	111.0
PMMA-13	13.0	-
PMMA-17	16.7	112.5
PMMA-20	20.0	-
PMMA-23	23.1	114.5
PMMA-29	28.5	113.7
PMMA-35	35.0	113/160

¹ All samples were not measured or wittingly the values were not presented in [39]

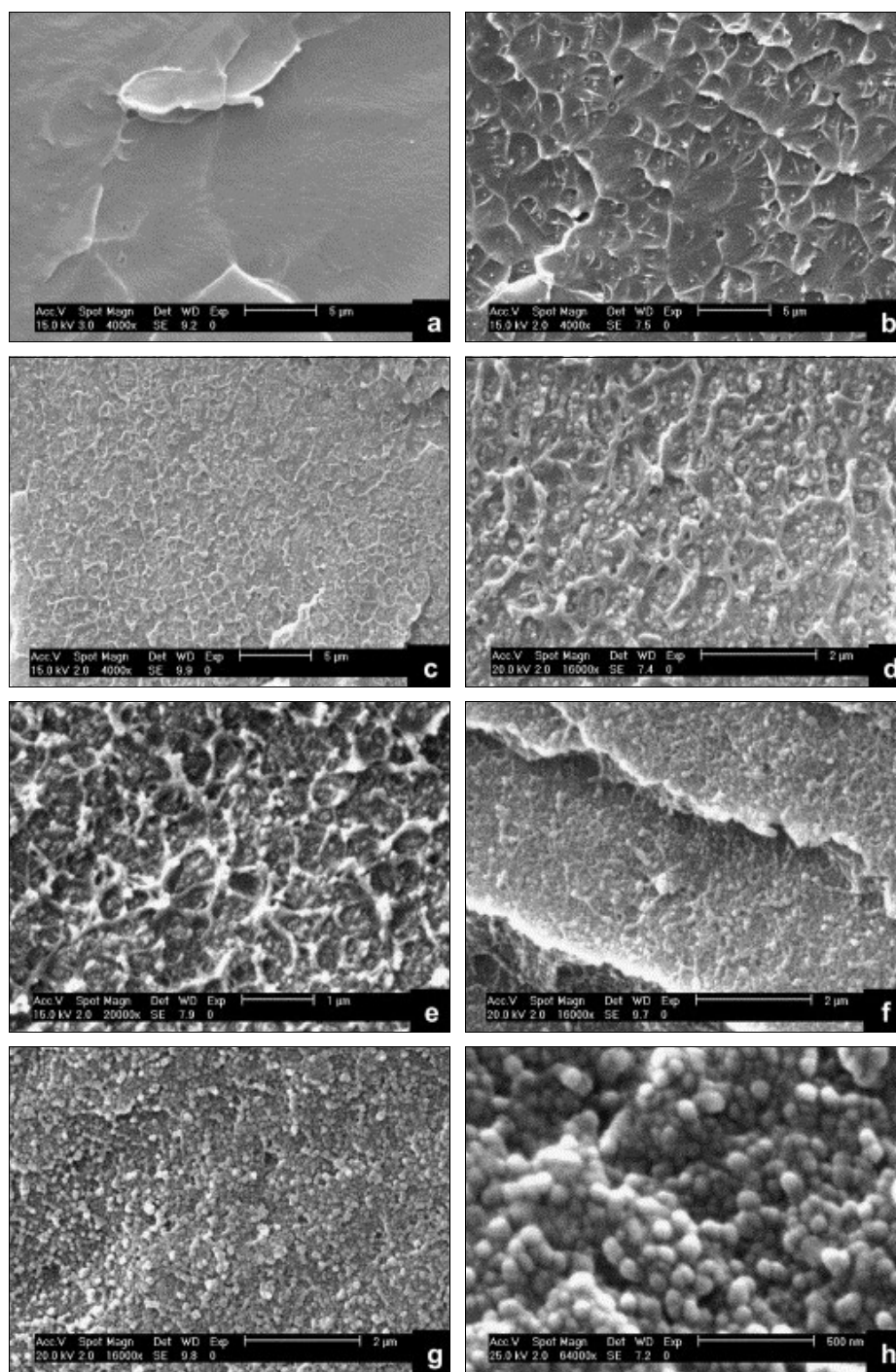


Fig. 57: SEM micrographs: a) pure PMMA; b) PMMA-1; c) PMMA-3; d) PMMA-9; e) PMMA-13; f) PMMA-20; g) PMMA-23; h) PMMA-35 at different magnitudes (Borrowed from [39])

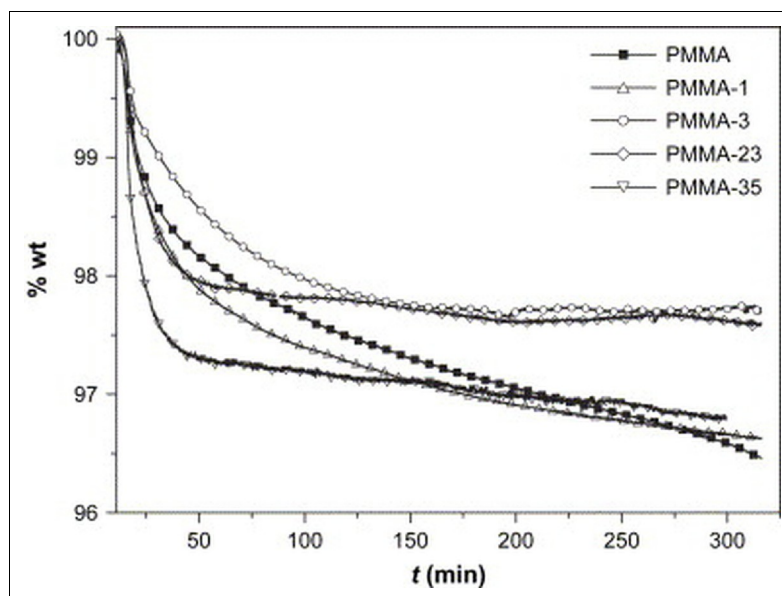


Fig. 58: Weight loss in nitrogen atmosphere at 220 °C (The weight loss percentage was normalised to the organic part) (Borrowed from [39])

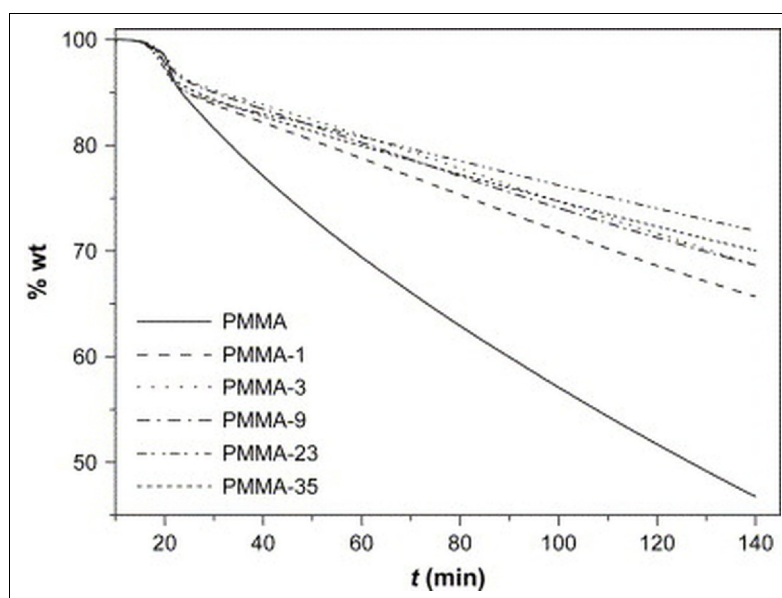


Fig. 59: Weight loss in nitrogen atmosphere at 300 °C (The weight loss percentage was normalised to the organic part) (Borrowed from [39])

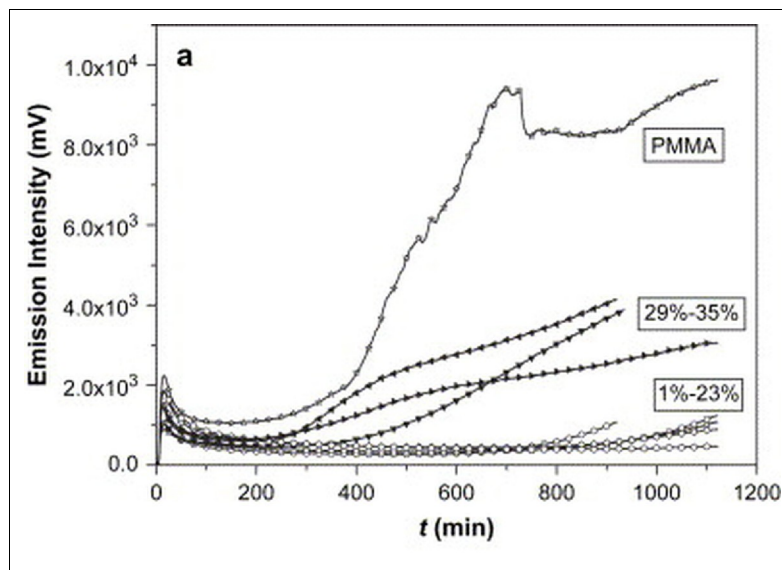


Fig. 60: Chemiluminescence emission curves in oxygen at 200°C. (Presented percentages are per cent by weight.) (Borrowed from [39])

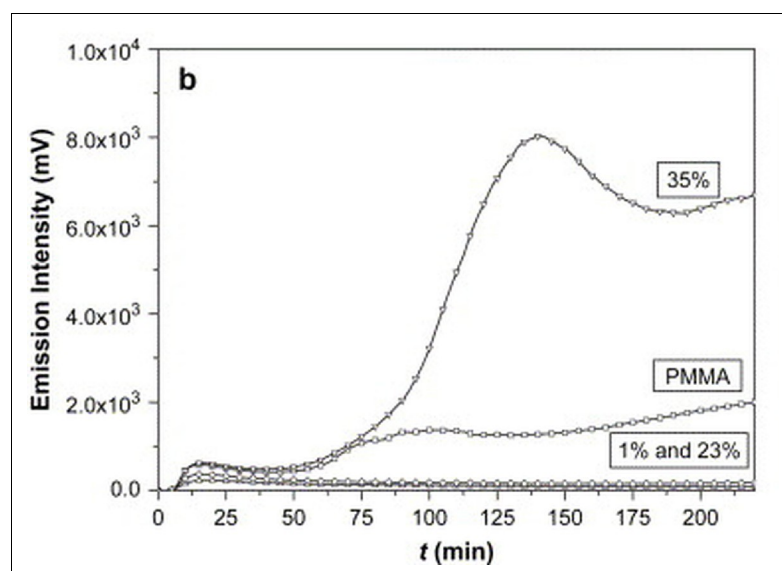


Fig. 61: Chemiluminescence emission curves in oxygen at 220°C. (Presented percentages are per cent by weight.) (Borrowed from [39])

García et al. found that T_g increases about 10°C up to 23 wt% of silica and over 30 wt% filling introduces a second glass transition at 160°C. The SEM showed nodular structure in the continuous phase, which disappears as the silica content increases. The thermal degradation of the composites changes due to elimination of initiation of degradation through labile chain ends. The minimal amount of silica was established as 3 wt% to reach this stabilisation even up to 300°C – as in nitrogen as in oxygen atmospheres. In contrary, the content of dust over 20 wt% increase the rate of random scission initiation on the chain. García et al. proposed that low silica ratio labile chain ends are trapped and stabilised at the

interface with the silica particle. At high silica ratio, the content of labile chains is decreased, but the number of formation of hydroperoxides at the chains is promoted what introduce labile sites.

Yang and Nelson [40] prepared nanocomposite material via *in situ* solution polymerisation. The fumed silicas were supplied by Degussa and they were at sizes of 40, 30, 20, 16 and 7 nm, respectively. Firstly the nano-dust was dispersed in ethanol and surface-treated by (3-acryloxypropyl)-methylmethoxysilane or by (3-acryloxypropyl)trimet-oxysilane. These particles were added to MMA in toluene (the reaction medium) and benzoyl benzenecarbo-peroxoate (initiator of free radical polymerisation) was immersed too. The reaction ran at 100°C for 24h. The resulting solution was moved on a Teflon sheet and it was dried¹.

Samples were tensile tested, thermal stability and flamability was investigated, molecular weight and FT-IR measurements was done too.

Conclusions from obtained data are similar to [39] in case of thermal stability. The ignition tests showed that presence of silica does not introduce fire retardancy or self-extinguishing. To the contrary the composite is easier to ignite, burn faster and it is harder to extinguish, but the burning material lost dripping. In another properties it was noted usual indirect proportion between improvement of the mechanical behaviour and silica particle diameter, and/or the nano-dust concentration. Finally, the surface-treated particles behaved better in polymer matrix than unmodified as it was observed also in other articles.

2.5 Polyesters/silica

2.5.1 PET/Silica

Poly(ethylene terephthalate) (PET) is a conventional and relatively good value polymer material with high performance. PET is potential material in fibre usage, packaging, bottles, films and so on. Liu et al. in [41] named some of previously investigated techniques to improve the PET properties, but he also remarked that the main problems with introduction of these methods in industry are the increased cost and the reduction of clarity of the material.

In [41] the purchased organic modified silica² was dispersed in ethylene glycol by sonication at room temperature. Afterwards the suspension was mixed with terephthalic

¹ In the paper [40], there is no description by which processing the testing sample pieces was made.

² In the paper [41] no further explanation or description was found.

acid, antimony acetate (as catalyst) and additional ethylene glycol. The mixture was agitated by mechanical stirring and consequently heated up to 260°C in nitrogenous atmosphere to esterify the mixture. The polymerisation was carried out at 260 – 270°C under pressure of 200 – 300 Pa. This reaction conditions also drain out residual ethylene glycol. The polymerisation level of the melt was denoted by watt-meter. Lastly the fused blend was extruded through an orifice and cooled with water.

TEM micrographs were obtained (See Fig. 62 and 63), DSC measures were done with findings presented in Table 9.

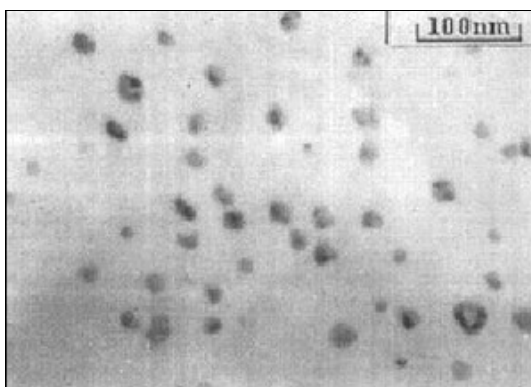


Fig. 62: TEM micrograph of PET/Silica 0.5 wt% (Borrowed from [41])

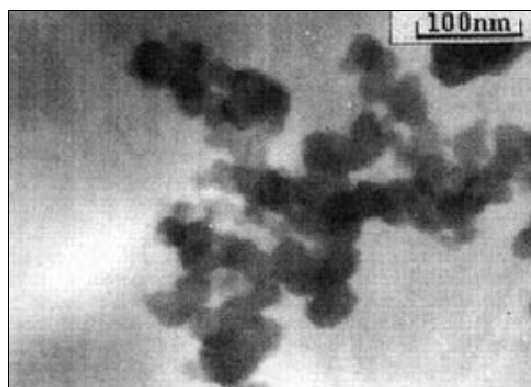


Fig. 63: TEM micrograph of PET/Silica 2.5 wt% (Borrowed from [41])

Table 9. Thermal property data by DSC (Reprinted from [41])

Specimen	T_g (°C)	T_c (°C)	T_m (°C)
Pure PET	73.8	195	243
PET/Silica 0.5 wt%	81.5	210	252
PET/Silica 2.5 wt%	83.4	213	254

It was concluded that the addition of nano-particles increases the crystallizing temperature and melting point of the matrix. The higher amount of dust deteriorate dispersion in *in situ* prepared polymer. Also was noted, that the presence of silica does not effect the process of synthesizing PET very much.

Crystallization and light transmissivity was studied also by Wu and Ke [42] who used core-shell type of particles. The silica was grafted and covered by PS. Another pure PS particles were prepared by dispersion polymerization for comparison of behaviour in PET matrix. The γ -methacrylic propyl trimethoxysilane modified and naked silica were mixed into PET as well.

The composite material was made by mixing of crushed PET powder in the ethanol suspension of the core-shell SiO₂/PS. Afterwards, the mixture was slowly heated under

mechanical agitation to remove the ethanol. The wet powder was dried under vacuum at 130°C. Finally the samples were compression moulded into 0.1 mm thick film at 275°C for 5 min. Another blends (PET-PS, PET-SiO₂(unmodified) and PET-SiO₂(modified)) were prepared by simple melting PET with particles.

Fig. 64 and 65 show TEM micrographs of untreated silica and core-shell silica/PS. Newly acquired materials were subjected to DSC measuring and the visible light transmittance and haziness were investigated. All obtained data are summarised in Tables 10 and 11.

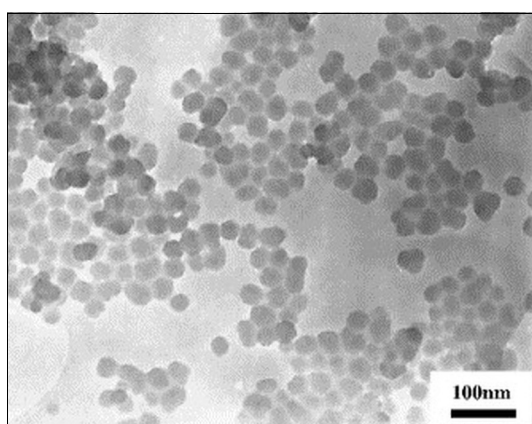


Fig. 64: TEM image of untreated silica (borrowed from [42])

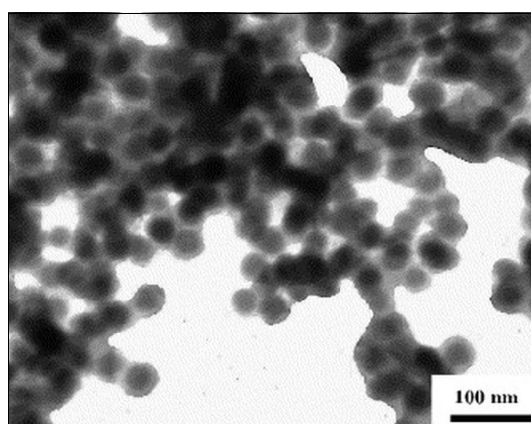


Fig. 65: TEM image of silica/PS core-shell (borrowed from [42])

Table 10. DSC data of PET with different surface treatment of SiO₂ nanoparticles (32 nm) (Reprinted from [42])

Sample	SiO ₂ (wt%)	PS (wt%)	T _m (°C)	T _c (°C)
PET	0	0	251.7	193.5
PET-PS	0	0.5	251.9	193.1
PET-SiO ₂ (unmodified)	2.0	0	252.7	197.7
PET-SiO ₂ (modified)	2.0	0	252.9	200.0
PET-SiO ₂ /PS	2.0	0.5	252.5	205.1

Table 11. DSC data of PET-SiO₂/PS nanocomposite films with different PS-encapsulated SiO₂ content (Reprinted from [42])

Sample	SiO ₂ (wt%)	PS (wt%)	T _m (°C)	T _c (°C)	T _{cc} ¹ (°C)	T _{b/2} ² (°C)
PET	0	0	251.7	193.5	135.2	22.0
PET-SiO ₂ /PS-0.5	0.5	0.1	251.9	196.5	134.2	20.9
PET-SiO ₂ /PS-1.0	1.0	0.2	253.5	197.7	133.6	16.1
PET-SiO ₂ /PS-2.0	2.0	0.5	252.5	205.1	130.4	6.8
PET-SiO ₂ /PS-3.0	3.0	0.7	251.0	202.6	131.4	7.6
PET-SiO ₂ /PS-5.0	5.0	1.2	251.2	202.1	130.6	9.3

1 T_{cc} = cold crystallization temperature from the glass state

2 T_{b/2} = half width temperature of crystallization peak

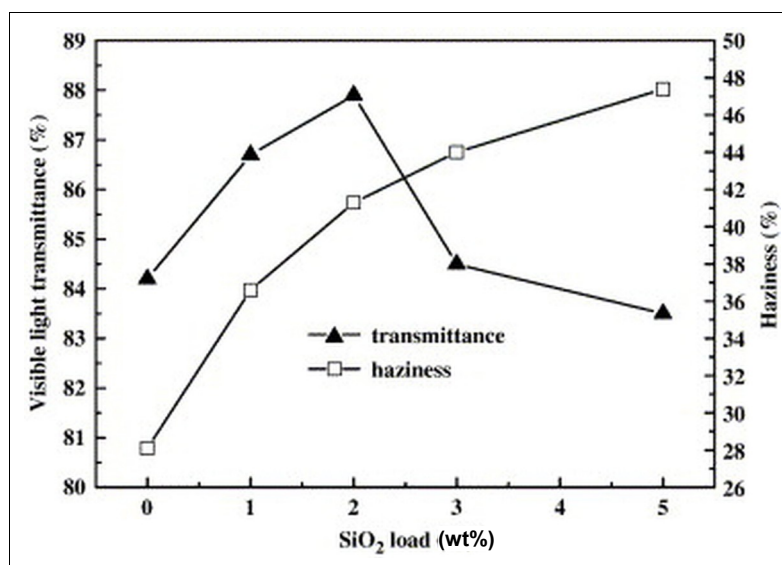


Fig. 66: Dependence of visible light transmittance and haziness of amorphous PET-SiO₂/PS nanocomposite on particle load. (Borrowed from [42])

Results which consequent from [42] are that encapsulated particles can accelerate more easily the crystallization of PET than modified or naked particles can. The highest crystallization temperature is achieved when PET matrix is filled by 2 wt%. At these load the transmittance is also the highest – around 87.9% (see Fig. 66). Finally, it is necessary to note that haziness increase continuously.

2.5.2 PBT/Silica

Besides PET there is another widely applied polyester – poly(butylene terephthalate) (PBT). This material have excellent comprehensive properties which have led to usage in automobile industry, electronics and electrical appliance. Main disadvantages of PBT are its low deformation temperature, relatively poor mechanical properties or low notched impact strength. In [43] Che et al. have modified thermoplastics PBT with surface treated silica. Used particles were an average diameter of 22 nm and were grafted with PBT chains synthesized *in situ* from butane-1,4-diol and dimethyl-*p*-phthalate with butyl titanate as catalyst. Mixture had been heated until the temperature reached 220°C. The suspension was finally centrifugated and separated dust was dried at 80 °C.

The composite material was prepared by high-speed mixing machine by simply immersion of different ratios of PBT resin pellets and grafted silica particles. Obtained blend was extruded by double-screw extruder and standard samples were prepared by injection moulding.

Finally, mechanical properties were investigated with results plotted in Fig. 67 – 69. This study shows that the tensile strength increases and reaches its maximum when the content of filler is 3 wt% and slow decrease come after. It is clearly seen in Fig. 67 that grafted silica holds tensile strength at relatively high value for wider range of silica content than in case of naked silica.

More dramatic changes were observed when elongation at break was studied. The composite filled with treated particles demonstrate great improvement of the property. Likewise the notched impact strength was increasing in low filled materials.

Che et al. concluded that besides mechanical improvements the grafted silica can be well dispersed in PBT matrix with no aggregation observed. Also the thermal stability of the composite was enhanced.

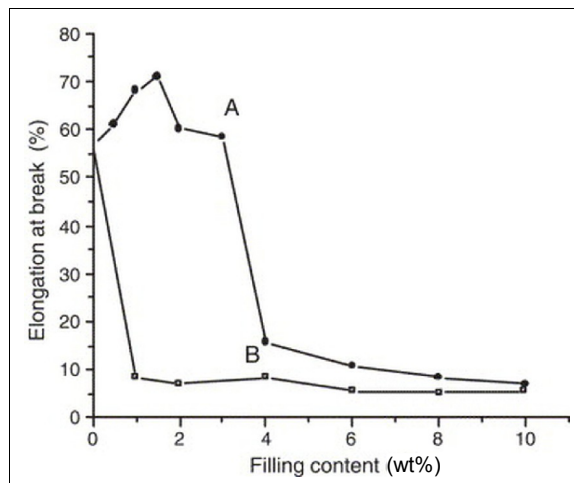
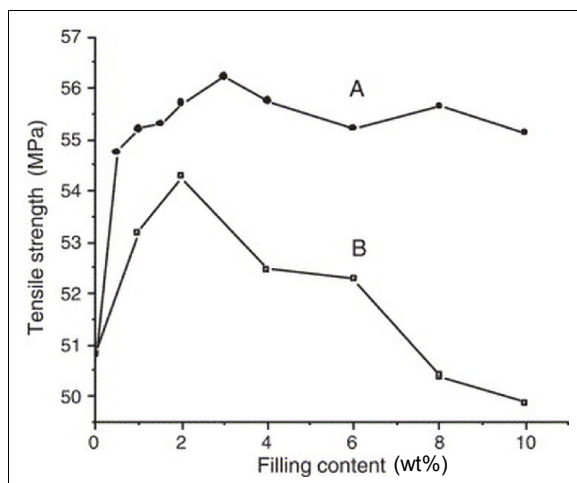


Fig. 67: Effect of the silica particles ratio on the tensile strength of PBT: A: grafted SiO₂, B: original SiO₂ (Borrowed from [43])

Fig. 68: Effect of the silica particles ratio on the elongation of PBT: A: grafted SiO₂, B: original SiO₂ (Borrowed from [43])

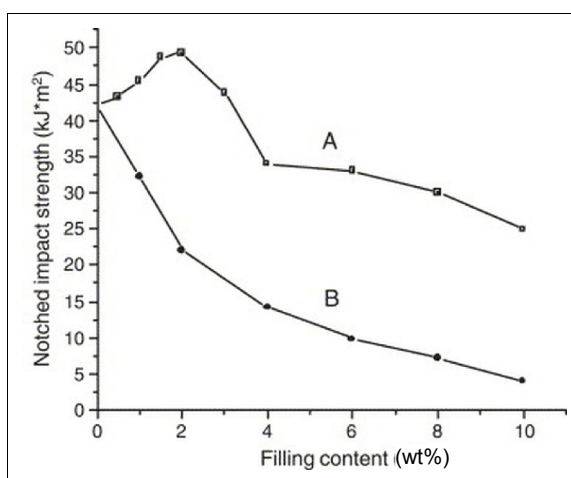


Fig. 69: Effect of the silica ratio on the notched impact strength of PBT: A: grafted SiO₂, B: original SiO₂ (Borrowed from [43])

2.6 Polyamide/silica

Polyamides (PA) are relatively expensive polymers [2]. Main types are PA6 and PA66 which differ in method of synthesis.

PA6/silica nanocomposites were studied by Yang et al. [44]. ϵ -Caprolactam was the monomer for preparation of the matrix which was filled with AEROSIL[®] R972. The silica surface was modified by aminobutyric acid and consequently dried in oven. Nanocomposite PA6/silica was finally prepared by dispersion of modified dust in melted ϵ -caprolactam (90°C) with consequent addition of aminocaproic acid as the initiator. Polymerisation ran as in “usual” preparation of PA6 – at high temperature under nitrogen atmosphere.

Concluded were the advantages of *in situ* polymerisation of PA6/silica – primarily the ability to avoid particle agglomeration and improvement of the interfacial interactions. Also in this case was proved that the organo-modified particles were dispersed more homogeneously in comparison to unmodified ones. DMA brought finding that the mechanical properties have tendencies to first increase and consequently decrease with the load of surface-modified silica ratio. The maximum appears at about 5 wt% of silica. Whereas the untreated particles caused decreasing tendency of mechanical properties.

Reynaud et al. [45] and García et al. [46] followed in studying PA6/silica nanocomposites. Mechanical and rheological properties and thermal transitions were investigated in [45], where the new material was prepared by *in situ* polycondensation of the polymer around the suspended silica. Besides the influence of filler load the impact of particle dimensions was also examined. Three sizes of silica particles were used – 17 nm, 30 nm and 80 nm in diameter, abbreviated in marks as S, M and L¹. Four samples varied in concentration (5, 10 and 15 wt%) were prepared as summarised in Table 12. Finally, the polymer was injection moulded into normed shapes for mechanical tests.

Table 12. Sample compositions and DSC data (Based on [45])

Sample	SiO ₂ diameter (nm)	SiO ₂ (wt.%)	T _m (°C)	T _c (°C)	ΔH_m (J g ⁻¹)	ΔH_c (J g ⁻¹)
Pure PA6	-	0	222	190	90	82
PA-05-S	17	5	219	188	93	86
PA-05-L	80	5	220	186	87	82
PA-10-M	30	10	219	186	90	82
PA-15-L	80	15	220	187	93	81

¹ S = small (17 nm), M = medium (30 nm), L = large (80 nm)

DSC and mechanical testing was executed and TEM images were obtained as WAXS and SAXS spectra too. Data from DSC analysis are included in Table 12. TEM micrographs are in Fig. 70 and 71. Loss factor plotted against temperature is in Fig. 72 and in Fig. 73 is conservation modulus presented. Fig. 74 represents graph of the composite evolution with respect to the filler content. Viscosity of the fused nanocomposite system at temperature 250 °C was measured and is plotted in Fig. 75. There can be seen that the non-Newtonian character of the liquid is increased with the decreasing of particle diameter even at low filling. Reynaud et al. suggest that it is caused by the particle-particle interaction due to their large specific surface, what is also demonstrated in Fig. 70 – TEM image shows more aggregated particles than with larger diameter. Relative moduli as dependency of filling at different temperatures are showed in Fig. 76 and in Fig. 77. Results of mechanical test are in Fig. 78 – 80¹. Another conclusion were that the presence of silica does not effect the crystalline phase within the nylon-based composites nor the quantity nor morphology of the spherulites.

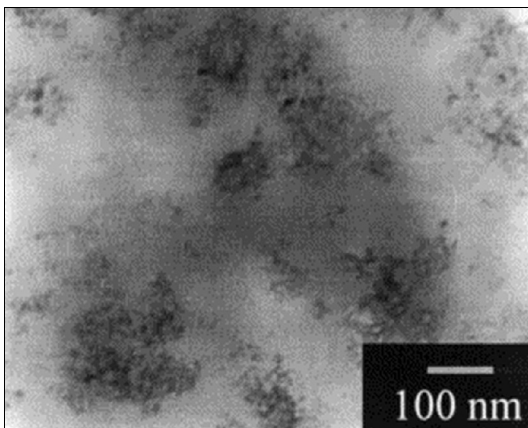


Fig. 70: TEM micrograph of PA-05-S (Borrowed from [45])

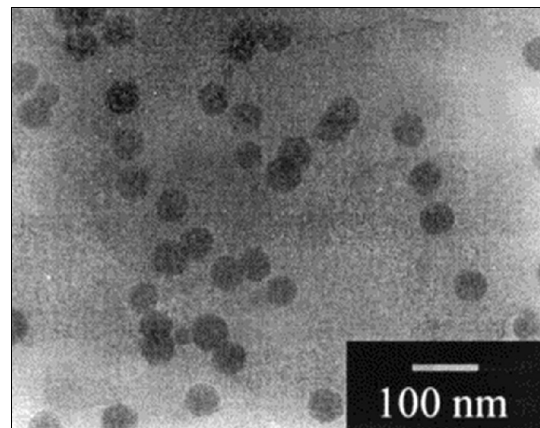


Fig. 71: TEM micrograph of PA-05-L (Borrowed from [45])

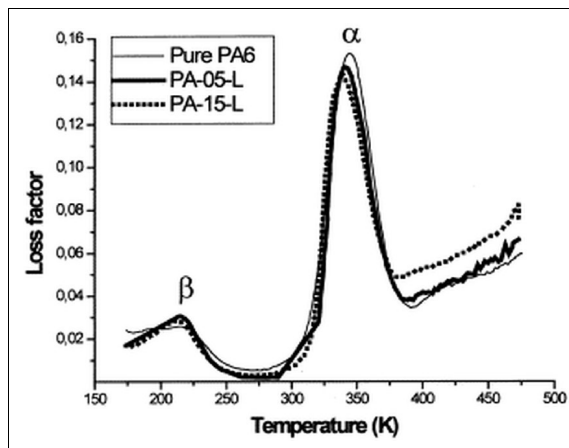


Fig. 72: Loss factor with respect to temperature (Borrowed from [45])

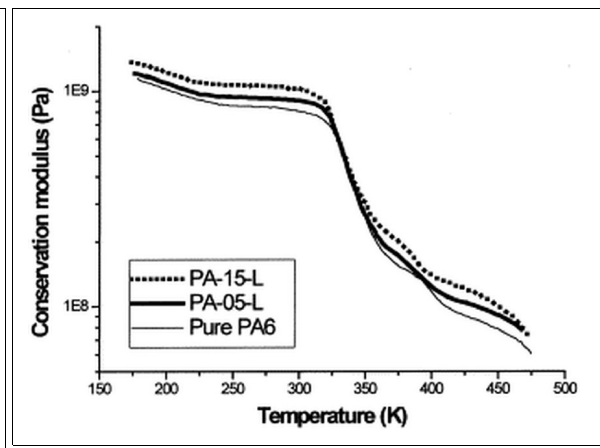


Fig. 73: Conservation modulus (G') with respect to temperature (Borrowed from [45])

¹ Only graphs were presented in [47] without summarising quantification

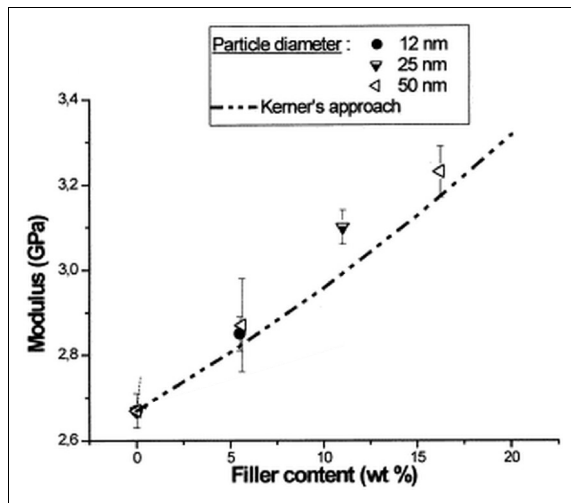


Fig. 74: The composite evolution versus the filler ratio (Borrowed from [45])

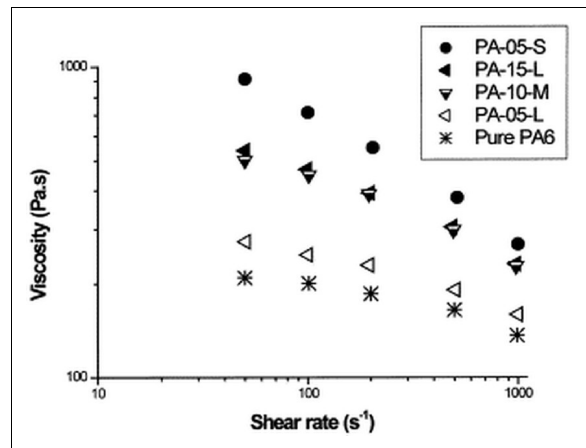


Fig. 75: Viscosity at temperature of 250 °C (Borrowed from [45])

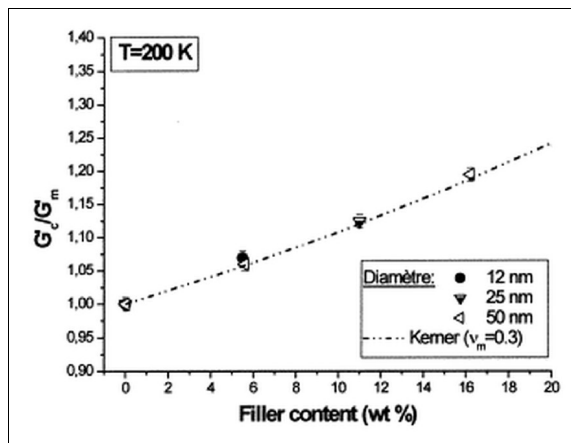


Fig. 76: Relative modulus evolution both below the main relaxation temperature of the pure matrix (Borrowed from [45])

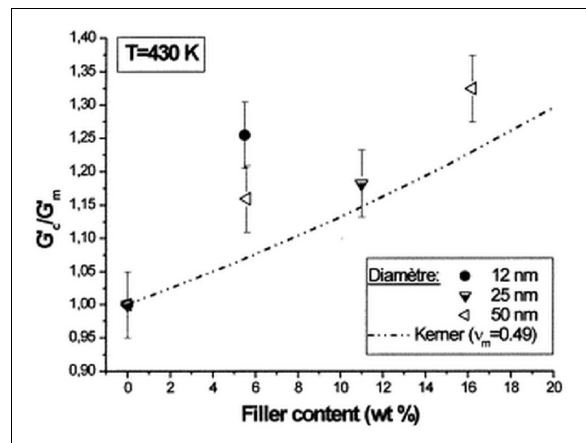


Fig. 77: Relative modulus evolution both above the main relaxation temperature of the pure matrix (Borrowed from [45])

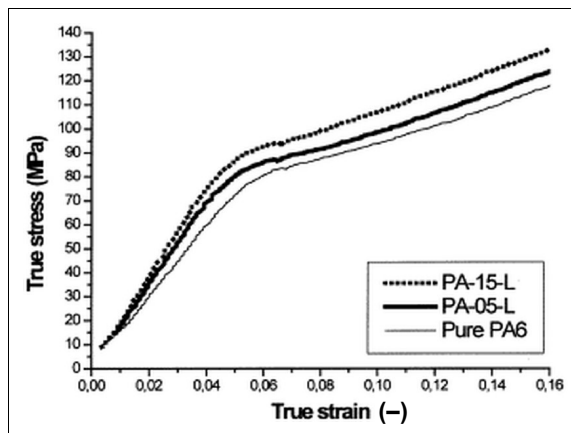


Fig. 78: Filler content influence on the mechanical behaviour in compression (Borrowed from [45])

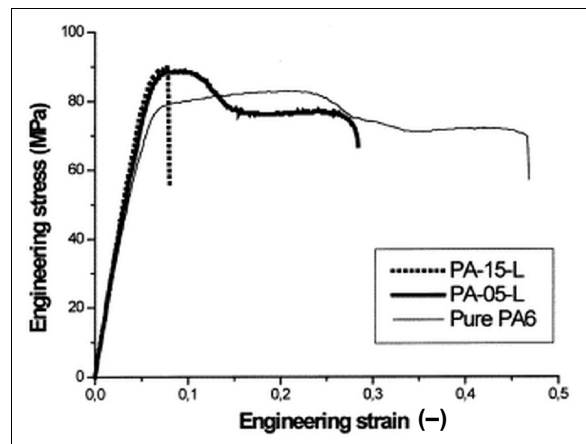


Fig. 79: Filler content influence on the mechanical behaviour in tension – systems with large particles (Borrowed from [45])

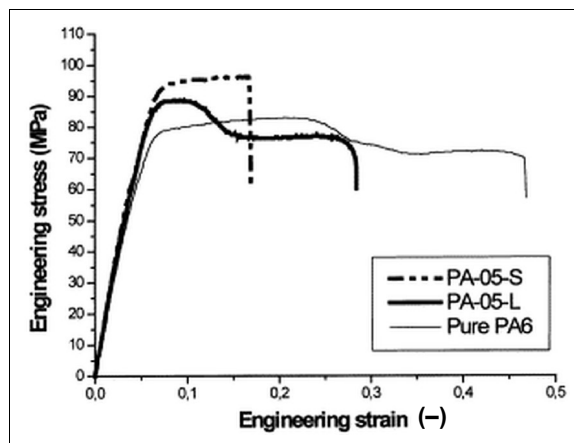


Fig. 80: Filler content influence on the mechanical behaviour in tension – low filled systems (Borrowed from [45])

García et al. [46] focused on gas penetration through nano-silica filled PA6. The membrane was prepared by solution casting of commercial Nylon-6 diluted in formic acid where silica dust was suspended. The mixture was smeared on glass and consequently placed into nitrogenous atmosphere to allow the membrane to dry. Afterwards, the measuring of CO₂ and N₂ fluxes was done using a soap bubble flow meter. It was concluded that low filling causes higher permeability but decrease the selectivity of the membranes. Conversely, higher amount of filler lowered permeabilities but kept the selectivity.

2.7 Epoxy resin/silica

Epoxy polymers are widely used for the matrices of fibre-reinforced composite materials and as adhesives. When cured, epoxides are amorphous and highly cross-linked polymers. However, the structure of cross-linked polymer also leads to a undesirable property – they are relatively brittle materials, with a poor resistance to crack initiation and growth. One of methods how to improve this disadvantage can be filling with nano-particles what was the interest of Johnsen et al. [48]. In their study the silica of mean diameter 20 nm was purchased as SiO₂ sol in the resin matrix. The polyepoxyde was standard diglycidyl ether bis-phenol A (DGEBA). The studied material was the unmodified resin and nano-silica-modified epoxy prepared by simple mixing of DGEBA with appropriate amount of nano-dust. Consequently, the curing agent (an accelerated methylhexahydro-phthalic acid anhydride) was added. Finally the mixture was poured into release-coated mould, precured at 90°C for 1 h and then cured at 160°C for 2 h.

The bulk sheets was investigated by DSC – results are summarised in Table 13. Mechanical testing such as stress-strain and Young's modulus was done as the fracture toughness

was investigated too (worked out into graphs in Fig. 81 and 82). Finally the micro-structure was observed via TEM and AFM – here presented as Fig. 83 – 85 and Fig. 88 – 91.

Table 13. Glass transition temperatures, modulus and fracture properties of the anhydride-cured epoxy polymer containing nano-particles (Based on [48])

Nanosilica content in wt. %	Nanosilica content in vol. %	T_g (°C) DSC	T_g (°C) DMTA	E (GPa)	G_{ic}^1 ($J m^{-2}$)
0	0	143	153	2.96	103
4.1	2.5	137	152	3.20	291
7.8	4.9	136	154	3.42	352
11.1	7.1	141	151	3.57	343
14.8	9.6	138	152	3.60	406
20.2	13.4	138	150	3.85	461

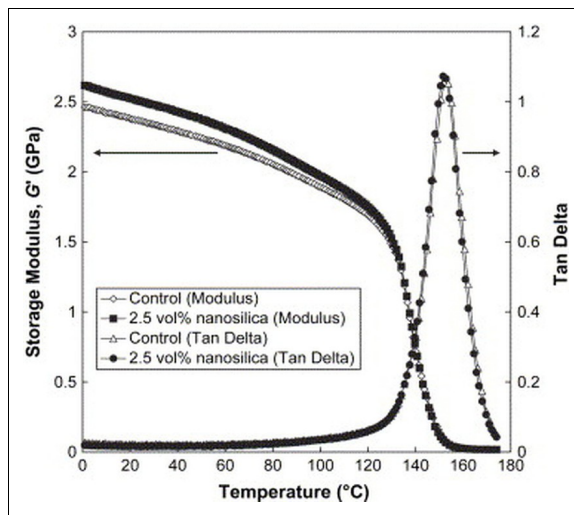


Fig. 81: DMTA data showing flexural modulus and loss factor, measured at 1 Hz. Epoxy polymer with 2.5 vol% of nano-silica (Borrowed from [48])

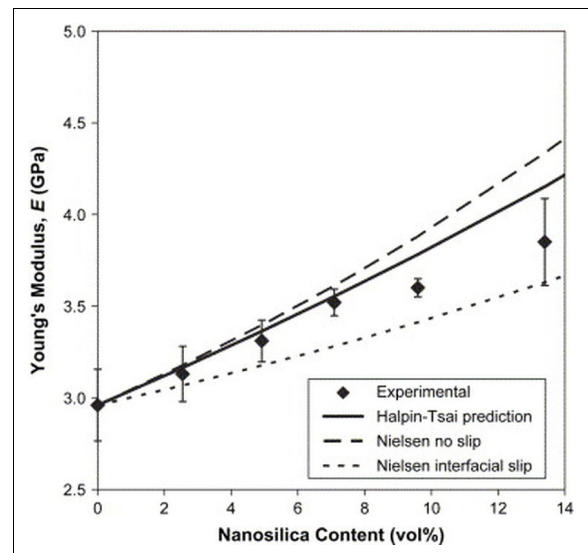


Fig. 82: Tensile modulus versus nano-silica content (Borrowed from [48])

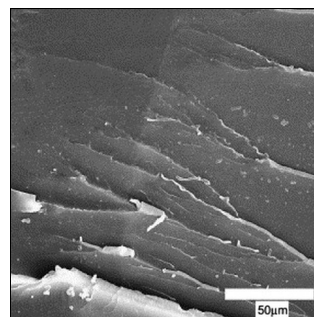


Fig. 83: SEM micrograph of fracture surface of pure epoxy (Borrowed from [48])

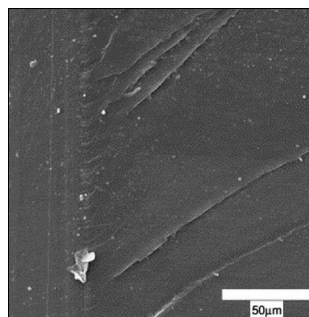


Fig. 84: SEM micrograph of fracture surface of EP/SiO₂ with 2.5 vol% (Borrowed from [48])

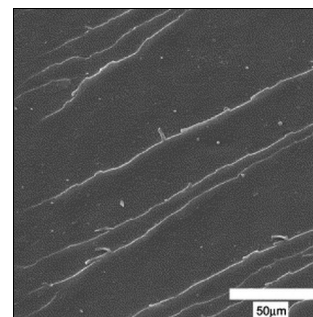


Fig. 85: SEM micrograph of fracture surface of EP/SiO₂ with 13 vol% (Borrowed from [48])

1 G_{ic} = fracture energy calculated using model – for details see [48]

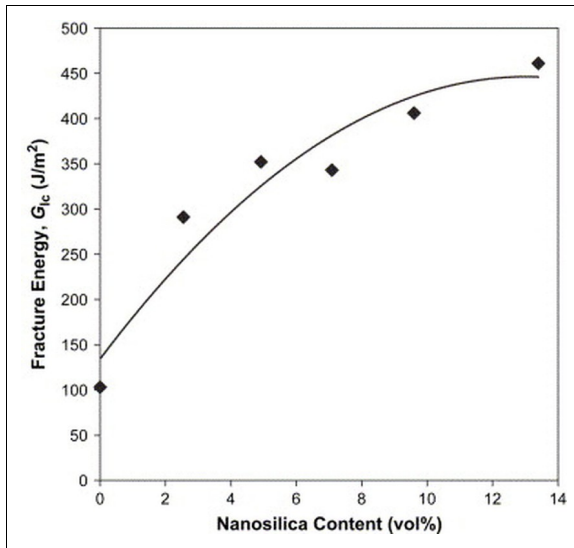


Fig. 86: Fracture energy as dependence of nano-silica content (Borrowed from [48])

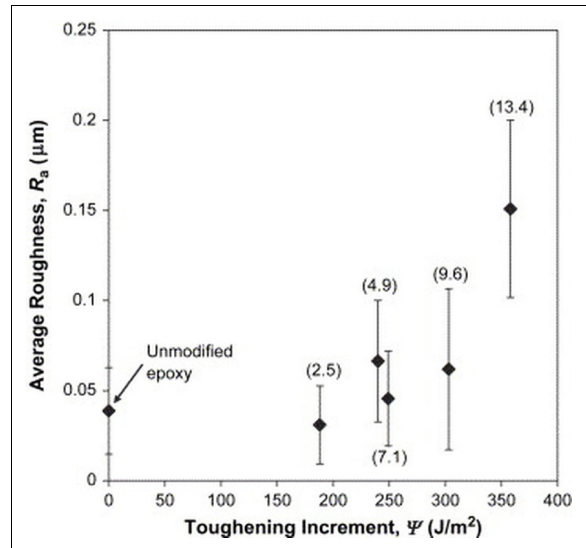


Fig. 87: Mean roughness of the fracture surface versus measured toughening increment. The numbers in brackets are the volume fractions of nano-particles. (Borrowed from [48])

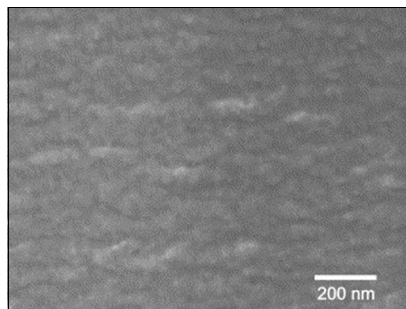


Fig. 88: SEM micrograph of the fracture surface of pure epoxy polymer (Borrowed from [48])

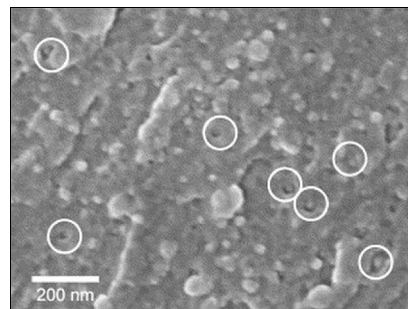


Fig. 89: SEM micrograph of the fracture surface of the epoxy polymer with 9.6 vol% silica – void particles are circled (Borrowed from [48])

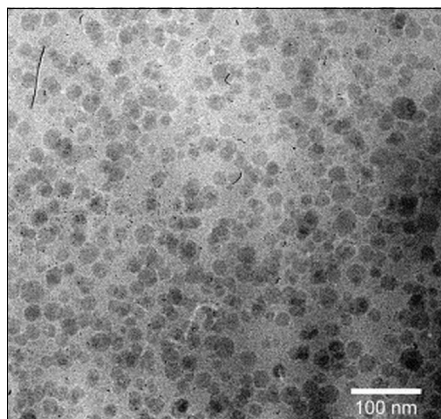


Fig. 90: TEM micrograph of the epoxy polymer containing 9.6 vol% of silica (Borrowed from [48])

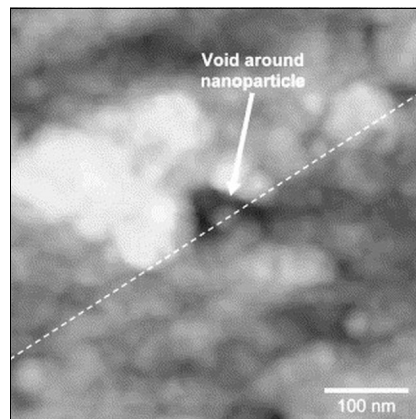


Fig. 91: AFM micrograph of fracture surface of the epoxy polymer with 9.6 vol% nano-silica (Borrowed from [48])

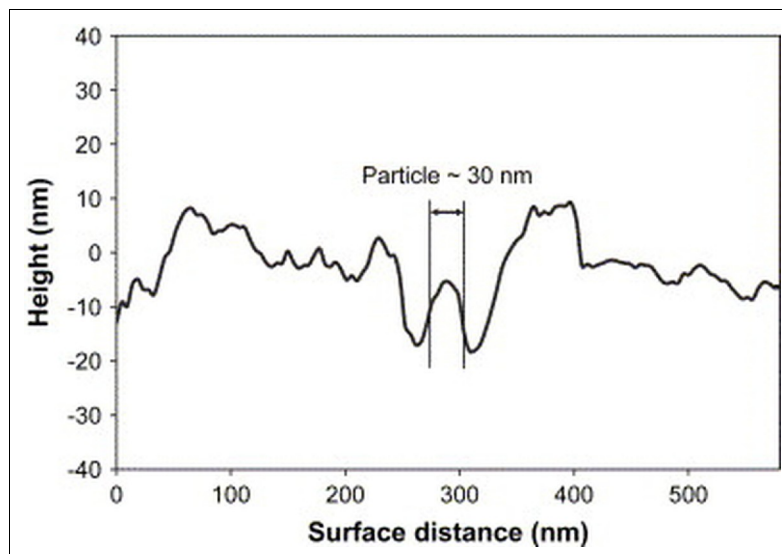


Fig. 92: Surface profile of the line drawn across the Fig. 91. (Borrowed from [48])

Johnsen et al. [48] concluded, that the glass transition temperature was not influenced by the presence of the filler as DSC and DMTA showed. From measurement of mechanical properties it was learnt that these properties were increased by addition of nano-particles. Furthermore, the calculated fracture energy increased by about 360 J/m^2 for the filling with 13 vol%. Observation of fractures by SEM and AFM brought ascertainment that the nano-particles are surrounded by voids (see Fig. 91 and 92) providing evidence of particle debonding and consequent growth of the plastic void. The model was used to confirm that this mechanisms could be the reason of toughening effect (Fig. 86). The calculated values concurred well with the measured ones (for more details see [48])

Preghenella et al. [49] discuss the phenomena of non-monotonic trends of thermo-mechanical properties. The untreated fumed silica was mixed with standard commercial DGEBA-based low molecular weight epoxy resin. This blend was consequently diluted with acetone and finally the curing agent was added and dispersed by sonication. Obtained paste was poured in Teflon mould and compressed. Testing pieces were punch-cut corresponding to appropriate standard.

DSC and TGA measuring were done as the mechanical behaviour was investigated too. Finally the SEM micrograph of fracture surfaces were obtained. Micrographs shows the existence of strong polymer-filler interactions in case of 16.7 wt% filled samples, what was suggested by acquired data from dynamic mechanical multi-frequency tests. Also in another parameters the values were decreasing as the silica content rose up to 16.7 wt%. From this load the trends are inverted. It was explained by the presence of polymer-filler

interactions which limits the cross-linking degree for low filled matrix. The inversion for high filled ones was supposed to be due to the increased physical immobilisation effects.

Preghenella et al. also mentions the possibility of different effects of nano-dust content in epoxy matrix in the range of lower or higher ratios than investigated ones (minimum was 6.3 wt%, maximum was about 17 wt%)

Influence of the curing temperature is the aim of [50] where Pascual-Sánchez and Martín-Martínez investigate epoxy/silica coatings. As in previously mentioned articles ([48], [49]) the resin was DGEBA, the isophoronediamine (IPDA) was used as a hardener and silica dust was hydrophilic AEROSIL® 200. It was found out that the addition of nano-silica decrease the gel time at any curing temperature and catalyse the curing reaction. This effect is ascribed to the formation of a nano-silica-DGEBA-IPDA network, which facilitated the creation of a silanol/oxirane ring active complex.

2.8 Polyurethane/silica

Polyurethane (PUR) is a versatile polymeric material, which can be modified to meet the diversified demands of modern technologies like coatings, adhesives, foams, reaction moulding, etc. The synthesis of polyether-based polyurethane-silica nanocomposites was the aim of Lee et al. work [51].

The composite was prepared via *in situ* polymerisation of NCO-terminated prepolymers (synthesised from 4,4'-diphenylmethane diisocyanate and poly(tetramethylene glycol) with presence of fumed silica. PUR chains were extended with butane-1,4-diol. The ratios of SiO₂ in polymer were from pure resin up to 10 wt% – and samples were abbreviated as PUR/S-1 for 1 wt%, PUR/S-3 for 3 wt%, etc. Whole process is drawn in Fig. 91, besides this the one sample with 3 wt% of silica dust was prepared by simple melt mixing with thermoplastic polyurethane¹. It was abbreviated as PUR/S-3b and was used for comparison of aggregation – see TEM micrographs (Fig. 94 – 97).

The thermal transitions and mechanical properties were investigated. The graphs are denoted as Fig. 98 – 100. Material was observed via TEM. Unfortunately, in [51] only graphs were presented and no more exact values were mentioned nor summarised in any table.

¹ Matrix was prepared as showed in Fig. 93 but without silica – nano-particles were added consequently during melt mixing.

Conclusion following from [51] is that the *in situ* preparation of the composite causes small aggregation in low ratio of filling. The tensile strength grows in dependence of nano-particles load until 3 wt% of silica. It was noted that even low filing can strongly increase the elongation against pure resin.

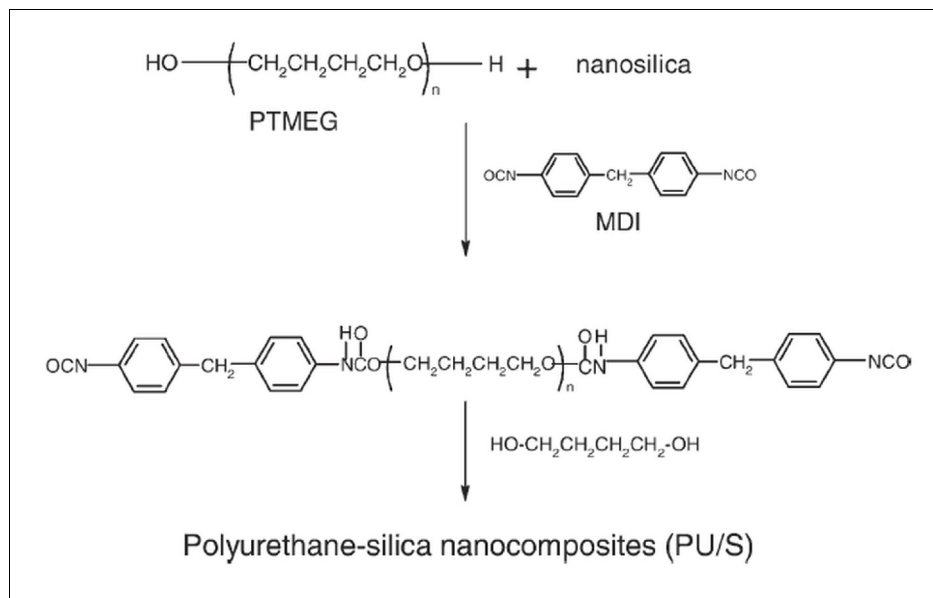


Fig. 93: Scheme of synthetic route to the PUR/S (Borrowed from [51])

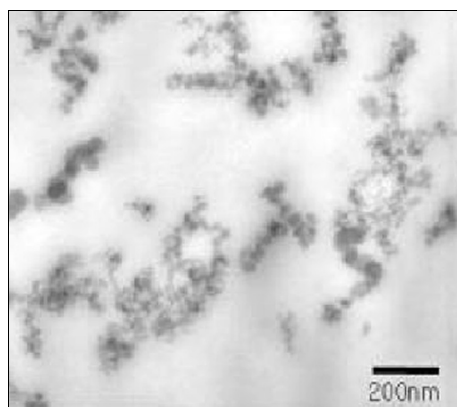


Fig. 94: TEM micrograph of PUR/S-1 (Borrowed from [51])

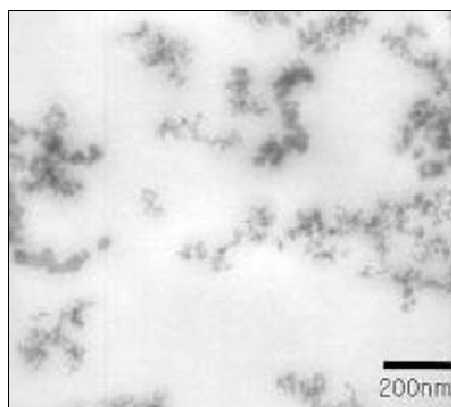


Fig. 95: TEM micrograph of PUR/S-3 (Borrowed from [51])

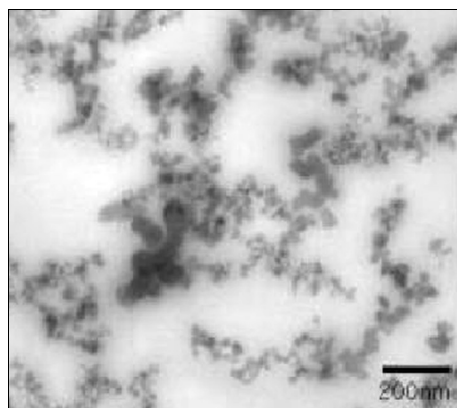


Fig. 96: TEM micrograph of PUR/S-7 (Borrowed from [51])

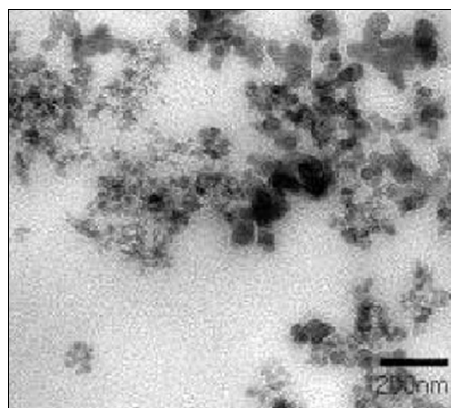


Fig. 97: TEM micrograph of PUR/S-3b (Borrowed from [51])

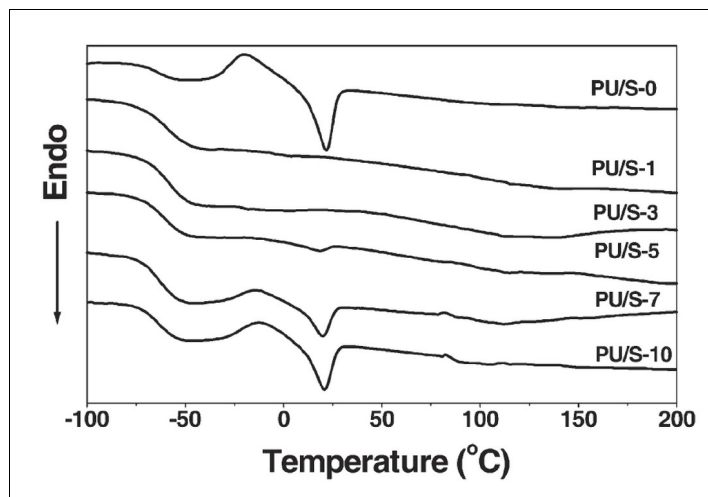


Fig. 98: DSC curves of PUR/silica nanocomposites (Borrowed from [51])

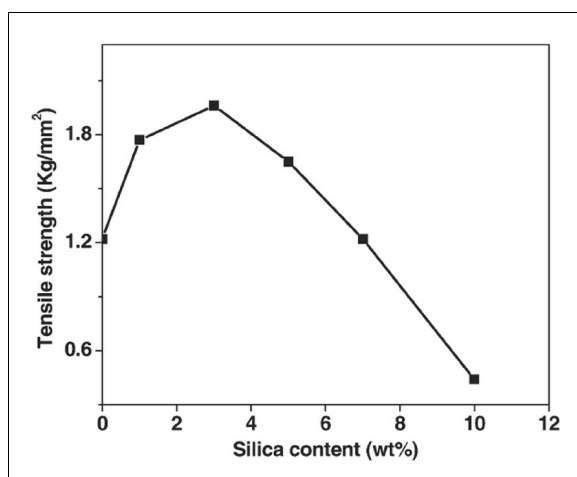


Fig. 99: Dependence of tensile strength on silica load (Borrowed from [51])

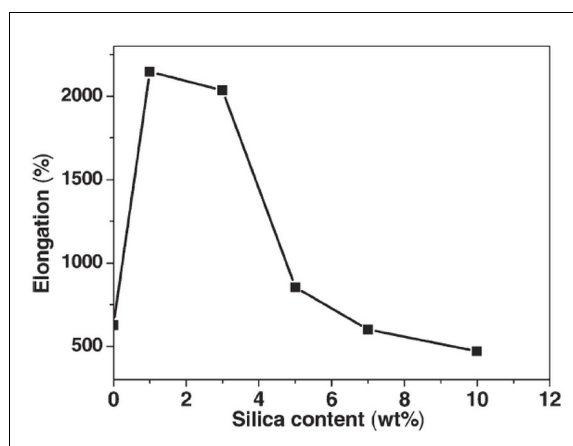


Fig. 100: Dependence of elongation on silica load (Borrowed from [51])

Chen et al. [52] have done more extended investigation of PUR/silica systems with composite prepared from particles synthesised according to Stöber's method (above described in chapter 1.1.1 or in [10]). The silica particles were introduced to form polyester polyol/nano-silica composites: One way was the dispersion of silica in monomers and then the polycondensation was carried out under the same conditions as for the preparation of pure polyester polyol. The second way was the blending method – the silica was directly immersed and mixed with fused polyester polyol resin at 160 °C by vigorous stirring.

Obtained polyester polyol/nano-silica composite was mixed with an isophorone diisocyanate trimer solution and the concentration was adjusted to 60 wt% by adding 4-methyl-pentan-2-one at room temperature. The nanocomposite coatings (about 45 μm) were prepared by casting the above mixtures onto glass substrates. The 10 μm coats were made by casting the above prepared solution onto a quartz panel using a drawdown rod.

Coatings were cured at 100°C for 30 min. and then they were kept at ambient temperature for two weeks before further investigation.

Films were characterised by FTIR and Ultraviolet-visible spectrograph (UV-vis), TGA, DMA, abrasion resistance and TEM micrographs were obtained as well.

Fig. 101 shows influence of silica particle diameter on the value of glass transition temperature of PUR/silica composite. It is clear that small particles (here up to 70 nm) increases the T_g point. Also in Fig. 102 and Fig. 103 can be seen that particles with diameter around 30 nm positively influence tensile strength and elongation at break. Moreover, these properties depend on filling ratio, which is showed in Fig. 104. Graphs representing dependency of macrohardness¹ (Fig. 105 and 106) shows analogous increases in property as tensile results dependence on particle dimension and content. Data obtained via UV-vis spectrography are here plotted at Fig 107 and 108.

Chen et al [52] concluded from these absorbance spectra that transparent nanocomposite polyurethane coatings can be obtained with improved weather resistance. Also was ascertained that UV-shielding coatings of composite prepared by *in situ* polymerisation has better attributes than the material made by melt mixing and the best properties were achieved with silica of diameter around 30 nm.

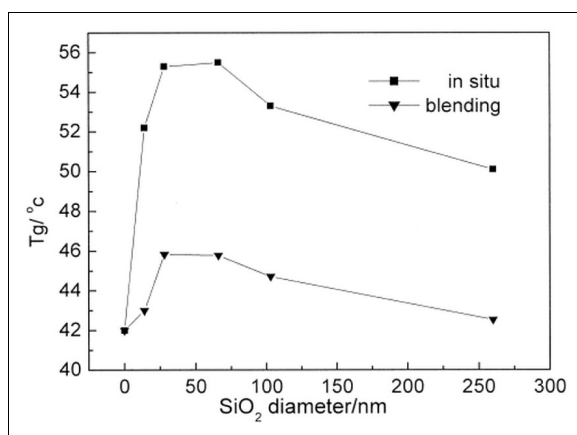


Fig. 101: Effect of silica particle size on the T_g of PUR/SiO₂ composites with 2.25 wt% SiO₂ content. (Borrowed from [52])

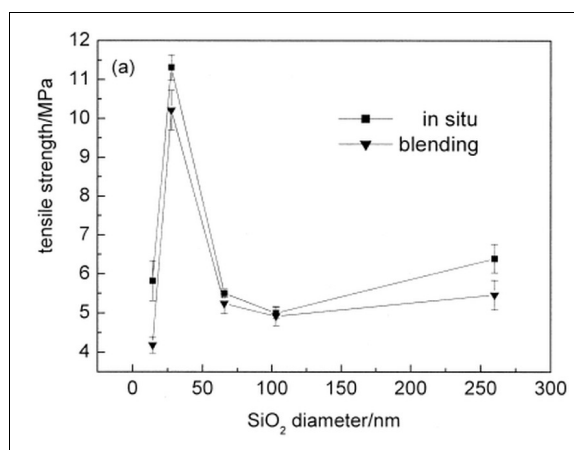


Fig. 102: Dependence of tensile strength of PUR/SiO₂ composites with 2.25 wt% SiO₂ content on silica particle diameter (Borrowed from [52])

¹ Macrohardness was determined using a pendulum hardness tester according to Chinese National Standard GB/T1730-93. Times, varying from 5 to 2° for the pendulum on the glass, with and without polymer films, were designated t and t_0 , respectively. The ratio of t/t_0 is regarded as macrohardness.

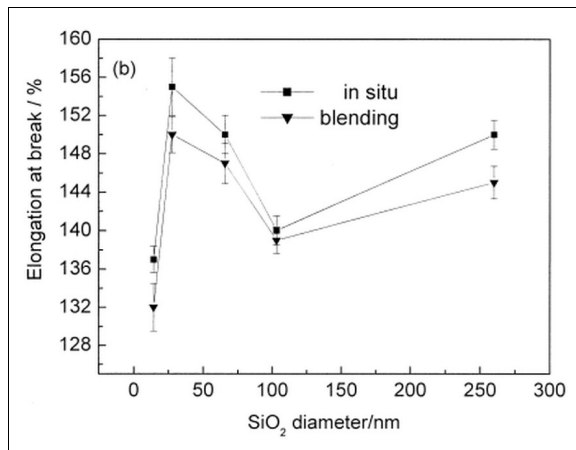


Fig. 103: Dependence of elongation at break of PUR/SiO₂ composites with 2.25 wt% SiO₂ content on silica particle diameter (Borrowed from [52])

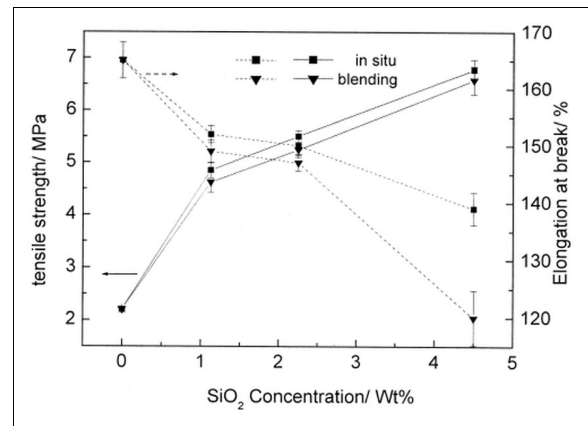


Fig. 104: Dependence of tensile strength and elongation at break of PUR/SiO₂ composites on silica concentration (silica particle size 66 nm) (Borrowed from [52])

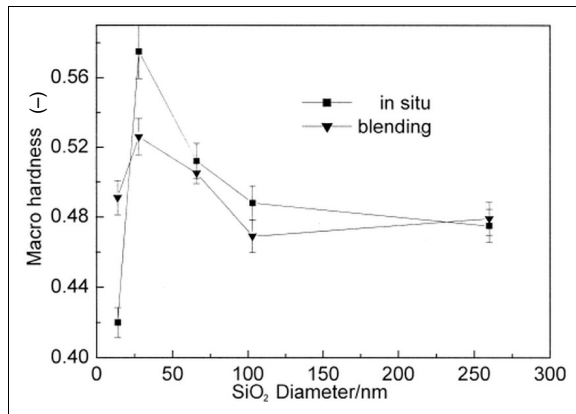


Fig. 105: Dependence of macrohardness of PUR/SiO₂ composites with 2.25 wt% SiO₂ content on silica particle diameter (Borrowed from [52])

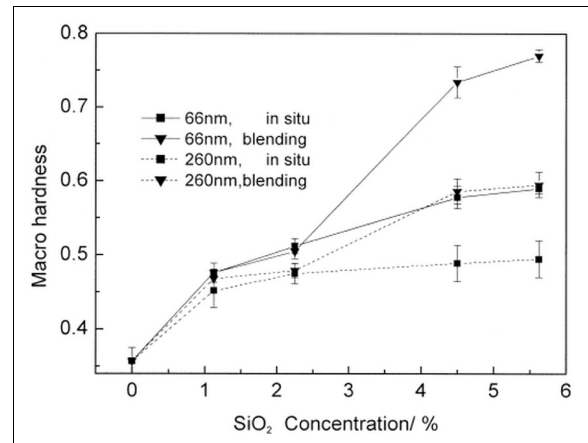


Fig. 106: Dependence of macrohardness of PUR/SiO₂ composites on silica particles load in wt% (Borrowed from [52])

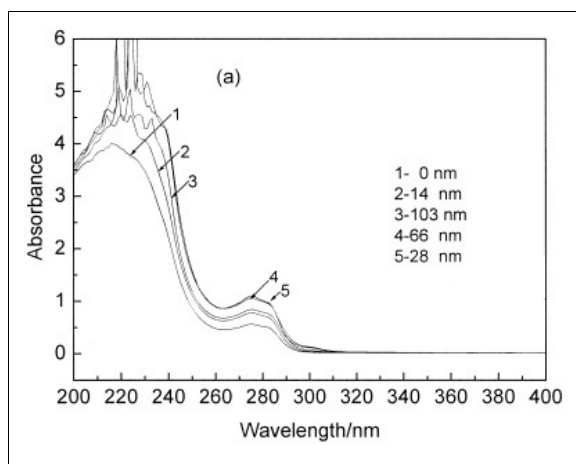


Fig. 107: Absorbance spectra of PUR/SiO₂ composites as a function of particle size embedded by in situ polymerization (Borrowed from [52])

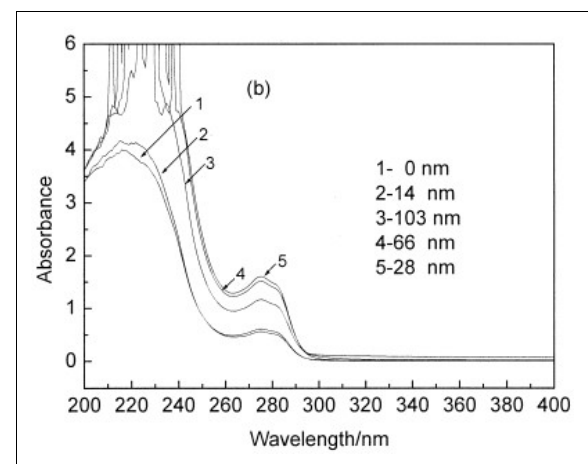


Fig. 108: Absorbance spectra of PUR/SiO₂ composites as a function of particle size embedded by blending polymerization (Borrowed from [52])

Xiang et al. [53] obtained similar conclusions in the study of properties of nano-silica-reinforced PUR for grouting.

The comparison of composites filled with micro-silica and nano-silica was given by Petrović et al. [54]. Several blends of PUR with nano-particles at different weight ratio of silica dust were prepared and compared with control series of samples prepared with micron-size particles. Petrović concluded that PUR/nano-silica materials were transparent at all the investigated loads of filler. Also as it was mentioned above, the mechanical properties of PUR matrix were significantly improved in comparison to micron-size silica particles. Even though the nano-silica showed stronger interaction with the polymer and water than the “conventional” filler, there were no cardinal differences in the dielectric behaviour between the two series of composites.

CONCLUSION

The aim of this bachelor thesis was to bring short literary study focused on the modification of polymeric matrices with silica particles of nanometre size. Search was done in several on-line databases of articles and book chapters including following publishers: John Wiley & Sons, Ltd., Elsevier, Ltd., and American Chemical Society as well.

As the spectra of available polymers is broad, only several main types were here described. It was learnt that in most cases filling with silica nano-dust brings mechanical improvement, as against pure matrix, namely tensile strength or notched impact stress. Presence of particles also modify rheological behaviour – for example the disappearance of “gel” behaviour or plateau of loss modulus in the low frequency range, what was observed in nanocomposite system PS/silica. Finally, in some types of degradations silica can effectively inhibit process of macromolecule destruction.

Dependences of thermal transitions of such gained materials with respect to filler load, mean particle size and surface modifications were observed. In many cases (LLDPE, PMMA, PET, PUR) the increase of glass transition temperature or melt temperature was noted. Whereas in another matrices (PP, PA) the presence of silica has negligible effect on characteristic temperatures. The formation of spherulites in semi-crystalline resins was also the object of interests. Ascertainments followed from these investigations were that silica can increase the rate of nucleation however the rate of spherulite growth is not influenced.

In many articles used in this thesis was played up the fact that less than several percent (mainly 0.5 wt% – 5 wt%) of nano-sized particles are needed to incur the same modification effect as with the micro-sized ones is reached with load about 20 wt%.

The stability and good dispersion in polymer matrix can be achieved by surface modifications of primarily particles – mainly by silane coupling agents. Dramatical improvements could be achieved by grafting macromolecular chains of same nature as the matrix is. This means that not only the same grafted polymer as matrix is – for example in chapter 2.5.1. where PET filled with silica grafted by PS was described.

BIBLIOGRAPHY

- [1] THOSTENSON, E.T., LI, C., CHOU, T. Nanocomposites in context. *Composites Science and Technology*, 2005, vol. 65, p. 491-516.
- [2] ROTHON, R.N., ROGER, N. *Particulate fillers for polymers*. Shrewsbury: Rapra, 2001. ISBN 185957310X
- [3] NAGANUMA, T., KAGAWA, Y. Effect of particle size on the optically transparent nano meter-order glass particle-dispersed epoxy matrix composites. *Composites Science and Technology*, 2002, vol. 62, p. 1187–1189.
- [4] GREENWOOD, N.N., EARNSHAW, A. *Chemie prvku*. Praha: Informatorium, 1993. ISBN 8085427389
- [5] *Quartz - SiO₂* [online]. [cit. 2007-03-26].
<<http://www.auburn.edu/~hameswe/Quartzpage.html>>.
- [6] *Silica Polymorphs* [online]. [cit. 2007-03-26].
<<http://www.uwsp.edu/geo/projects/geoweb/participants/dutch/PETROLOGY/Silica%20Poly.HTM>>.
- [7] *Tectosilicates* [online]. [cit. 2007-03-26].
<<http://www.geoclassroom.com/mineralogy/tectosilicates.html>>.
- [8] *Biogenic silica* [online]. [cit. 2007-03-26].
<http://en.wikipedia.org/wiki/Biogenic_silica>.
- [9] KNECHT, M.R., WRIGHT, D.W. Amine-terminated dendrimers as biomimetic templates for silica nanosphere formation. *Langmuir*, 2004, vol. 11, p. 4728-4732.
- [10] STÖBER, W., FINK, A., BOHN, E. Controlled growth of monodisperse silica spheres in the micron size range. *Journal of Colloid and Interface Science*, 1968, vol. 26, p. 62-69.
- [11] BOGUSH, G.H., TRACY, M.A., ZUKOSKI C.F. Preparation of monodisperse silica particles: Control of size and mass fraction. *Journal of Non-Crystalline Solids*, 1988, vol. 104, p. 95-106.
- [12] *Technical bulletin: Fine particles*. Degussa AG. Vol. 11. [online]
<<https://www.aerosil.com/page/en/literature>>
- [13] ULRICH, G. D., RIEH, J. W. Aggregation and growth of submicron oxide particles in flames. *Journal of Colloid and Interface Science*, 1982, vol. 87, p. 257-265.

- [14] BALABANOVA E. Mechanism of nanoparticle generation by high-temperature methods. *Vacuum*, 2000, vol. 58, p. 174-182.
- [15] BALABANOVA E. Nanoparticle production under conditions of a non-isothermal aerosol flow reactor. *Vacuum*, 2003, vol. 69, p. .
- [16] WYPYCH, G. *Handbook of Fillers*. Toronto: ChemTec Publishing, 1999. ISBN 1884207693
- [17] ZHANG G. ET AL. Silica nanobottles templated from functional polymer spheres. *Journal of Colloid and Interface Science*, 2003, vol. 263, p. 467-472.
- [18] CHEN, X., CUI, Z., CHEN, Z., ZHANG, K., LU, G., ZHANG, G., YANG, B. The synthesis and characterization of monodisperse cross-linked polymer microspheres with carbonyl on the surface. *Polymer*, 2002, vol. 43, p. 4147-1452.
- [19] IJIMA, M., TSUKADA, M., KAMIYA, H. Effect of particle size on surface modification of silica nanoparticles by using silane coupling agents and their dispersion stability in methylethylketone. *Journal of Colloid and Interface Science*, 2007, vol. 307, p. 418-424.
- [20] HASENZ AHL, S., BRAUNAGEL, A. New and innovative silica based formulation concepts for color cosmetics. Degussa AG. [online]
<<https://www.aerosil.com/page/en/literature>>
- [21] BAGWE, R.P., HILLIARD, L.R., TAN, W. Surface modification of silica nanoparticles to reduce aggregation and nonspecific binding. *Langmuir*, 2006, vol. 22, p. 4357-4362.
- [22] TAKAHASHI, S., PAUL, D.R. Gas permeation in poly(ether imide) nanocomposite membranes based on surface-treated silica. Part 2: With chemical coupling to matrix. *Polymer*, 2006, vol. 47, p. 7535-7547.
- [23] OSSENKAMP, G.C., KEMMITT, T., JOHNSTON, J.H. New approaches to surface-alkoxylated silica with increased hydrolytic stability. *Chemistry of materials*, 2001, vol. 11, p. 3975-3980.
- [24] SHIMADA, T., AOKI, K., SHINODA, YO., NAKAMURA, T., TOKUNAGA, N., INAGAKI, S., HAYASHI, T. Functionalization on silica gel with allylsilanes. A new method of covalent attachment of organic functional groups on silica gel. *Journal of American chemical society*, 2003, vol. 16, p. 4688-4689.

- [25] EL HARRAK, A., CARROT, G., OBERDISSE, J., EYCHENNE-BARON, C., BOUE, F. Surface-atom transfer radical polymerization from silica nanoparticles with controlled colloidal stability. *Macromolecules*, 2004, vol. 37, p. 6376-6384.
- [26] AVELLA, M., BONDIOLI, F., CANNILLO, V., PACE, E., ERRICO, M.E., FERRARI, A.M., FOCHER, B., MALINCONICO, M. Poly(ϵ -caprolactone)-based nanocomposites: Influence of compatibilization on properties of poly(ϵ -caprolactone)-silica nanocomposites. *Composites Science and Technology*, 2006, vol. 66, p. 886-894.
- [27] CAI, L.F., HUANG, X.B., RONG, M.Z., RUAN, W.H., ZHANG, M.Q. Effect of grafted polymeric foaming agent on the structure and properties of nano-silica/polypropylene composites. *Polymer*, 2006, vol. 47, p. 7043-7050.
- [28] YOKOYAMA, R., SUZUKI, S., SHIRAI, K., YAMAUCHI, T., TSUBOKAWA, N., TSUCHIMOCHI, M. Preparation and properties of biocompatible polymer-grafted silica nanoparticle. *European Polymer Journal*, 2006, vol. 42, p. 3221-3229.
- [29] RONG, M.Z., ZHANG, M.Q., ZHENG, Y.X., ZENG, H.M., WALTER, R., FRIEDRICH, K. Structure-property relationships of irradiation grafted nanoinorganic particle filled polypropylene composites. *Polymer*, 2001, vol. 42, p. 167-183.
- [30] KONTOU, E., NIAOUNAKIS, M. Thermo-mechanical properties of LLDPE/SiO₂ nanocomposites. *Polymer*, 2006, vol. 47, p. 1267-1280.
- [31] ZHANG, M.Q., RONG, M.Z., ZHANG, H.B., FRIEDRICH, K. Mechanical properties of low nano-silica filled high density polyethylene composites. *Polymer engineering and science*, 233, vol. 43, p. 490-500.
- [32] WU, C.L., ZHANG, M.Q., RONG, M.Z., FRIEDRICH, K. Tensile performance improvement of low nanoparticles filled-polypropylene composites. *Composites science and technology*, 2002, vol. 62, p. 1327-1340.
- [33] WU, C.L., ZHANG, M.Q., RONG, M.Z., FRIEDRICH, K. Silica nanoparticles filled polypropylene: effects of particle surface treatment, matrix ductility and particle species on mechanical performance of the composites. *Composites science and technology*, 2005, vol. 65, p. 635-645.
- [34] ZHOU, H.J., RONG, M.Z., ZHANG, M.Q., RUAN, W.H., FRIEDRICH, K. Role of Reactive Compatibilization in Preparation of Nanosilica/Polypropylene Composites.

- Polymer engineering and science*, 2007, vol. 47, p. 499-509.
- [35] NITTA, K., ASUKA, K., LIU, B., TERANO, M. The effect of the addition of silica particles on linear spherulite growth rate of isotactic polypropylene and its explanation by lamellar cluster model. *Polymer*, 2006, vol. 47, p. 6457-6463.
- [36] BARTHOLOME, C., BEYOU, E., BOURGEAT-LAMI, E., CASSAGNAU, P., CHAUMONT, P., DAVID, L., ZYDOWICZ, N. Viscoelastic properties and morphological characterization of silica/polystyrene nanocomposites synthesized by nitroxide-mediated polymerization. *Polymer*, 2005, vol. 46, p. 9965-9973.
- [37] DAGRÉOU, S., KASSEH, A., ALLAL, A., MARIN, G., AÏT-KADI, A. Linear viscoelastic properties of suspensions of rigid hairy particles in a polymeric matrix. *The Canadian journal of chemical engineering*, 2002, vol. 80, p. 1126-1134.
- [38] LIU, Y.L., HSU, C.Y., HSU, K.Y. Poly(methylmethacrylate)-silica nanocomposites films from surface-functionalized silica nanoparticles. *Polymer*, 2005, vol. 46, p. 1851-1856.
- [39] GARCÍA, N., CORRALES, T., GUZMÁN, J., TIEMBLO, P. Understanding the role of nanosilica particle surface in the thermal degradation of nanosilica-poly(methyl methacrylate) solution-blended nanocomposites: From low to high silica concentration. *Polymer degradation and stability*, 2007, vol. 92, p. 635-643.
- [40] YANG, F., NELSON, G.L. PMMA/Silica nanocomposite studies: Synthesis and Properties. *Journal of applied polymer science*, 2004, vol. 91, p. 3884-3850.
- [41] LIU, W., TIAN, X., CUI, P., LI, Y., ZHENG, K. YANG, Y. Preparation and characterisation of PET/Silica nanocomposites. *Journal of applied polymer science*, 2004, vol. 91, p. 1229-1232.
- [42] WU, T., KE, Y. Melting, crystallization and optical behaviors of poly(ethylene terephthalate)-silica/polystyrene nanocomposite films. *Thin solid films*, 2007, vol. 515, p. 5220-5226.
- [43] CHE, J., LUAN, B., YANG, X., LU, L., WANG, X. Graft polymerization onto nano-sized SiO₂ surface and its application to the modification of PBT. *Materials letters*, 2005, vol. 59, p. 1603-1609.
- [44] YANG, F., OU, Y., YU, Z. Polyamide 6/Silica nanocomposites prepared by in situ polymerization. *Journal of applied polymer science*, 1998, vol. 69, p. 355-361.

- [45] REYNAUD, E., JOUEN, T., GAUTHIER, C., VIGIER, G., VARLET, J. Nanofillers in polymeric matrix: a study on silica reinforced PA6. *Polymer*, 2001, vol. 42, p. 8759-8768.
- [46] GARCÍA, M., BARSEMA, J., GALINDO, R.E., CANGIALOSI, D., GARCIA-TURIEL, J., VAN ZYL, W.E., VERWEIJ, H., BLANK, D.H.A. Hybrid organic inorganic nylon-6/SiO₂ nanocomposites: Transport properties. *Polymer engineering and science*, 2004, vol. 44, p. 1240-1248.
- [47] REYNAUD, E., JOUEN, T., GAUTHIER, C., VIGIER, G., VARLET, J. Nanofillers in polymeric matrix: a study on silica reinforced PA6. *Polymer*, 2001, vol. 42, p. 8759-8768.
- [48] JOHNSEN, B.B., KINLOCH, A.J., MOHAMED, R.D., TAYLOR, A.C., SPRENGER, S. Toughening mechanism of nanoparticle-modified epoxy polymers. *Polymer*, 2007, vol. 48, p. 530-541.
- [49] PREGHENELLA, M., PEGORETTI, A., MIGLIARESI, C. Thermo-mechanical characterisation of fumed silica-epoxy nanocomposites. *Polymer*, 2005, vol. 46, p. 12065-12072.
- [50] PASCUAL-SÁNCHEZ, V., MARTÍN-MARTÍNEZ, J.M. Influence of the curing temperature in the mechanical and thermal properties of nanosilica filled epoxy resin coating. *Macromolecular symposia*, 2006, vol. 233, p. 137-146.
- [51] LEE, S.I., HAHN, Y.B., NAHM, K.S., LEE, Y.S. Synthesis of polyether-based polyurethane-silica nanocomposites with high elongation property. *Polymers for advanced technologies*, 2005, vol. 16, p. 328-331.
- [52] CHEN, Y., ZHOU, S., YANG, H., WU, L. Structure and properties of polyurethane/nanosilica composites. *Journal of applied polymer science*, 2005, vol. 95, p. 1032-1039.
- [53] XIANG, X.J., QIAN, J.W., YANG, W.Y., FANG, M.H., QIAN, X.Q. Synthesis and properties of nanosilica-reinforced polyurethane for grouting. *Journal of applied polymer science*, 2006, vol. 100, p. 4333-4337.
- [54] PETROVIĆ, Z.S., JAVNI, I., WADDON, A., BÁNHEGYI, G. Structure and properties of polyurethane-silica nanocomposites. *Journal of applied polymer science*, 2000, vol. 76, p. 133-151.

LIST OF SYMBOLS AND ABBREVIATIONS

AFM	atomic force microscopy
CL	chemiluminescence
DGEBA	diglycidyl ether bis-phenol A
DLS	dynamic light scattering
DMTA	dynamic mechanical thermal analysis
DSC	differential scanning calorimetry
E	complex Young's modulus
E'	storage modulus
E''	loss modulus
E _c	modulus of the composite
E _m	modulus of pure matrix
FTIR	Fourier transform infra-red spectroscopy
G	complex shear modulus
G'	storage shear modulus
G''	loss shear modulus
G _{ic}	calculated fracture energy
HDPE	high density polyethylene
iPP	isotactic polypropylene
LLDPE	linear low density polyethylene
MFI	melt flow index
MMA	methyl methacrylate
M _n	number average molecular weight
M _w	weight average molecular weight
PA	polyamide
PBA	poly(butyl acrylate)
PBT	poly(butylene terephthalate)
PCL	polycaprolactame
PE	polyethylene
PEA	poly(ethyl acrylate)
PET	poly(ethylene terephthalate)
PMMA	poly(methyl methacrylate)
PP	polypropylene
PS	polystyrene
PUR	polyurethane
SAXS	small angle X-ray scattering

SEM	scanning electron microscopy
T_{β}	β -transition temperature
T_{γ}	γ -transition temperature
$T_{b/2}$	half width temperature of crystallization peak
T_c	crystallization temperature
T_{cc}	cold crystallization temperature from the glass state
TEM	transmission electron microscopy
TEOS	tetraethyl orthosilicate
T_g	glass transition temperature
TGA	thermogravimetric analysis
T_m	melting temperature
WAXS	wide angle X-ray scattering
x_c	crystallinity
ΔH_c	heat of crystallization
ΔH_m	heat of fusion

LIST OF PICTURES

Fig. 1: Models of structure of α -quartz and β -quartz. (Borrowed from [5]).....	9
Fig. 2: Models of a) α -tridymite and b) α -quartz. (Borrowed from [6]).....	9
Fig. 3: Structure of α -cristobalite. (Borrowed from [7]).....	9
Fig. 4: Relations between crystal modifications of silica. (Reprinted from [4]).....	10
Fig. 5: Picture of diatoms trough the microscope. (Borrowed from [8]).....	10
Fig. 6: Production of fumed silica – flow chart.....	13
Fig. 7: Scheme of silica nano-bottle preparation. (Borrowed from [17]).....	14
Fig. 8: Interactions between silanol groups: 1. free groups, 2. geminal group, 3. bridged groups, 4. siloxane group. (Reprinted from [12]).....	15
Fig. 9: The effect of particle curvature on surface silanol structure and the accessibility of water molecules. (a) bridged groups, (b) isolated groups. (Reprinted from [19]).....	16
Fig. 10: Substitution of silanol hydrogen by organic silicon.....	16
Fig. 11: The difference between hydrophilic silica and hydrophobic silica silylate (the amount of water and dust is always the same). (Borrowed from [20]).....	17
Fig. 12: Esterification of the particle surface. (Based on schemes in [21], [22]).....	18
Fig. 13: Reaction studied by Shimada et al. (Based on schemes in [24]).....	18
Fig. 14: Silica surface treatment studied by El Harrak et al. (Scheme based on [25]).....	19
Fig. 15: Grafting poly(ϵ -caprolactone) on silica surface. (Scheme based on [26]).....	20
Fig. 16: Grafting of silica onto poly(ether imide) chain. (Scheme based on [22]).....	21
Fig. 17: SEM micrograph of the mLLDPE/SiO ₂ nanocomposites with the silica content of 4 wt%. (Borrowed from [30]).....	22
Fig. 18: SEM micrograph of the mLLDPE/SiO ₂ nanocomposites with the silica content of 8 wt%. (Borrowed from [30]).....	22
Fig. 19: SEM micrograph of the zLLDPE/SiO ₂ nanocomposites with the silica content of 4 wt%. (Borrowed from [30]).....	23
Fig. 20: SEM micrograph of the zLLDPE/SiO ₂ nanocomposites with the silica content of 8 wt%. (Borrowed from [30]).....	23
Fig. 21: Storage modulus (E') dependence on temperature of the mLLDPE/SiO ₂ nanocomposites at frequency of 1 Hz. Percentages are percent by weight of particles load. (Borrowed from [30]).....	23
Fig. 22: Storage modulus (E') dependence on temperature of the zLLDPE/SiO ₂ nanocomposites at frequency of 1 Hz. Percentages are percent by weight of particles load. (Borrowed from [30]).....	24

- Fig. 23: Loss modulus (E'') dependence on temperature of the mLLDPE/SiO₂ nanocomposites at frequency of 1 Hz. Percentages are percent by weight of particles load. The curves are shifted in the y-direction to make them distinguishable. (Borrowed from [30])..... 24
- Fig. 24: Loss modulus (E'') dependence on temperature of the zLLDPE/SiO₂ nanocomposites at frequency of 1 Hz. Percentages are percent by weight of particles load. The curves are shifted in the y-direction to make them distinguishable. (Borrowed from [30])..... 25
- Fig. 25: Tensile stress–strain curves of the mLLDPE/SiO₂ nanocomposites. Percentages are percent by weight of particles load. (Borrowed from [30])..... 26
- Fig. 26: Tensile stress–strain curves of the mLLDPE/SiO₂ nanocomposites in the low strain range – detail indicated by rectangle in Fig. 25. Percentages are percent by weight of particles load. (Borrowed from [30])..... 26
- Fig. 27: Tensile stress–strain curves of the zLLDPE/SiO₂ nanocomposites. Percentages are percent by weight of particles load. (Borrowed from [30])..... 27
- Fig. 28: Tensile stress–strain curves of the mLLDPE/SiO₂ nanocomposites in the low strain range – detail indicated by rectangle in Fig. 27. Percentages are percent by weight of particles load. (Borrowed from [30])..... 27
- Fig. 29: Young's modulus of HDPE reinforced by different modifications of silica (Borrowed from [31])..... 29
- Fig. 30: Notched charpy impact strength of HDPE reinforced by different modifications of silica (Borrowed from [31])..... 29
- Fig. 31: Tensile properties of PP composites as a function of nano-SiO₂ volume fraction: (a) Young's modulus, (b) tensile strength, (c) elongation at break, and (d) area under stress–strain curve. Crosshead speed was 50 mm·min⁻¹. (Borrowed from [32])..... 30
- Fig. 32: SEM pictures of tensile fractured surface of: (a) neat PP; (b) and (c) PP/SiO₂ (silica content 0.86 vol%) at different magnification; (d) PP/SiO₂-g-PS (silica content 1.06 vol%); (e) PP/SiO₂-g-PEA (silica content 0.86 vol%) (Borrowed from [32])..... 30
- Fig. 33: SEM micrographs of tensile fractured surface of: (a) and (b) PP/SiO₂ (silica content 2.74 vol%); (c) and (d) PP/SiO₂-g-PS (silica content 2.75 vol%); (e) and (f) PP/SiO₂-g-PEA (silica content 2.75 vol%). Micrographs are at different magnitudes. (Borrowed from [32])..... 31
- Fig. 34: Young's modulus as a function of silica content (Borrowed from [33])..... 32

Fig. 35: Elongation at break as a function of silica content (Borrowed from [33]).....	32
Fig. 36: Tensile strength as a function of silica content (Borrowed from [33]).....	32
Fig. 37: Impact strength as a function of silica content (Borrowed from [33]).....	32
Fig. 38: Young's modulus versus silica content – the comparison of different silica types: p-SiO ₂ – precipitated and f-SiO ₂ – fumed silica (Borrowed from [33]).....	33
Fig. 39: Tensile strength versus silica content – the comparison of different silica types: p-SiO ₂ – precipitated and f-SiO ₂ – fumed silica (Borrowed from [33]).....	33
Fig. 40: Elongation at break versus silica content – the comparison of different silica types: p-SiO ₂ – precipitated and f-SiO ₂ – fumed silica (Borrowed from [33]).....	33
Fig. 41: Impact strength versus silica content – the comparison of different silica types: p-SiO ₂ – precipitated and f-SiO ₂ – fumed silica (Borrowed from [33]).....	33
Fig. 42: TEM micrograph of untreated SiO ₂ /PP (silica particles load 3 wt%) (Borrowed from [34]).....	34
Fig. 43: TEM micrograph of untreated SiO ₂ /PP (silica particles load 5 wt%) (Borrowed from [34]).....	34
Fig. 44: TEM micrograph of SiO ₂ -g-PGMA/PP (particles load 3 wt%) (Borrowed from [34]).....	34
Fig. 45: TEM micrograph of SiO ₂ -g-PGMA/PP-g-NH ₂ /PP (particles load 3 wt%) (Borrowed from [34]).....	34
Fig. 46: Results of mechanical tests of different blends. The highest material property of blends was observed with presented particle volume ratio. (Borrowed from [34])....	35
Fig. 47: The dependence of the spherulite growth rates on silica content isothermally measured at 407K. (Borrowed from [35]).....	37
Fig. 48: The dependence of the spherulite growth rates on silica content isothermally measured at 403K. (Borrowed from [35]).....	37
Fig. 49: The dependence of the spherulite growth rates on silica content isothermally measured at 399K. (Borrowed from [35]).....	37
Fig. 50: The scheme of grafting silica by PS chains (Borrowed from [36]).....	38
Fig. 51: TEM micrograph of unmodified silica gel (Borrowed from [36]).....	39
Fig. 52: TEM micrograph of PS/silica gel – sample 3 (Borrowed from [36]).....	39
Fig. 53: Complex shear modulus versus frequency: Master curves (T _{ref} = 160°C). PS-grafted silica (●G', ■G'') (sample 2) and polystyrene matrix (–). (Borrowed from [36]).....	40
Fig. 54: Complex shear modulus versus frequency: Master curves (T _{ref} = 160 °C). PS-	

grafted silica (○G', □G'') (sample 3) and polystyrene matrix (-). (Borrowed from [36]).....	40
Fig. 55: Complex shear modulus versus frequency: Master curves (Tref = 160 °C). PS-grafted silica (●G', ■G'') (sample 1) and polystyrene matrix (-). (Borrowed from [36])	41
Fig. 56: Storage shear modulus of blends of polystyrene and PS-grafted silica (samples 1 – 3 in Table 7) (Borrowed from [36]).....	41
Fig. 57: SEM micrographs: a) pure PMMA; b) PMMA-1; c) PMMA-3; d) PMMA-9; e) PMMA-13; f) PMMA-20; g) PMMA-23; h) PMMA-35 at different magnitudes (Borrowed from [39]).....	43
Fig. 58: Weight loss in nitrogen atmosphere at 220 °C (The weight loss percentage was normalised to the organic part) (Borrowed from [39]).....	44
Fig. 59: Weight loss in nitrogen atmosphere at 300 °C (The weight loss percentage was normalised to the organic part) (Borrowed from [39]).....	44
Fig. 60: Chemiluminescence emission curves in oxygen at 200°C. (Presented percentages are per cent by weight.) (Borrowed from [39]).....	45
Fig. 61: Chemiluminescence emission curves in oxygen at 220°C. (Presented percentages are per cent by weight.) (Borrowed from [39]).....	45
Fig. 62: TEM micrograph of PET/Silica 0.5 wt% (Borrowed from [41]).....	47
Fig. 63: TEM micrograph of PET/Silica 2.5 wt% (Borrowed from [41]).....	47
Fig. 64: TEM image of untreated silica (borrowed from [42]).....	48
Fig. 65: TEM image of silica/PS core-shell (borrowed from [42]).....	48
Fig. 66: Dependence of visible light transmittance and haziness of amorphous PET-SiO ₂ /PS nanocomposite on particle load. (Borrowed from [42]).....	49
Fig. 67: Effect of the silica particles ratio on the tensile strenght of PBT: A: grafted SiO ₂ , B: original SiO ₂ (Borrowed from [43]).....	50
Fig. 68: Effect of the silica particles ratio on the elongation of PBT: A: grafted SiO ₂ , B: original SiO ₂ (Borrowed from [43]).....	50
Fig. 69: Effect of the silica ratio on the notched impact strength of PBT: A: grafted SiO ₂ , B: original SiO ₂ (Borrowed from [43]).....	50
Fig. 70: TEM micrograph of PA-05-S.....	52
Fig. 71: TEM micrograph of PA-05-L.....	52
Fig. 72: Loss factor with respect to temperature (Borrowed from [45]).....	52
Fig. 73: Conservation modulus (G') with respect to temperature (Borrowed from [45]).....	52

Fig. 74: The composite evolution versus the filler ratio (Borrowed from [45]).....	53
Fig. 75: Viscosity at temperature of 250 °C (Borrowed from [45]).....	53
Fig. 76: Relative modulus evolution both below the main relaxation temperature of the pure matrix (Borrowed from [45]).....	53
Fig. 77: Relative modulus evolution both above the main relaxation temperature of the pure matrix (Borrowed from [45]).....	53
Fig. 78: Filler content influence on the mechanical behaviour in compression (Borrowed from [45]).....	53
Fig. 79: Filler content influence on the mechanical behaviour in tension – systems with large particles (Borrowed from [45]).....	53
Fig. 80: Filler content influence on the mechanical behaviour in tension – low filled systems (Borrowed from [45]).....	54
Fig. 81: DMTA data showing flexural modulus and loss factor, measured at 1 Hz. Epoxy polymer with 2.5 vol% of nano-silica (Borrowed from [48]).....	55
Fig. 82: Tensile modulus versus nano-silica content (Borrowed from [48]).....	55
Fig. 83: SEM micrograph of fracture surface of pure epoxy (Borrowed from [48]).....	55
Fig. 84: SEM micrograph of fracture surface of EP/SiO ₂ with 2.5 vol% (Borrowed from [48]).....	55
Fig. 85: SEM micrograph of fracture surface of EP/SiO ₂ with 13 vol% (Borrowed from [48]).....	55
Fig. 86: Fracture energy as dependence of nano-silica content (Borrowed from [48]).....	56
Fig. 87: Mean roughness of the fracture surface versus measured toughening increment. The numbers in brackets are the volume fractions of nano-particles. (Borrowed from [48]).....	56
Fig. 88: SEM micrograph of the fracture surface of pure epoxy polymer (Borrowed from [48]).....	56
Fig. 89: SEM micrograph of the fracture surface of the epoxy polymer with 9.6 vol% silica – void particles are circled (Borrowed from [48]).....	56
Fig. 90: TEM micrograph of the epoxy polymer containing 9.6 vol% of silica (Borrowed from [48]).....	56
Fig. 91: AFM micrograph of fracture surface of the epoxy polymer with 9.6 vol% nano- silica (Borrowed from [48]).....	56
Fig. 92: Surface profile of the line drawn across the Fig. 91. (Borrowed from [48]).....	57
Fig. 93: Scheme of synthetic route to the PUR/S (Borrowed from [51]).....	59

Fig. 94: TEM micrograph of PUR/S-1 (Borrowed from [51]).....	59
Fig. 95: TEM micrograph of PUR/S-3 (Borrowed from [51]).....	59
Fig. 96: TEM micrograph of PUR/S-7 (Borrowed from [51]).....	59
Fig. 97: TEM micrograph of PUR/S-3b (Borrowed from [51]).....	59
Fig. 98: DSC curves of PUR/silica nanocomposites (Borrowed from [51]).....	60
Fig. 99: Dependence of tensile strength on silica load (Borrowed from [51]).....	60
Fig. 100: Dependence of elongation on silica load (Borrowed from [51]).....	60
Fig. 101: Effect of silica particle size on the Tg of PUR/SiO ₂ composites with 2.25 wt% SiO ₂ content. (Borrowed from [52]).....	61
Fig. 102: Dependence of tensile strength of PUR/SiO ₂ composites with 2.25 wt% SiO ₂ content on silica particle diameter (Borrowed from [52]).....	61
Fig. 103: Dependence of elongation at break of PUR/SiO ₂ composites with 2.25 wt% SiO ₂ content on silica particle diameter (Borrowed from [52]).....	62
Fig. 104: Dependence of tensile strength and elongation at break of PUR/SiO ₂ composites on silica concentration (silica particle size 66 nm) (Borrowed from [52]).....	62
Fig. 105: Dependence of macrohardness of PUR/SiO ₂ composites with 2.25 wt% SiO ₂ content on silica particle diameter (Borrowed from [52]).....	62
Fig. 106: Dependence of macrohardness of PUR/SiO ₂ composites on silica particles load in wt% (Borrowed from [52]).....	62
Fig. 107: Absorbance spectra of PUR/SiO ₂ composites as a function of particle size embedded by in situ polymerization (Borrowed from [52]).....	62
Fig. 108: Absorbance spectra of PUR/SiO ₂ composites as a function of particle size embedded by blending polymerization (Borrowed from [52]).....	62

LIST OF TABLES

Table 1. Obtained DSC data (Reprinted from [30]).....	23
Table 2. DMA results (Reprinted from [30]).....	25
Table 3. Tensile properties (Reprinted from [30]).....	28
Table 4. Melt flow indexes (MFI) and equilibrium torques recorded at steady-state (10 min. after feeding) in the mixer of PP and its composites (Reprinted from [34])....	35
Table 5. DSC results of PP and its composites (Reprinted from [34]).....	35
Table 6. Influence of SiO ₂ -g-PGMA content on crystallization and melting behaviours of PP composites (Reprinted from [34]).....	36
Table 7. Polystyrene grafting densities, molecular weights of the grafted PS chains and hydrodynamic diameters of a series of PS-grafted silica samples (reprinted from [36])	38
Table 8. Compositions and glass transition temperatures (Reprinted from [39]).....	42
Table 9. Thermal property data by DSC (Reprinted from [41]).....	47
Table 10. DSC data of PET with different surface treatment of SiO ₂ nano-particles (32 nm) (Reprinted from [42]).....	48
Table 11. DSC data of PET-SiO ₂ /PS nanocomposite films with different PS-encapsulated SiO ₂ content (Reprinted from [42]).....	48
Table 12. Sample compositions and DSC data (Based on [45]).....	51
Table 13. Glass transition temperatures, modulus and fracture properties of the anhydride- cured epoxy polymer containing nano-particles (Based on [48]).....	55

LIST OF APPENDICES

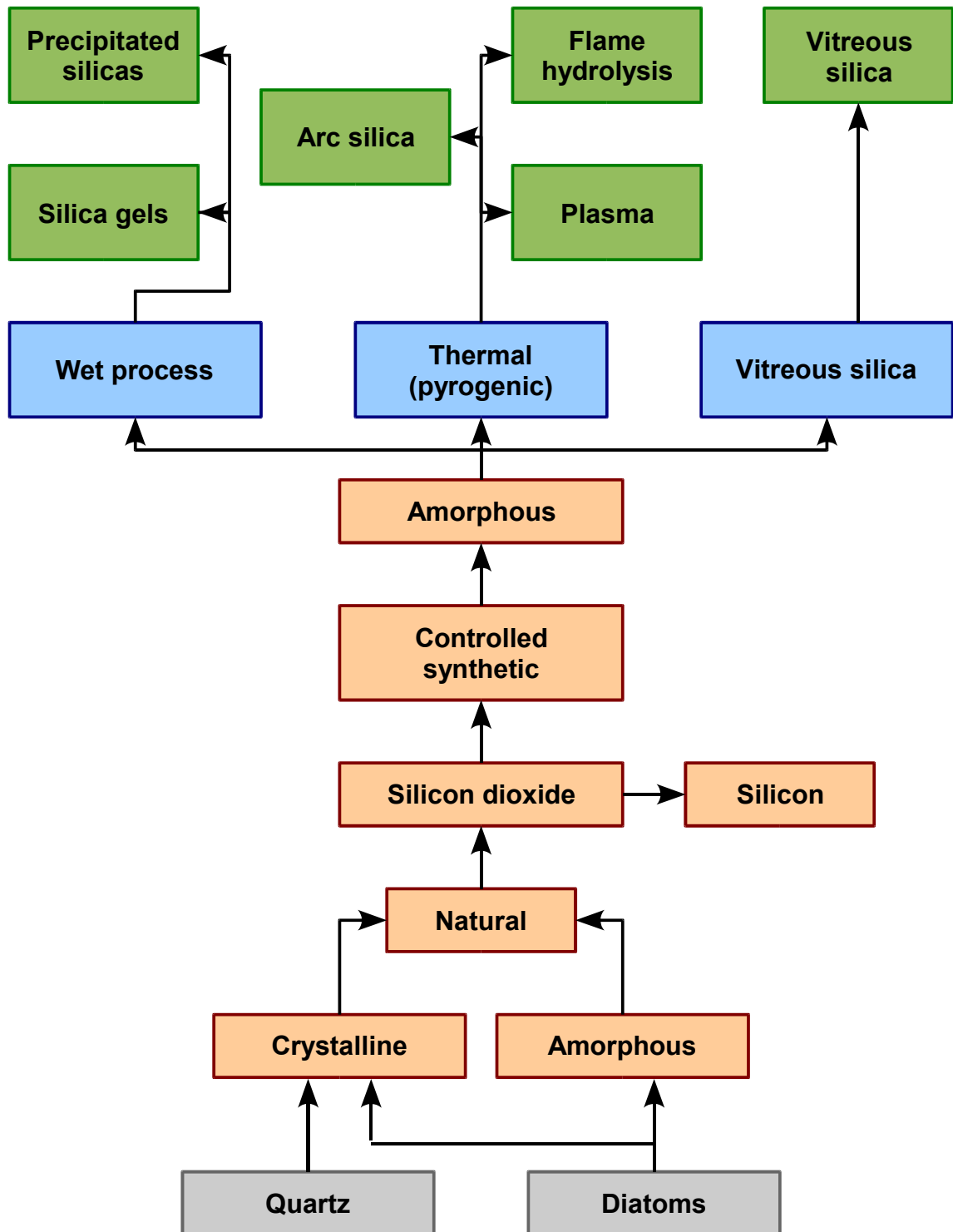
Appendix A1: Silica family tree.

Appendix A2: Characterisation of particles obtained by Stöber.

Appendix A3: Data sheets of some named and commercially available nano-silicas

APPENDIX A1: SILICA FAMILY TREE.

Diagram based on image published in: Technical bulletin: Fine particles. Degussa AG. Vol. 11. [online]. [cit. 2007-03-12] <<https://www.aerosil.com/page/en/literature>>



APPENDIX A2: CHARACTERISATION OF PARTICLES OBTAINED BY STÖBER.

Reprinted from: Stöber, W., Fink, A., Bohn E. Controlled growth of monodisperse silica spheres in the micron size range. *Journal of Colloid and Interface Science*, 1968, vol. 26 p. 62-69

Components	Final pH	Test					
		1		2		3	
		D (µm)	σ_{geom}	D (µm)	σ_{geom}	D (µm)	σ_{geom}
10 ml pentyl ester; 10 ml ammonium hydroxide (sat.); 50 ml propanol saturated with NH ₃	12.7	1.53	1.06	1.35	1.06	1.22	1.10
8 ml pentyl ester; 8 ml ammonium hydroxide (sat.); 50 ml propanol-methanol (3:1) saturated with NH ₃	12.7	1.68	1.07	1.26	1.05	1.30	1.50
8 ml pentyl ester; 8 ml ammonium hydroxide (sat.); 50 ml propanol saturated with NH ₃	12.6	1.57	1.07	1.21	1.07	1.35	1.45
6 ml pentyl ester; 6 ml ammonium hydroxide (sat.); 50 ml ethanol	11.8	1.10	1.07	0.42	1.03	0.99	1.09
6 ml pentyl ester; 5 ml ammonium hydroxide (sat.); 50 ml ethanol	11.6	0.37	1.06	0.64	1.14	0.42	1.06
6 ml pentyl ester; 4 ml ammonium hydroxide (sat.); 50 ml propanol-methanol (3:1)	11.4	0.60	7.03	0.63	1.08	0.64	1.10
4 ml pentyl ester; 4 ml ammonium hydroxide (sat.); 50 ml ethanol	11.6	0.29	1.02	0.36	1.05	0.44	1.03
4 ml pentyl ester; 4 ml ammonium hydroxide (sat.); 50 ml propanol-methanol (3:1)	11.5	0.44	1.04	0.66	1.05	0.64	1.06
4 ml pentyl ester; 3 ml ammonium hydroxide (sat.); 50 ml ethanol	11.4	0.25	1.08	0.25	1.06	0.27	1.12
4 ml pentyl ester; 2 ml ammonium hydroxide (sat.); 50 ml ethanol	11.3	0.05	1.07	0.08	1.05	0.08	1.05
4 ml pentyl ester; 2 ml ammonium hydroxide (sat.); 50 ml propanol-methanol (3:1)	11.2	0.11	1.06	0.17	1.07	0.20	1.06

APPENDIX A3: DATA SHEETS OF SOME NAMED AND COMMERCIALY AVAILABLE NANO-SILICAS

Data sheets are available on-line on producers/distributors web sites. Selection was made on the frequency of usage in cited articles and also the commercial importance of the producer was considered.

Namely:

- Degussa AG *<http://www.aerosil.com>*
- Sigma Aldrich *<http://sigmaaldrich.com>*
- Cabot corporation *<http://www.cabot-corp.com>*
- Harwick Standard Distribution Corporation
<http://www.harwickstandard.com>

Due to the copyright of the data sheet publisher, the documents are not modified or shorted and are here inserted as downloaded from web sites.

Product Information

▶ AEROSIL[®] 200

Hydrophilic Fumed Silica

AEROSIL[®] 200 is a hydrophilic fumed silica with a specific surface area of 200 m²/g.

Applications and Properties

Applications

- Paints and coatings
- Unsaturated polyester resins, laminating resins and gel coats
- HTV- and RTV-2K-silicone rubber
- Adhesives and sealants
- Printing inks
- Cable compounds and cable gels
- Plant protection
- Food and cosmetics

Properties

- Rheology and thixotropy control of liquid systems, binders, polymers, etc.
- Used as anti-settling, thickening and anti-sagging agent.
- Reinforcement of HTV- and RTV-2K silicone rubber.
- Improvement of free flow and anticaking characteristics of powders.

Physico-chemical Data

Properties	Unit	Typical Value
Specific surface area (BET)	m ² /g	200 ± 25
Average primary particle size	nm	12
Tapped density (approx. value)* acc. to DIN EN ISO 787/11, Aug. 1983	g/l	approx. 50
Moisture* 2 hours at 105 °C	wt. %	≤ 1.5
Ignition loss 2 hours at 1000 °C based on material dried for 2 hours at 105 °C	wt. %	≤ 1.0
pH in 4% dispersion		3.7 - 4.7
SiO₂ - content based on ignited material	wt. %	≥ 99.8

* ex plant

The data represents typical values and not production parameters.

Safety and Handling

With every sample or initial shipment of our products we will send a Material Safety Data Sheet. Of course, you can also request an MSDS or any other information regarding product safety at any time, or download it as a registered user at www.aerosil.com.

Packaging and Storage

AEROSIL® 200 is supplied in multiple layer 10 kg bags. We recommend to store the product in closed containers under dry conditions and to protect the material from volatile substances. AEROSIL® 200 should be used within 2 years after production.

Registration

AEROSIL® 200					
CAS-No.	EINECS	TSCA (USA), AICS (Australia), DSL (Canada)	ENCS (Japan)	ECL (Korea)	IECS (China)
112 945-52-5 7631-86-9	231-545-4	Registered	1-548	KE-30953 (KE-31032)	Registered

► For further information please contact:

Commercial Contact

Degussa AG

Business Line Aerosil
Weissfrauenstrasse 9
D-60287 Frankfurt am Main,
Germany
Phone: +49 69/218-2532
Fax: +49 69/218-2533
E-Mail: aerosil@degussa.com
<http://www.aerosil.com>

NAFTA

Degussa Corporation
Business Line Aerosil
379 Interpace Parkway,
P. O. Box 677
Parsippany, NJ 07054-0677
Phone: +1 (800) AEROSIL
Phone: +1 (973) 541-8510
Fax: +1 (973) 541-8501

Asia (without Japan)

Aerosil Asia Marketing Office
c/o NIPPON AEROSIL CO., LTD.
P. O. Box 7015
Shinjuku Monolith 13F
3-1, Nishi-Shinjuku 2-chome
Shinjuku-ku, Tokyo
163-0913 Japan
Phone: +81-3-3342-1786
Fax: +81-3-3342-1761

Japan

NIPPON AEROSIL CO., LTD.
Sales & Marketing Division
P. O. Box 7015
Shinjuku Monolith 13F
3-1, Nishi-Shinjuku 2-chome
Shinjuku-ku, Tokyo
163-0913 Japan
Phone: +81-3-3342-1763
Fax: +81-3-3342-1772

Technical Contact

Degussa AG

Technical Service Aerosil
Rodenbacher Chaussee 4
P. O. Box 1345
D-63403 Hanau-Wolfgang,
Germany
Phone: +49 6181/59-3936
Fax: +49 6181/59-4489

NAFTA

Degussa Corporation
Technical Service Aerosil
2 Turner Place
Piscataway, NJ 08855-0365
Phone: +1 (888) SILICAS
Phone: +1 (732) 981-5000
Fax: +1 (732) 981-5275

Asia (without Japan)

Degussa AG
Technical Service Aerosil
Rodenbacher Chaussee 4
P. O. Box 1345
D-63403 Hanau-Wolfgang,
Germany
Phone: +49 6181/59-3936
Fax: +49 6181/59-4489

Japan

NIPPON AEROSIL CO., LTD.
Applied Technology Service
3 Mita-cho
Yokkaichi, Mie
510-0841 Japan
Phone: +81-593-45-5270
Fax: +81-593-46-4657

Or your local Degussa Representative

The information in this document is based on our best knowledge. We disclaim any warranty and liability whatsoever as to accuracy and completeness of such information as well as to the potential infringement of any proprietary rights. We reserve the right to effect technical alterations. Any user of our products shall bear the full risk connected to their use including but not limited to their properties and fitness for any purpose.

Product Information

▶ AEROSIL® R 972

Hydrophobic Fumed Silica

AEROSIL® R 972 is a hydrophobic fumed silica after treated with DDS (Dimethyldichlorosilane) based on a hydrophilic fumed silica with a specific surface area of 130 m²/g

Applications and Properties

Applications

- Silicone rubber and silicone sealants
- Paints and coatings
- Printing inks and toner
- Adhesives
- Cable compounds and gels
- Plant protection

Properties

- Hydrophobic component for thickening and reinforcement of RTV-1 K silicone sealants.
- Improves shelf-life of silicone sealants.
- Water resistant, hydrophobising of liquid systems.
- Rheology control of (complex) liquid systems.
- For use in coatings as anti-settling agent, for pigment stabilization and improvement of corrosion protection.
- Improves hydrophobicity and rheology of offset printing inks.
- Improvement and maintenance of free flow and anti-caking characteristics of powders.

Physico-chemical Data

Properties	Unit	Typical Value
Specific surface area (BET)	m ² /g	110 ± 20
Carbon content	wt. %	0.6 – 1.2
Average primary particle size	nm	16
Tapped density* (approx. value) acc. to DIN EN ISO 787/11, Aug. 1983	g/l	approx. 50
Moisture * 2 hours at 105 °C	wt. %	≤ 0.5
Ignition loss, 2 hours at 1000 °C, based on material dried for 2 hours at 105 °C	wt. %	≤ 2.0
pH in 4% dispersion		3.6 – 4.4
SiO ₂ -content based on ignited material	wt. %	≥ 99.8

* ex plant

The data represents typical values and not production parameters.

Safety and Handling

With every sample or initial shipment of our products we will send a Material Safety Data Sheet. Of course you can also ask at any time for a MSDS or any other information regarding product safety.

Packing and Storage

AEROSIL® R 972 is supplied in multiple layer 10 kg bags. We recommend to store the product in closed containers under dry conditions and to protect the material from volatile substances. AEROSIL® R 972 should be used within 2 years after production.

Registration

	CAS-No.	EINECS	TSCA (USA) AICS (Australia) CEPA (Canada) PICCS (Philippines) IECS (China)	MITI (Japan)	ECL (Korea)
AEROSIL® R 972	68 611-44-9	271-893-4	Registered	1-548 / 7-476	KE-10116

▶ For further information please contact:

Commercial Contact

Degussa AG

Business Line Aerosil
Weissfrauenstrasse 9
D-60287 Frankfurt am Main,
Germany
Phone: +49 69/218-2532
Fax: +49 69/218-2533
E-Mail: aerosil@degussa.com
<http://www.aerosil.com>

NAFTA

Degussa Corporation

Business Line Aerosil
379 Interpace Parkway,
P.O. Box 677
Parsippany, NJ 07054-0677
Phone: +1 (800) AEROSIL
Phone: +1 (973) 541-8510
Fax: +1 (973) 541-8501

Asia (without Japan)

Aerosil Asia Marketing Office

c/o NIPPON AEROSIL CO., LTD.
P. O. Box 7015
Shinjuku Monolith 13F
3-1, Nishi-Shinjuku 2-chome
Shinjuku-ku, Tokyo
163-0913 Japan
Phone: +81-3-3342-1786
Fax: +81-3-3342-1761

Japan

NIPPON AEROSIL CO., LTD.

Sales & Marketing Division
P. O. Box 7015
Shinjuku Monolith 13F
3-1, Nishi-Shinjuku 2-chome
Shinjuku-ku, Tokyo
163-0913 Japan
Phone: +81-3-3342-1763
Fax: +81-3-3342-1772

Technical Contact

Degussa AG

Technical Service Aerosil
Rodenbacher Chaussee 4
P. O. Box 1345
D-63403 Hanau-Wolfgang,
Germany
Phone: +49 6181/59-3936
Fax: +49 6181/59-4489

NAFTA

Degussa Corporation

Technical Service Aerosil
2 Turner Place
Piscataway, NJ 08855-0365
Phone: +1 (888) SILICAS
Phone: +1 (732) 981-5000
Fax: +1 (732) 981-5275

Asia (without Japan)

Degussa AG

Technical Service Aerosil
Rodenbacher Chaussee 4
P. O. Box 1345
D-63403 Hanau-Wolfgang,
Germany
Phone: +49 6181/59-3936
Fax: +49 6181/59-4489

Japan

NIPPON AEROSIL CO., LTD.

Applied Technology Service
3 Mita-cho
Yokkaichi, Mie
510-0841 Japan
Phone: +81-593-45-5270
Fax: +81-593-46-4657

Or your local Degussa Representative

The information in this document is based on our best knowledge. We disclaim any warranty and liability whatsoever as to accuracy and completeness of such information as well as to the potential infringement of any proprietary rights. We reserve the right to effect technical alterations. Any user of our products shall bear the full risk connected to their use including but not limited to their properties and fitness for any purpose.

Product Information

▶ AEROSIL[®] R 9200

Hydrophobic Fumed Silica

AEROSIL[®] R 9200 is a structure modified, hydrophobic fumed silica.

Applications and Properties

Applications

- Paints and coatings
- Silicone rubber
- Free flow

Properties

- Improves the scratch resistance of paints and coatings
- Low rheological effect and excellent processability enable high loading levels of polymer systems
- Effective free flow agent for fine powders, easily to incorporate, does not form agglomerates, allows short mixing time and gentle mixing conditions..

Physico-chemical Data

Properties	Unit	Typical Value
Specific surface area (BET)	m ² /g	170 ± 20
Carbon content	wt. %	0.7 - 1.3
Tapped density (approx. value) acc. to DIN EN ISO 787/11, Aug. 1983	g/l	approx. 200
Moisture 2 hours at 105 °C	wt. %	≤ 1.5
pH in 4% dispersion		3.0 - 5.0
SiO₂ -content based on ignited material	wt. %	≥ 99.8
Al₂O₃ -content	wt. %	≤ 0.10
Fe₂O₃ -content	wt. %	≤ 0.01
TiO₂ -content	wt. %	≤ 0.03
HCl -content	wt. %	≤ 0.025

* ex plant

The data represents typical values and not production parameters.

Safety and Handling

With every sample or initial shipment of our products we will send a Material Safety Data Sheet. Of course, you can also request an MSDS or any other information regarding product safety at any time, or download it as a registered user at www.aerosil.com.

Packaging and Storage

AEROSIL® R 9200 is supplied in multiple layer 15 kg bags. We recommend to store the product in closed containers under dry conditions and to protect the material from volatile substances. AEROSIL® R 9200 should be used within 2 years after production.

Registration

AEROSIL® R 9200					
CAS-No.	EINECS	TSCA (USA), AICS (Australia), DSL (Canada), PICCS (Philippines)	ENCS (Japan)	ECL (Korea)	ECS (China)
68611-44-9	271-893-4	registered	1-548/7-476	KE-10116	registered

► For further information please contact:

Commercial Contact

Degussa GmbH

Business Line Aerosil
Weissfrauenstrasse 9
D-60287 Frankfurt am Main,
Germany
Phone: +49 69/218-2532
Fax: +49 69/218-2533
E-Mail: aerosil@degussa.com
<http://www.aerosil.com>

NAFTA

Degussa Corporation
Business Line Aerosil
379 Interpace Parkway,
P. O. Box 677
Parsippany, NJ 07054-0677
Phone: +1 (800) AEROSIL
Phone: +1 (973) 541-8510
Fax: +1 (973) 541-8501

Asia (without Japan)

Aerosil Asia Marketing Office
c/o NIPPON AEROSIL CO., LTD.
P. O. Box 7015
Shinjuku Monolith 13F
3-1, Nishi-Shinjuku 2-chome
Shinjuku-ku, Tokyo
163-0913 Japan
Phone: +81-3-3342-1786
Fax: +81-3-3342-1761

Japan

NIPPON AEROSIL CO., LTD.
Sales & Marketing Division
P. O. Box 7015
Shinjuku Monolith 13F
3-1, Nishi-Shinjuku 2-chome
Shinjuku-ku, Tokyo
163-0913 Japan
Phone: +81-3-3342-1763
Fax: +81-3-3342-1772

Technical Contact

Degussa GmbH

Technical Service Aerosil
Rodenbacher Chaussee 4
P. O. Box 1345
D-63403 Hanau-Wolfgang,
Germany
Phone: +49 6181/59-3936
Fax: +49 6181/59-4489

NAFTA

Degussa Corporation
Technical Service Aerosil
2 Turner Place
Piscataway, NJ 08855-0365
Phone: +1 (888) SILICAS
Phone: +1 (732) 981-5000
Fax: +1 (732) 981-5275

Asia (without Japan)

Degussa GmbH
Technical Service Aerosil
Rodenbacher Chaussee 4
P. O. Box 1345
D-63403 Hanau-Wolfgang,
Germany
Phone: +49 6181/59-3936
Fax: +49 6181/59-4489

Japan

NIPPON AEROSIL CO., LTD.
Applied Technology Service
3 Mita-cho
Yokkaichi, Mie
510-0841 Japan
Phone: +81-593-45-5270
Fax: +81-593-46-4657

Please visit our website www.aerosil.com to find your local contact.

This information and all further technical advice are based on Degussa's present knowledge and experience. However, Degussa assumes no liability for providing such information and advice including the extent to which such information and advice may relate to existing third party intellectual property rights, especially patent rights. In particular, Degussa disclaims all CONDITIONS AND WARRANTIES, WHETHER EXPRESS OR IMPLIED, INCLUDING THE IMPLIED WARRANTIES OF FITNESS FOR A PARTICULAR PURPOSE OR MERCHANTABILITY. DEGUSSA SHALL NOT BE RESPONSIBLE FOR CONSEQUENTIAL, INDIRECT OR INCIDENTAL DAMAGES (INCLUDING LOSS OF PROFITS) OF ANY KIND. Degussa reserves the right to make any changes according to technological progress or further developments. It is the customer's responsibility and obligation to carefully inspect and test any incoming goods. Performance of the product(s) described herein should be verified by testing and carried out only by qualified experts. It is the sole responsibility of the customer to carry out and arrange for any such testing. Reference to trade names used by other companies is neither a recommendation, nor an endorsement of any product and does not imply that similar products could not be used.



Product Information

FUMED SILICA

Product Code **38,127-6**

Replacement for Product Number **S 5380**

CAS NUMBER: 112945-52-5

SYNONYMS: fumed silicon dioxide, Aerosil™, Cab-O-Sil™

PHYSICAL DESCRIPTION:

Appearance:¹

S5130 blue-grey powder

S2128 white fluffy powder

S5255 white powder

S5505 white powder with very faint blue cast

S5380 white powder

Fumed silica is composed of submicron-sized spheres, which are 40-60% fused into short chains, very highly branched, 0.1-0.2 microns long. The spheres are quite uniform in size for a given product, but the chain lengths are quite variable, 10 to 30 units in length. The surface area, which varies with the particle size, gives a good approximation of the sphere diameter. The smaller the particles, the larger the estimated surface area.²

Sigma product	Particle size (µm)	Surface area (m ² /gram)	Density (lb/cu. ft)
S5130	0.007	390 ± 40	2.3
S5255	0.008	325 ± 25	2.3
S5380	0.011	255 ± 15	4.5 ± 0.5
S2128	0.012	200 ± 25	2.3
S5505	0.014	200 ± 25	2.3

METHOD OF PREPARATION:²

Silicon tetrachloride is burned in a flame of hydrogen and oxygen (at approximately 1800°C) to produce molten spheres of silicon dioxide (and hydrogen chloride). Depending on process parameters, the size of these silica spheres can be varied and, within a given batch, show excellent uniformity (by electron micrograph). The molten spheres collide and fuse with one another to form branched, three-dimensional chain-like aggregates.

FUMED SILICA
Sigma Prod. Nos. S5130, S5255,
S5380, S2128 and S5505

METHOD OF PREPARATION:² (continued)

Many aggregates have chains from 10 to 30 spheres in length, or from 0.1 to 0.2 microns (μm) in length. As the aggregates cool down below the fusion temperature of silica (approximately 1710°C), further collisions result in some reversible mechanical entanglement or agglomeration. Further agglomeration occurs during the collection process; this can be reversed by proper dispersion in a suitable medium.

During the formation of the product, hydroxyl groups become attached to some of the silicon atoms on the surface of the silica particles, making the surface hydrophilic and capable of hydrogen bonding with suitable molecules. There are (estimated) 3.5-4.5 hydroxyl groups per square millimicron of silica surface, compared to a theoretical maximum of 7.85. The structure of fumed silica is amorphous (as indicated by absence of lines in its X-ray diffraction pattern.)

The surface area was determined by calculation using a nitrogen adsorption method of Brunauer³, and the value used to calculate particle diameter.

The residual hydrogen chloride on the surface of the fumed silica was reduced to less than 200 ppm by calcining.² The moisture content of the product will vary, depending on storage conditions. Moisture adsorbed on the surface can be removed by evacuation at room temperature (at 10^{-2} mm Hg) or by heating at 110°C . (If the product is heated above 800°C , it sinters irreversibly.)

STORAGE / STABILITY AS SUPPLIED:

These products are stable indefinitely at room temperature if kept dry. Their tendency to adsorb moisture suggests an effective shelflife of about two years, once opened.

SOLUBILITY / SOLUTION STABILITY:²

Fumed silica will form dispersions in water, glycerine, butyl alcohol, mineral oil and a variety of other liquids, causing them to thicken or form gels. The dispersions often have thixotropic properties, i.e., viscosity that varies with rate of stirring.

For liquids with minimal hydrogen bonding, small amounts of fumed silica will increase the viscosity. Addition from 3 to 5% by weight usually suffices to cause the liquid to form a gel. After an initial thorough dispersion, increasing the mixing time has little effect on the viscosity for a given percent of silica.

For liquids with a high degree of hydrogen bonding, small amounts of fumed silica will also increase the viscosity. However, usually 10% or more (by weight) will be needed to form gels. The initial dispersion is rapid. If the dispersion is mixed too long, the result will be an irreversible decrease in viscosity.

SOLUBILITY / SOLUTION STABILITY:²

Dispersions formed with fumed silica are quite stable, remaining unchanged for weeks to months, over a range of temperatures.

FUMED SILICA
Sigma Prod. Nos. S5130, S5255,
S5380, S2128 and S5505

USAGE:

Fumed silica have been used commercially in a wide range of applications to enhance viscosity of many liquids, including paints. The most common application in biochemistry is for clarifying sera by removing lipids.

For years, serum could be delipidized very easily using a solvent, 1,1,2-trichlorotrifluoroethane (Sigma product number T5271). This was offered under a trade name "Lipoclean", and cited methods suggested the use of three parts solvent to two parts serum - or vice versa.⁴ In 1993, OSHA-directed regulations became effective concerning the labeling of products exposed to chlorofluorocarbons (CFC's) during their manufacture. This has led to the need for alternate methods of clarifying serum-related products, especially if they are to be sold commercially.

Two methods are reported to be successful, each with its own limitations: dextran sulfate extraction and fumed silica precipitation. The use of dextran sulfate MW 500,000 (Sigma product number D6001) has been reported.⁵ However, it does tend to bind blood clotting factors and, in fact, has been used to isolate factors II and X.⁶ Use of fumed silica has generally been successful; one trade name reported is Aerosil 380; Sigma's comparable product is S5130, 0.007 micron particles.

GENERAL PROCEDURE FOR DELIPIDIZING SERUM:⁶

Add 20 g of fumed silica, Sigma product S5130/L serum (or 20 mg/mL serum), mix well for 2-3 hours or overnight. Centrifuge at 2000 g for 15 minutes. Wash the pelleted silica with buffer, then recentrifuge the supernatant liquid. Any pellet can be re-washed to recover as much serum as possible.

Disadvantages:

- a. About 15% of the sample volume will be irretrievably lost, adsorbed to the silica.
- b. The fumed silica is extremely fluffy and somewhat difficult to handle. The use of a fine-dust filter respirator is recommended. The fumed silica must be added as a dry powder to the serum, since once it is wet, the silica becomes very slimy and is extremely hard to handle as a heavy precipitate.
- c. The silica is suitable for serum but cannot be used on plasma. The surface will activate clotting factors.

REFERENCES:

1. Sigma quality control.
2. Supplier data.
3. Brunauer, S. et al., *J. Am. Chem. Soc.*, 60, 309 (1938).
4. *Clin. Chim. Acta*, 148, 125-130 (1985) and *Clin. Chem.*, 36, 1675-1678 (1990).
5. Agnese et al., *Clin. Biochem.*, 16, 98-100 (1983).
6. Sigma production department.

Sigma warrants that its products conform to the information contained in this and other Sigma-Aldrich publications. Purchaser must determine the suitability of the product(s) for their particular use. Additional terms and conditions may apply. Please see reverse side of the invoice or packing slip.

CAB-O-SIL® LM-150



CAB-O-SIL® LM-150 untreated fumed silica is a synthetic, amorphous, colloidal silicon dioxide that is generally regarded as unique in industry because of its unusual particle characteristics. CAB-O-SIL® fumed silica's extremely small particle size, enormous surface area, its high purity, and its chain-forming tendencies set it apart in a class of its own. CAB-O-SIL® fumed silica is a light, fluffy powder that is white in appearance and is used in many applications and in a variety of industries.

Product Form

Powder

Typical Properties

B.E.T. Surface Area	150 m ² /g
pH (4% aqueous slurry)	3.7 – 4.3
325 Mesh Residue (44 microns)	0.02% max.
Tamped Density	50 g/l
Loss on Heating*	< 0.5%
Specific Gravity	2.2 g/cm ³
Wt. per gallon	18.3 lb
Refractive Index	1.46
X-ray Form	Amorphous
Assay (% SiO ₂)	> 99.8
Average Particle (Aggregate) Length	0.2 – 0.3 microns

*At time of packaging.

Functions

Reheology Control
Reinforcement

Applications

Adhesives & Sealants
Silicone Rubber Systems



Packaging Options

CAB-O-SIL® fumed silicas are packaged in color-coded, multi-wall Kraft paper bags. Grade LM-150 is packaged in North America in 10-lb bags and in Europe in 10 kg. bags. The bags are unitized and sized to provide product protection, facilitate efficient handling, and maximize payloads. Specific information regarding standard and custom packaging may be obtained by contacting a sales service representative at the Cabot Corporation office in your region.

MSDS

A Material Safety Data Sheet for this product may be obtained by contacting the Cabot Corporation office in your region or visiting our website.

This information is provided as a convenience and for informational purposes only. No guarantee or warranty as to this information, or any product to which it relates, is given or implied. This information may contain inaccuracies, errors or omissions and CABOT DISCLAIMS ALL WARRANTIES EXPRESS OR IMPLIED, INCLUDING MERCHANTABILITY OR FITNESS FOR A PARTICULAR PURPOSE AS TO (i) SUCH INFORMATION, (ii) ANY PRODUCT OR (iii) INTELLECTUAL PROPERTY INFRINGEMENT. In no event is Cabot responsible for, and Cabot does not accept and hereby disclaims liability for, any damages whatsoever in connection with the use of or reliance on this information or any product to which it relates.

NORTH AMERICA	EUROPE	ASIA/ PACIFIC	SOUTH AMERICA	MIDDLE EAST/ AFRICA
Cabot Corporation Business and Technical Center 157 Concord Road Billerica, MA 01821-7001 USA Customer Service: Phone: (800) 526-7591 Technical Service: Phone: +1 (978) 663-3455 Phone: (800) 462-2313 Fax: +1 (978) 670-6167	Cabot Interleuvenlaan 15 I B-3001 Leuven BELGIUM Tel: +32 16 39 24 00 Fax: +32 16 39 24 44	Cabot Specialty Chemicals Level 21 MNI Tower 2 11, Jalan Pinang 50450 Kuala Lumpur MALAYSIA Phone: +60 3 2164 8352 Fax: +60 3 2161 0253 Cabot Specialty Chemicals Shiba Boat Bldg. 5F 3-1-15 Shiba, Minato-ku Tokyo 105-0014 JAPAN Phone: +81 3 3457 7354 Fax: +81 3 3457 7658	Cabot Latin America Division Rua do Paraíso, 148 - 5º andar CEP 04103-000, São Paulo SP BRAZIL Customer Service: Phone: +55 11 2144 6400 Fax: +55 11 3253 0051	Cabot Specialty Chemicals Jebel Ali Free Zone LOB 15, Office 424 Dubai UNITED ARAB EMIRATES Phone: +971 4 8871 800 Fax: +971 4 8871 801

UNTREATED FUMED SILICA



CAB-O-SIL® M-5



CAB-O-SIL® M-5 untreated fumed silica is a synthetic, amorphous, colloidal silicon dioxide that is generally regarded as unique in industry because of its unusual particle characteristics. CAB-O-SIL® fumed silica's extremely small particle size, its enormous surface area, its high purity, and its chain-forming tendencies set it apart in a class of its own. CAB-O-SIL® fumed silica is a light, fluffy powder that is white in appearance and is used in many applications and in a variety of industries.

Product Form

Powder

Typical Properties

B.E.T. Surface Area	200 m ² /g
pH (4% aqueous slurry)	3.7 – 4.3
325 Mesh Residue (44 microns)	0.02% max.
Tamped Density	50 g/l
Loss on Heating*	< 1.5%
Specific Gravity	2.2 g/cm ³
Wt. per gallon	18.3 lb
Refractive Index	1.46
X-ray Form	Amorphous
Assay (% SiO ₂)	> 99.8
Oil Adsorption	~350 g/100 g oil
Average Particle (Aggregate) Length	0.2 – 0.3 microns

*At time of packaging.





Functions

Rheology Control
Reinforcement
Free Flow
Suspension
Adsorbant

Applications

Adhesives & Sealants
Coatings
Composites
Cosmetics
Foods
Inks
Pharmaceuticals

Packaging Options

CAB-O-SIL® fumed silicas are packaged in color-coded, multi-wall Kraft paper bags. Grade M-5 is packaged in North America in 10-lb bags and in Europe in 10 kg. bags. The bags are unitized and sized to provide product protection, facilitate efficient handling, and maximize payloads. Specific information regarding standard and custom packaging may be obtained by contacting a sales service representative at the Cabot Corporation office in your region.

MSDS

A Material Safety Data Sheet for this product may be obtained by contacting the Cabot Corporation office in your region or visiting our website.

This information is provided as a convenience and for informational purposes only. No guarantee or warranty as to this information, or any product to which it relates, is given or implied. This information may contain inaccuracies, errors or omissions and CABOT DISCLAIMS ALL WARRANTIES EXPRESS OR IMPLIED, INCLUDING MERCHANTABILITY OR FITNESS FOR A PARTICULAR PURPOSE AS TO (i) SUCH INFORMATION, (ii) ANY PRODUCT OR (iii) INTELLECTUAL PROPERTY INFRINGEMENT. In no event is Cabot responsible for, and Cabot does not accept and hereby disclaims liability for, any damages whatsoever in connection with the use of or reliance on this information or any product to which it relates.

NORTH AMERICA	EUROPE	ASIA/ PACIFIC	SOUTH AMERICA	MIDDLE EAST/ AFRICA
Cabot Corporation Business and Technical Center 157 Concord Road Billerica, MA 01821-7001 USA Customer Service: Phone: (800) 526-7591 Technical Service: Phone: +1 (978) 663-3455 Phone: (800) 462-2313 Fax: +1 (978) 670-6167	Cabot Interleuvenlaan 15 I B-3001 Leuven BELGIUM Tel: +32 16 39 24 00 Fax: +32 16 39 24 44	Cabot Specialty Chemicals Level 21 MNI Tower 2 11, Jalan Pinang 50450 Kuala Lumpur MALAYSIA Phone: +60 3 2164 8352 Fax: +60 3 2161 0253 Cabot Specialty Chemicals Shiba Boat Bldg. 5F 3-1-15 Shiba, Minato-ku Tokyo 105-0014 JAPAN Phone: +81 3 3457 7354 Fax: +81 3 3457 7658	Cabot Latin America Division Rua do Paraíso, 148 - 5º andar CEP 04103-000, São Paulo SP BRAZIL Customer Service: Phone: +55 11 2144 6400 Fax: +55 11 3253 0051	Cabot Specialty Chemicals Jebel Ali Free Zone LOB 15, Office 424 Dubai UNITED ARAB EMIRATES Phone: +971 4 8871 800 Fax: +971 4 8871 801

UNTREATED FUMED SILICA



CAB-O-SIL® EH-5



CAB-O-SIL® EH-5 untreated fumed silica is a synthetic, amorphous, colloidal silicon dioxide that is generally regarded as unique in industry because of its unusual particle characteristics. CAB-O-SIL® fumed silica's extremely small particle size, its enormous surface area, its high purity, and its chain-forming tendencies set it apart in a class of its own. CAB-O-SIL® fumed silica is a light, fluffy powder that is white in appearance and is used in many applications and in a variety of industries.

Product Form

Powder

Typical Properties

B.E.T. Surface Area	380 m ² /g
pH (4% aqueous slurry)	3.7 – 4.3
325 Mesh Residue (44 microns)	0.02% max.
Tamped Density	50 g/l
Loss on Heating*	< 1.5%
Specific Gravity	2.2 g/cm ³
Wt. per gallon	18.3 lb
Refractive Index	1.46
X-ray Form	Amorphous
Assay (% SiO ₂)	> 99.8
Oil Adsorption	~300-350 g/100 g oil
Average Particle (Aggregate) Length	0.2 – 0.3 microns

*At time of packaging.





Functions

Rheology Control
Reinforcement
Free Flow
Suspension
Adsorbant

Applications

Adhesives & Sealants
Coatings
Cosmetics
Foods
Inks

Packaging Options

CAB-O-SIL® fumed silicas are packaged in color-coded, multi-wall Kraft paper bags. Grade EH-5 is packaged in North America in 10-lb bags and in Europe in 10 kg. bags. The bags are unitized and sized to provide product protection, facilitate efficient handling, and maximize payloads. Specific information regarding standard and custom packaging may be obtained by contacting a sales service representative at the Cabot Corporation office in your region.

MSDS

A Material Safety Data Sheet for this product may be obtained by contacting the Cabot Corporation office in your region or visiting our website.

This information is provided as a convenience and for informational purposes only. No guarantee or warranty as to this information, or any product to which it relates, is given or implied. This information may contain inaccuracies, errors or omissions and CABOT DISCLAIMS ALL WARRANTIES EXPRESS OR IMPLIED, INCLUDING MERCHANTABILITY OR FITNESS FOR A PARTICULAR PURPOSE AS TO (i) SUCH INFORMATION, (ii) ANY PRODUCT OR (iii) INTELLECTUAL PROPERTY INFRINGEMENT. In no event is Cabot responsible for, and Cabot does not accept and hereby disclaims liability for, any damages whatsoever in connection with the use of or reliance on this information or any product to which it relates.

NORTH AMERICA	EUROPE	ASIA/ PACIFIC	SOUTH AMERICA	MIDDLE EAST/ AFRICA
Cabot Corporation Business and Technical Center 157 Concord Road Billerica, MA 01821-7001 USA Customer Service: Phone: (800) 526-7591 Technical Service: Phone: +1 (978) 663-3455 Phone: (800) 462-2313 Fax: +1 (978) 670-6167	Cabot Interleuvenlaan 15 I B-3001 Leuven BELGIUM Tel: +32 16 39 24 00 Fax: +32 16 39 24 44	Cabot Specialty Chemicals Level 21 MNI Tower 2 11, Jalan Pinang 50450 Kuala Lumpur MALAYSIA Phone: +60 3 2164 8352 Fax: +60 3 2161 0253 Cabot Specialty Chemicals Shiba Boat Bldg. 5F 3-1-15 Shiba, Minato-ku Tokyo 105-0014 JAPAN Phone: +81 3 3457 7354 Fax: +81 3 3457 7658	Cabot Latin America Division Rua do Paraíso, 148 - 5º andar CEP 04103-000, São Paulo SP BRAZIL Customer Service: Phone: +55 11 2144 6400 Fax: +55 11 3253 0051	Cabot Specialty Chemicals Jebel Ali Free Zone LOB 15, Office 424 Dubai UNITED ARAB EMIRATES Phone: +971 4 8871 800 Fax: +971 4 8871 801

CAB-O-SIL® TS-610



CAB-O-SIL® TS-610 treated fumed silica is a high-purity, large particle size silica which has been treated with dimethyldichlorosilane. The treatment replaces many of the surface hydroxyl groups on the fumed silica with methyl groups. This renders the silica less hydrophylic, having very different properties from untreated silica.

Product Form

Powder

Typical Properties

B.E.T. Surface Area	125 m ² /g
Carbon	0.85
pH (4% slurry; 1:1 v/v isopropanol/water)	> 4.0
Tamped Density	60 g/l
Loss on Heating*	< 0.5% max.
Specific Gravity	2.2 g/cm ³
Wt. per gallon	18.3 lb
Refractive Index	1.46
X-ray Form	Amorphous
Average Particle (Aggregate) Length	0.2–0.3 microns

*At time of packaging.

Typical Applications

The unique properties of TS-610 treated fumed silica offer special benefits in many applications:

- The silica's low moisture content makes it usable without expensive drying when incorporated into moisture-sensitive systems.
- The hydrophobic nature of TS-610 allows it to be used in materials which are produced to protect ferrous substrates from corrosion or as moisture barriers. Also, the hydrophobic nature of the TS-610 renders systems more resistant to emulsification with water.
- TS-610 is an excellent free flow agent. The hydrophobic characteristic allows it to be especially useful in free flowing hygroscopic materials and in preventing clumping in these materials.
- TS-610 is a rheology control agent. It offers a different thixotropic response than a hydrophilic, untreated fumed silica and can offer improved flow and leveling characteristics.
- TS-610 is an excellent reinforcing filler. The reduced thickening behavior of TS-610 allows higher loadings for attainment of very high physical properties while still having a polymer system with a processible viscosity.





creating what matters

Packaging Options

CAB-O-SIL® TS-610 treated fumed silica is packaged in North America in 10-lb multi-wall Kraft bags and is available in 24 x 10-lb poly-shrouded units. Specific information regarding standard and custom packaging may be obtained by contacting a sales service representative at the Cabot Corporation office in your region.

MSDS

A Material Safety Data Sheet for this product may be obtained by contacting the Cabot Corporation office in your region.

This information is provided as a convenience and for informational purposes only. No guarantee or warranty as to this information, or any product to which it relates, is given or implied. This information may contain inaccuracies, errors or omissions and CABOT DISCLAIMS ALL WARRANTIES EXPRESS OR IMPLIED, INCLUDING MERCHANTABILITY OR FITNESS FOR A PARTICULAR PURPOSE AS TO (i) SUCH INFORMATION, (ii) ANY PRODUCT OR (iii) INTELLECTUAL PROPERTY INFRINGEMENT. In no event is Cabot responsible for, and Cabot does not accept and hereby disclaims liability for, any damages whatsoever in connection with the use of or reliance on this information or any product to which it relates.

NORTH AMERICA

Cabot Corporation
Business and Technical Center
157 Concord Road
Billerica, MA 01821-7001
USA
Customer Service:
Phone: (800) 526-7591
Technical Service:
Phone: +1 (978) 663-3455
Phone: (800) 462-2313
Fax: +1 (978) 670-6167

EUROPE

Cabot
Interleuvenlaan 15 I
B-3001 Leuven
BELGIUM
Tel: +32 16 39 24 00
Fax: +32 16 39 24 44

ASIA/ PACIFIC

Cabot Specialty Chemicals
Level 21 MNI Tower 2
11, Jalan Pinang
50450 Kuala Lumpur
MALAYSIA
Phone: +60 3 2164 8352
Fax: +60 3 2161 0253

Cabot Specialty Chemicals
Shiba Boat Bldg. 5F
3-1-15 Shiba, Minato-ku
Tokyo 105-0014
JAPAN
Phone: +81 3 3457 7354
Fax: +81 3 3457 7658

SOUTH AMERICA

Cabot Latin America Division
Rua do Paraíso, 148 - 5º andar
CEP 04103-000, São Paulo
SP BRAZIL
Customer Service:
Phone: +55 11 2144 6400
Fax: +55 11 3253 0051

MIDDLE EAST/ AFRICA

Cabot Specialty Chemicals
Jebel Ali Free Zone
LOB 15, Office 424
Dubai
UNITED ARAB EMIRATES
Phone: +971 4 8871 800
Fax: +971 4 8871 801

CAB-O-SIL® TS-530



CAB-O-SIL® TS-530 treated fumed silica is a high-purity silica which has been treated with a hexamethyldisilazane. The treatment replaces many of the surface hydroxyl groups on the fumed silica with trimethylsilyl groups. This treatment makes the silica extremely hydrophobic.

Product Form

Powder

Typical Properties

B.E.T. Surface Area	225 m ² /g
Carbon	4.25
pH (4% slurry; 1:1 v/v isopropano/water)	4.5 - 6.5
Tamped Density	60 g/l
Specific Gravity	2.2 g/cm ³
Wt. per gallon	18.3 lb
Refractive Index	1.46
X-ray Form	Amorphous
Average Particle (Aggregate) Length	0.2–0.3 microns

*At time of packaging.

Typical Applications

The unique properties of TS-530 treated fumed silica offer special benefits in many applications:

- TS-530 is an excellent reinforcing filler for elastomers. Its full surface treatment gives a low viscosity and its high surface area provide excellent reinforcement properties, such as tear strength.
- As a free flow agent, TS-530 is the most efficient of all the treated and untreated fumed silicas. This, combined with the potential to enhance the charging properties of a powder, makes TS-530 especially attractive for free flow applications in toners and powder coatings.
- TS-530 can function as an anti-settling agent in coatings. With its reduced thickening potential, it will not raise the viscosity of the system which is of great benefit in high-solids systems.
- TS-530 reduces the water permeability of a coating, thereby increasing its corrosion and humidity resistance.
- TS-530 is an effective dry powder carrier for oils such as perfumes, fragrances, pesticides, herbicides, and veterinary products.





creating what matters

Packaging Options

CAB-O-SIL® TS-530 treated fumed silica is packaged in North America in 10-lb multi-wall Kraft bags and is available in 24 x 10-lb poly-shrouded units. Specific information regarding standard and custom packaging may be obtained by contacting a sales service representative at the Cabot Corporation office in your region.

MSDS

A Material Safety Data Sheet for this product may be obtained by contacting the Cabot Corporation office in your region.

This information is provided as a convenience and for informational purposes only. No guarantee or warranty as to this information, or any product to which it relates, is given or implied. This information may contain inaccuracies, errors or omissions and CABOT DISCLAIMS ALL WARRANTIES EXPRESS OR IMPLIED, INCLUDING MERCHANTABILITY OR FITNESS FOR A PARTICULAR PURPOSE AS TO (i) SUCH INFORMATION, (ii) ANY PRODUCT OR (iii) INTELLECTUAL PROPERTY INFRINGEMENT. In no event is Cabot responsible for, and Cabot does not accept and hereby disclaims liability for, any damages whatsoever in connection with the use of or reliance on this information or any product to which it relates.

NORTH AMERICA	EUROPE	ASIA/ PACIFIC	SOUTH AMERICA	MIDDLE EAST/ AFRICA
Cabot Corporation Business and Technical Center 157 Concord Road Billerica, MA 01821-7001 USA Customer Service: Phone: (800) 526-7591 Technical Service: Phone: +1 (978) 663-3455 Phone: (800) 462-2313 Fax: +1 (978) 670-6167	Cabot Interleuvenlaan 15 I B-3001 Leuven BELGIUM Tel: +32 16 39 24 00 Fax: +32 16 39 24 44	Cabot Specialty Chemicals Level 21 MNI Tower 2 11, Jalan Pinang 50450 Kuala Lumpur MALAYSIA Phone: +60 3 2164 8352 Fax: +60 3 2161 0253 Cabot Specialty Chemicals Shiba Boat Bldg. 5F 3-1-15 Shiba, Minato-ku Tokyo 105-0014 JAPAN Phone: +81 3 3457 7354 Fax: +81 3 3457 7658	Cabot Latin America Division Rua do Paraíso, 148 - 5º andar CEP 04103-000, São Paulo SP BRAZIL Customer Service: Phone: +55 11 2144 6400 Fax: +55 11 3253 0051	Cabot Specialty Chemicals Jebel Ali Free Zone LOB 15, Office 424 Dubai UNITED ARAB EMIRATES Phone: +971 4 8871 800 Fax: +971 4 8871 801



WACKER

SILICONES

HDK®

PRODUCT OVERVIEW
HDK® – PYROGENIC SILICA

CREATING TOMORROW'S SOLUTIONS

A SURVEY OF HDK[®] PRODUCT DATA

Typical General Properties		
Appearance		Loose white powder
Color		Transparent
Crystal structure SiO ₂		Amorphous
SiO ₂ content ¹ DIN EN ISO 3262-19	[wt. %]	>99.8 %
Loss on ignition ² DIN EN ISO 3262-19, at 1,000 °C/2 h	[wt. %]	<2 % (hydrophilic)
Density of SiO ₂ (primary structure)	[g/l]	2,200
Refractive index		1.46 (hydrophilic)
Silanol group density		2 SiOH/nm ² (hydrophilic)
Electrical resistance at densities of 50–60 g/l	[cm]	>10 ¹³

1 Based on the substance incinerated for 2 h at 1,000 °C

2 Based on the substance dried for 2 h at 105 °C

Hydrophilic HDK[®]

Hydrophilic HDK[®] is manufactured by the hydrolysis of volatile chlorosilanes in an oxyhydrogen flame. In chemical terms, it consists of highly pure amorphous silicon dioxide with the appearance of a loose white powder. Hydrophilic silica is wetted by water and can be dispersed in water.

Hydrophobic HDK[®]

Hydrophobic HDK[®] is produced by the chemical reaction of hydrophilic HDK[®] with reactive silanes, e.g. methyl chlorosilanes or hexamethyldisilazane. It has water-repellent properties and is no longer dispersible in water.

HDK[®] Dispersions

HDK[®] dispersions are produced by the dispersion of hydrophilic HDK[®] in water using high shear forces. They obtain their stability by electrostatic and steric stabilization.

HDK® Hydrophilic Grades – Physicochemical Properties

HDK®		D05	C10	S13	V15	V15P	N20	N20P	T30	T40
BET surface area DIN EN ISO 9277/DIN 66132	[m ² /g]	50 ± 20	100 ± 20	125 ± 15	150 ± 20	150 ± 20	200 ± 30	200 ± 30	300 ± 30	400 ± 40
pH DIN EN ISO 787-9 in 4 % H ₂ O dispersion		3.8 – 4.5	3.8 – 4.5	3.8 – 4.5	3.8 – 4.3	3.8 – 4.3	3.8 – 4.3	3.8 – 4.3	3.8 – 4.3	3.6 – 4.3
Apparent density after tamping DIN EN ISO 787-11	[g/l]	ca. 70	ca. 60	ca. 50	ca. 50	ca. 100	ca. 40	ca. 100	ca. 40	ca. 40
Loss on drying¹ DIN EN ISO 787-2 2 h at 105 °C	[wt. %]	<1.0	<1.0	<1.0	<1.0	<1.0	<1.5	<1.5	<1.5	<1.5
Screen residue DIN EN ISO 787-18 (acc. to Mocker >40 µm)	[wt. %]	<0.04	<0.03	<0.03	<0.03	<0.03	<0.04	<0.04	<0.04	<0.04

Note: These figures are intended as a guide and should not be used in preparing specifications.

¹ On leaving the factory

HDK® Hydrophobic Grades – Physicochemical Properties

HDK®		H15	H20	H30	H18	H2000	H2050EP ¹	H3004 ¹
BET Surface area² DIN EN ISO 9277/DIN 66132	[m ² /g]	150 ± 20	200 ± 30	300 ± 30	200 ± 30	200 ± 30	250 ± 30	300 ± 30
pH DIN EN ISO 787-9 in water:methanol = 1:1		3.8 – 4.8	3.8 – 4.8	3.8 – 4.5	4.0 – 6.5	6.5 – 8.0	8.0 – 9.0	6.0 – 8.0
Apparent density after tamping DIN EN ISO 787-11	[g/l]	ca. 40	ca. 40	ca. 40	ca. 40	ca. 200	ca. 200	ca. 100
Loss on drying³ DIN EN ISO 787-2 2 h at 105 °C	[wt. %]	<0.6	<0.6	<0.6	<0.6	<0.6	<1.0	<1.0
Screen residue DIN EN ISO 787-18 (acc. to Mocker >40 µm)	[wt. %]	<0.05	<0.05	<0.05	<1.0	n. a.	n. a.	n. a.
Carbon content	[wt. %]	ca. 0.8	ca. 1.1	ca. 1.8	ca. 4.0	ca. 2.8	ca. 7.0	ca. 4.0
Surface modification		-OSi(CH ₃) ₂ -	-OSi(CH ₃) ₂ -	-OSi(CH ₃) ₂ -	-OSi(CH ₃) ₂ -	-OSi(CH ₃) ₃	-OSi(CH ₃) ₂ - -NR ₂ / ⁺ -NR ₃	-OSi(CH ₃) ₃

Note: These figures are intended as a guide and should not be used in preparing specifications.

¹ Special grades for electrophotographic toners and developers. Other grades available on request.

² Hydrophilic silica

³ On leaving the factory

HDK® Dispersions – Physicochemical Properties

		D1515B	D2012B	D3017B	A2012	A3017	XK20030
BET Surface area silica DIN EN ISO 9277/DIN 66132	[m ² /g]	150 ± 20	200 ± 30	300 ± 30	200 ± 30	300 ± 30	200 ± 30
Solids content	[%]	15	12	17	12	17	30
pH		4 – 6	4 – 6	4 – 6	8 – 10	8 – 10	9 – 11
Viscosity	[mPa s at 200 s ⁻¹]	<100	<100	<100	<100	<100	<100
Zeta potential	[mV]	<-10	<-10	<-10	<-10	<-10	<-10

Note: These figures are intended as a guide and should not be used in preparing specifications.

THE MANY USES OF HDK®

Applications of HDK®

Application	Grade	Amount used [%]	Effect	Equipment
Unsaturated polyester (GRP)				
– Laminating resins	N20	0.8–1.5	Thickening, thixotropic agent, antisedimentation	Dissolvers, kneaders, roll mills, ultrasonic dispersion
– Gel coats	N20, T30	2.0–3.0		
– Grouting compounds	N20	0.5–1.0		
– Polar resin systems, e.g. vinyl ester resins	H18	0.5–3.0		
PVC				
– Plastisols	N20, T30, T40	0.3–2.5	Thickening, thixotropic agent, antisedimentation, anti-sticking agent, free-flow agent, increase of dielectric properties	Dissolvers, roll mills, fluid mixers
– Organosols	N20, T30, T40	0.3–2.5		
– Plasticized PVC compounds	N20, T30	0.1–0.8		
– Cable compounds	T30, T40	1.0–3.0		
– Dry blend compounds	H20	0.05–0.5		
– Film & sheet	N20, T30, H20	0.1–1.0		
Printing inks				
– Letterpress printing	N20	0.5–2.0	Thickening, thixotropic agent, antisedimentation, regulation of water content, improved brilliance and contrast	Dissolvers, roll mills, fluid mixers
– Silk-screen printing	N20, T40	1.0–10.0		
– Gravure printing	N20	0.5–2.0		
– Flexographic printing	N20, T30, H15, H20, H30	0.5–2.5		
– Offset printing	H15, H20	0.5–2.5		
Paints and coatings				
– Polyester coatings	N20, T30, T40	0.5–2.5	Thickening, thixotropic agent, antisedimentation, in powder paint systems also for optimizing free flow and triboelectric application	Dissolvers, roll mills, mills, stirrers
– Epoxy resin and polyurethane coatings	H15, H20, H30, H18	1.0–4.5		
– Alkyd resin coatings	N20, T30, T40, H15, H20, H30, H18	0.5–5.0		
– Acrylic resin coatings	N20, T30, T40	0.3–2.0		
– Zinc-rich paints	H15, H20, N20, H18	0.5–2.0		
– Powder coatings	N20, H15, H20, H2000,	0.5–5.0		
Adhesives				
– Polychloroprene-based	N20, H2000	0.8–5.0	Thickening, thixotropic agent, antisedimentation, processing aids, adhesion improvers	Dissolvers, roll mills, stirrers
– Epoxy resin, polyurethane resin, cyanoacrylate-based	N20, H2000, H18	0.8–5.0		
– Dispersion-based	N20, H2000	0.8–5.0		
Insulating gels				
– Cable and splice fillings for conventional copper and fiber-optic technology	N20, H15, H20, H30	5.0–10.0	Thickening, thixotropic agent, water repellency	Stirrers, kneaders, roll mills
Accumulators				
– Battery acids	N20P	2.0–6.0	Thickening, thixotropic agent	Dissolvers, stirrers
CMP				
– Chemical-mechanical planarizing	K1012, K1020, A5012 C10, S13, T30 *)	1.0–25.0	Polishing and planarizing semiconductor device surfaces	Special polishing machines
Natural and synthetic rubber				
	N20, H15, H20, H2000	5.0–40.0	Reinforcement	Internal mixers, roll mills

*) Customer-formulated, ready-to-use dispersions for CMP processes are available from our "Planar Solutions" joint venture.

Applications of HDK®

Application	Grade	Amount used [%]	Effect	Equipment
Silicone elastomers				
- HTV/LSR silicone rubber	N20, T30, H30, H2000	15.0 – 35.0	Reinforcement, increase of dielectric properties	Roll mills, kneaders
- RTV-2 silicone rubber	S13, V15, H2000	3.0 – 30.0		
Grouting compound				
- RTV-1 silicone rubber	S13, V15, H2000, H15, H20	3.0 – 30.0	Reinforcement, thixotropic agent	Planetary mixers, Dissolvers, extruders
- Polyurethanes	V15, H20	3.0 – 25.0		
- Polysulfides (thiokols)	V15, N20, H15, H20	0.7 – 3.0		
- Acrylates	V15, H20	0.5 – 1.5		
Toners and developers				
- Magnetic and non-magnetic 1-part toners, 2-part toners Polymerization toner	H3004, H2050EP	0.2 – 2.0	Free-flow agents, external charge control for positive and negative systems, self-cleaning	Powder mixers
Cosmetics, pharmaceuticals, animal feed and foods				
- Toothpaste	N15, N20, N20P	1.5 – 5.0	Thickening, thixotropic agent, antisedimentation, free-flow agents, carriers for actives, tableting aids	Dissolvers, roll mills, mechanical mixers, pneumatic mixers
- Tablets	N20, N20Pharma	1.5 – 10.0		
- Dragees	N20, N20Pharma	3.0 – 12.0		
- Dusting agents	N20, N20Pharma	2.0 – 5.0		
- Powders	N20, H20, N20Pharma	0.1 – 2.0		
- Aerosols	N20, N20Pharma	0.1 – 3.0		
- Suspensions	V15, N20Pharma, N20	0.2 – 3.0		
- Ointments, creams	V15, N20Pharma, N20	2.0 – 10.0		
Bulk materials				
- Fire-extinguisher powders	H15, H2000	0.5 – 1.0	Free-flow agents, processing aids flow enhancers	Mechanical and pneumatic mixers
- Fly ashes	H15, H20, H2000	0.4 – 1.0		
- Plastic powders	N20, H15, H20, H2000	0.05 – 1.0		
- Pigments	N20, H20, H2000	0.1 – 1.0		
- Salts	N20, H20, H30	0.1 – 1.0		
Textile impregnation				
	D1515B D3017B, A3017	3.0	Stabilization	Stirrers

Further Information

More detailed information on particular applications is given in the following application brochures. Chemical-Mechanical Planarization, Coatings and Printing Inks, Toners, Adhesives and Sealants, Synthetic Resins and Composites. Copies of the brochures can be obtained direct from WACKER SILICONES, from your technical support staff, or via the internet at: www.wacker.com/hdk

PACKAGED TO CUSTOMERS' NEEDS



Multilayer Bags

Multilayer valved bags are the standard packaging for HDK®. The plastic layer keeps out moisture, allowing the product to be kept for several months in dry conditions.

Depending on the HDK® grade and bulk density, the bags are available in various weights to suit market demands. They are shrink wrapped in PE film. The data sheet indicates which form of packaging is used for a particular product.

Big Bags

Special HDK® grades are available in Big Bags. These woven super sacks are delivered on an individual pallet. The Big Bags are also shrink-wrapped in polyethylene film as reliable moisture protection and to ensure stability during transport. Another advantage of this form of container is dust-free HDK® processing.

Bulk Vehicles

WACKER SILICONES offers delivery in bulk vehicles. Since the full load must be accepted, this form of delivery assumes that the customer has a storage silo big enough to receive the entire delivery.

Supply of HDK® Dispersions

All HDK® dispersions are delivered in 200-liter PE drums, or alternatively in road tankers.

Handling and Product Safety

HDK® is not classified as a hazardous substance as defined by the German chemicals law (Chem G) and the law on the transport of hazardous goods (GG BefG).

Further information on toxicology is given in the appropriate material safety data sheets. Detailed information on handling can be found in the product data sheets.

The data presented in this brochure are in accordance with the present state of our knowledge, but do not absolve the user from carefully checking all supplies immediately upon receipt. We reserve the right to alter product constants within the scope of technical progress or new developments. The information given in this brochure should be checked by preliminary trials because of conditions during processing over which we have no control, especially where other companies' raw materials are also being used. The information provided by us does not absolve the user from the obligation of investigating the possibility of infringement of third parties' rights and, if necessary, clarifying the position. Recommendations for use do not constitute a warranty, either express or implied, of the fitness or suitability of the product for a particular purpose.

WACKER

SILICONES

Wacker Chemie AG
Hanns-Seidel-Platz 4
81737 München, Germany

hdk@wacker.com
www.wacker.com/hdk

Wacker Chemical Corporation
3301 Sutton Road
Adrian, MI 49221-9397
USA

Tel. +1 517 264-8500
Fax +1 517 264-8246

hdk@wacker.com
www.wacker.com/hdk

Wacker Chemicals Trading
(Shanghai) Co. Ltd.
31 F., Bank of China Tower
200 Yin Cheng Road Central
Pudong
Shanghai 200 120
China

Tel. +86 21 6100-3400
Fax +86 21 6100-3500

hdk@wacker.com
www.wacker-chemicals.com.cn